

---

Doctoral Dissertations

Student Theses and Dissertations

---

Fall 2015

## Synthesis and electrochemical studies of novel ionic liquid based electrolytes

Avinash Raju Vadapalli

Follow this and additional works at: [https://scholarsmine.mst.edu/doctoral\\_dissertations](https://scholarsmine.mst.edu/doctoral_dissertations)

 Part of the [Chemistry Commons](#)

Department: Chemistry

---

### Recommended Citation

Vadapalli, Avinash Raju, "Synthesis and electrochemical studies of novel ionic liquid based electrolytes" (2015). *Doctoral Dissertations*. 2460.

[https://scholarsmine.mst.edu/doctoral\\_dissertations/2460](https://scholarsmine.mst.edu/doctoral_dissertations/2460)

This thesis is brought to you by Scholars' Mine, a service of the Missouri S&T Library and Learning Resources. This work is protected by U. S. Copyright Law. Unauthorized use including reproduction for redistribution requires the permission of the copyright holder. For more information, please contact [scholarsmine@mst.edu](mailto:scholarsmine@mst.edu).

SYNTHESIS AND ELECTROCHEMICAL STUDIES OF NOVEL IONIC LIQUID  
BASED ELECTROLYTES

by

AVINASH RAJU VADAPALLI

A DISSERTATION

Presented to the Faculty of the Graduate School of the

MISSOURI UNIVERSITY OF SCIENCE AND TECHNOLOGY

In Partial Fulfillment of the Requirements for the Degree

DOCTOR OF PHILOSOPHY

in

CHEMISTRY

2015

Approved by:

Dr. V. Prakash Reddy, Advisor

Dr. Nicholas Leventis

Dr. Jeffrey G. Winiarz

Dr. Paul Nam

Dr. K. Chandrashekhara

© 2015

Avinash Raju Vadapalli

All Rights Reserved

## ABSTRACT

Room temperature ionic liquids (RTILs) have received substantial interest as nonaqueous electrolytes in lithium ion- and metal-air batteries in recent years due to their low volatility, non-flammability, wide liquid range, and thermal stability characteristics. Towards developing a new generation of high specific energy lithium ion batteries, a series of imidazolium and pyrrolidinium based ionic liquids were synthesized and explored as nonaqueous electrolytes in lithium-, lithium ion-, and lithium-air batteries. Pyrrolidinium-TFSI based ionic liquids have wide electrochemical stability (5.7 – 6.2 V vs Li/Li<sup>+</sup>); however, they show limited thermal stabilities and lithium cell discharge characteristics. TFSI-based ionic liquids are thermally and electrochemically more stable when compared with their BF<sub>4</sub>-based analogues. A series of fluorinated ionic liquid electrolytes were synthesized and investigated for their use in lithium-air batteries. These ionic liquids have improved the diffusion coefficient and higher solubility of oxygen when compared with currently used nonaqueous electrolytes.

Cathode materials, such as LiNi<sub>1/3</sub>Mn<sub>1/3</sub>Co<sub>1/3</sub>O<sub>2</sub> and LiFePO<sub>4</sub>, were chemically delithiated using nitronium tetrafluoroborate (NO<sub>2</sub>BF<sub>4</sub>), or disodium peroxydisulfate (Na<sub>2</sub>S<sub>2</sub>O<sub>8</sub>), to explore their effect on the oxidative degradation of the carbonate based electrolytes. Using fluoroethylene carbonate as the electrolyte additive, electrolyte degradation was monitored by <sup>19</sup>F NMR spectroscopy. Formation of the solid electrolyte interface (SEI) on the delithiated cathode materials was probed using surface techniques, such as X-ray photoelectron spectroscopy (XPS) and scanning electron microscopy (SEM).

## ACKNOWLEDGMENTS

First and foremost, I would like to thank my advisor, Dr V. Prakash Reddy for his continuous guidance and support during my pursuit of graduate studies at Missouri University of Science and Technology.

I want to thank my advising committee members, Dr. Nicholas Leventis, Dr. Jeffrey G. Winiarz, Dr. Paul Nam and Dr. K. Chandrashekhara for their support and guidance throughout the completion of my Ph.D. program.

I would like to thank my former and current lab members Dr Nanditha Nair, Ninu Madria and Jatin Mehta and all undergraduates for their help and expertise in helping complete my research work. The author would like to thank the Department of Chemistry at the Missouri University of Science and Technology for the financial support provided through teaching assistantships and other resources. I am also thankful to all teaching and non-teaching staff, and students of the Department of Chemistry for their help with course work and making my stay comfortable at Missouri University of Science and Technology.

## TABLE OF CONTENTS

	Page
ABSTRACT.....	iii
ACKNOWLEDGMENTS .....	iv
LIST OF ILLUSTRATIONS.....	viii
LIST OF TABLES.....	x
NOMENCLATURE .....	xi
SECTION	
1. IONIC LIQUIDS.....	1
1.1. INTRODUCTION .....	1
1.2. HISTORY OF IONIC LIQUIDS .....	3
1.3. CHARACTERISTICS OF IONIC LIQUIDS.....	4
1.3.1. Melting Point.....	5
1.3.2. Viscosity.....	8
1.3.3. Density.....	11
1.3.4. Thermal Stability.....	12
1.3.5. Surface Tension.....	14
1.3.6. Conductivity.....	15
1.3.7. Electrochemical Windows.....	18
1.3.8. Water Miscibility.....	19
1.3.9. Flammability of Ionic Liquids.....	20
1.3.10. Vapor Pressure .....	21
1.4. IONIC LIQUID SYNTHESIS .....	21
1.5. RESEARCH GOALS .....	23
2. SYNTHESIS AND ELECTROCHEMICAL PROPERTIES OF NOVEL IONIC LIQUIDS.....	24
2.1. INTRODUCTION .....	24
2.2. EXPERIMENTAL.....	26
2.2.1. Materials and Methods.....	26
2.3. SYNTHESIS OF IONIC LIQUIDS.....	27
2.3.1. 1-Ethoxymethyl-3-methyl-imidazolium bis(trifluoromethanesulfonyl)imide.....	27

2.3.2. 1-Ethoxymethyl-1-methyl-pyrrolidinium bis(trifluoromethanesulfonyl)imide.....	28
2.3.3. 1-(3-cyanopropyl)-3-methylimidazolium bis(trifluoromethanesulfonyl)imide.....	29
2.3.4. 1-(3,3,3-trifluoropropyl)-3-methylimidazolium bis(trifluoromethanesulfonyl)imide.....	31
2.3.5. 1-(3,3,3-trifluoropropyl)-1-methylpyrrolidinium bis(trifluoromethanesulfonyl)imide.....	32
2.3.6. 1-(2-fluoroethyl)-1-methylpyrrolidinium bis(trifluoromethanesulfonyl)imide.....	33
2.3.7. 1-(2-fluoroethyl)-3-methylimidazolium bis(trifluoromethanesulfonyl)imide.....	34
2.3.8. 1-Ethoxymethyl-3-methyl-imidazolium tetrafluoroborate.....	36
2.3.9. 1-Ethoxymethyl-1-methyl-pyrrolidinium tetrafluoroborate.....	37
2.4. RESULTS AND DISCUSSION.....	38
2.4.1. Synthesis.....	38
2.4.2. Thermal Stability.....	41
2.4.3. Electrochemical Studies.....	42
2.5. FLUORINATED IONIC LIQUID IN LITHIUM/OXYGEN BATTERY.....	43
2.5.1. Introduction.....	43
2.5.2. Materials and Methods.....	45
2.5.3. Synthesis of Fluorinated Ionic Liquids.....	46
2.5.3.1 1-Methyl-3-(3,3,4,4,5,5,6,6,7,7,8,8,8-tridecafluorooctyl)- imidazolium bis(trifluoromethanesulfonyl)imide.....	46
2.5.3.2 1-Methyl-3-(3,3,4,4,4-pentafluorobutyl)-imidazolium bis(trifluoromethanesulfonyl)imide.....	48
2.5.3.3 1-Methyl-3-butylimidazolium bis(trifluoromethanesulfonyl)imide.....	50
2.5.4. Preliminary Results.....	51
2.6. BORON BASED ANION RECEPTORS.....	52
2.6.1. Introduction.....	52
2.6.2. Materials and Methods.....	55
2.6.3. Synthesis of Boron Based Anion Receptors.....	56
2.6.3.1 3,9-diphenyl-2,4,8,10-tetraoxa-3,9-diborasp[5.5] undecane.....	56

2.6.3.2 3,9-bis(3-nitrophenyl)-2,4,8,10-tetraoxa-3,9-diborasp[5.5]undecane.....	57
2.7. CONCLUSION.....	57
3. CHEMICAL DELITHIATION OF LiFePO <sub>4</sub> ; EFFECT ON THE SOLID ELECTROLYTE INTERFACE .....	59
3.1. INTRODUCTION .....	59
3.2. EXPERIMENTAL.....	61
3.2.1. Material and Methods.....	61
3.2.2. Chemical Delithiation of Cathode Materials.....	62
3.2.2.1 Delithiation using Na <sub>2</sub> S <sub>2</sub> O <sub>8</sub> .....	62
3.2.2.2 Delithiation using NO <sub>2</sub> BF <sub>4</sub> .....	62
3.3. RESULTS AND DISCUSSION.....	63
3.3.1. <sup>19</sup> F NMR Studies.....	63
3.3.2. X-ray Photoelectron Spectrometry Studies (XPS).....	64
3.3.3. Scanning Electron Microscopy Studies (SEM).....	66
3.4. PROBABLE SEI FORMATION MECHANISM. ....	66
3.5. CONCLUSION.....	67
APPENDIX.....	69
REFERENCES .....	111
VITA.....	126



## LIST OF ILLUSTRATIONS

	Page
Figure 1.1. Commonly used ionic liquids. ....	2
Figure 1.2. A “functionalized ionic liquid” based on the miconazole cation. ....	4
Figure 1.3. Viscosities of [C <sub>n</sub> MIM][BF <sub>4</sub> ] (n = 2 to n = 6) vs temperature. ....	9
Figure 1.4. Density of [C <sub>n</sub> MIM][BF <sub>4</sub> ](n = 2-6) vs temperature ....	11
Figure 1.5. Schematic representation of Hofmann elimination. ....	13
Figure 1.6. Scheme showing thermal decomposition of [C <sub>4</sub> MIM][X] ....	13
Figure 1.7. Variation in surface tension vs change in temperature for different ionic liquid.....	15
Figure 2.1. Alkoxyalkyl and fluoroalkyl-derived imidazolium and pyrrolidinium ionic liquids. ....	25
Figure 2.2. Structure of 1-Ethoxymethyl-3-methyl-imidazolium bis(trifluoromethanesulfonyl)imide.....	28
Figure 2.3. Structure of 1-Ethoxymethyl-1-methyl-pyrrolidinium bis(trifluoromethanesulfonyl)imide.....	29
Figure 2.4. Structure of 1-(3-cyanopropyl)-3-methylimidazolium bis(trifluoromethanesulfonyl)imide.....	30
Figure 2.5. Synthesis of 1-(3,3,3-trifluoropropyl)-3-methylimidazolium bis(trifluoromethanesulfonyl) imide.....	31
Figure 2.6. A) Synthesis of 1-(3,3,3-trifluoropropyl)-1-methylpyrrolidinium bis(trifluoromethanesulfonyl)imide.....	33
Figure 2.7. Structure of 1-(2-fluoroethyl)-1-methylpyrrolidinium bis(trifluoromethanesulfonyl)imide.....	34
Figure 2.8. Structure of 1-(2-fluoroethyl)-3-methylimidazolium bis(trifluoromethanesulfonyl)imide.....	35
Figure 2.9. Structure of 1-ethoxymethyl-3-methyl-imidazolium tetrafluoroborate.....	37
Figure 2.10. Structure of 1-ethoxymethyl-1-methyl-pyrrolidinium tetrafluoroborate.....	38
Figure 2.11. Synthesis of 1-methyl-1-fluoroethylpyrrolidinium and 1-methyl-3-fluoroethylimidazolium bis(trifluoromethylsulfonyl)imide ionic liquids. ....	39
Figure 2.12. Synthesis of 1-methyl-1-ethoxymethylpyrrolidinium and 1-methyl-3-ethoxymethylimidazolium bis(trifluoromethylsulfonyl)imide ionic liquids. ....	40
Figure 2.13. Thermogravimetric analysis of 1-trifluoropropyl-3-methylimidazolium bis(trifluoromethanesulfonyl)imide.....	42

Figure 2.14. Gravimetric energy densities (W·h/kg) for various types of rechargeable batteries compared to gasoline .....	44
Figure 2.15. Synthesis of 1-Methyl-3-(3,3,4,4,5,5,6,6,7,7,8,8,8-tridecafluorooctyl)-imidazolium bis(trifluoromethanesulfonyl)imide. ....	48
Figure.2.16. Synthesis of 1-methyl-3-(3,3,4,4,4-pentafluorobutyl)-imidazolium bis(trifluoromethanesulfonyl)imide.....	49
Figure 2.17. Synthesis of 1-methyl-3-butylimidazolium bis(trifluoromethanesulfonyl)imide.....	51
Figure 2.18. Structure of tris(pentafluorophenyl)borane (TPFPB).....	54
Figure 2.19. Structure of borate ester based anion receptors. ....	55
Figure 2.20. Structure of boron based anion receptor.....	55
Figure 2.21. Synthesis of 3,9-diphenyl-2,4,8,10-tetraoxa-3,9-diborasp[5.5]undecane .....	56
Figure 2.22. Synthesis of 3,9-bis(3-nitrophenyl)-2,4,8,10-tetraoxa-3,9-diborasp[5.5]undecane .....	57
Figure 3.1. A range of lithium-ion battery electrodes either currently available or under development and comparison of their theoretical and practical capacity. ....	60
Figure 3.2. The reaction mixture of fluoroethylene carbonate (FEC) and delithiated LiFePO <sub>4</sub> at various time intervals with trifluorotoluene as an internal standard. ....	64
Figure 3.3. C 1s, O 1s, Li 1s and F 1s XPS spectra of the pristine and delithiated LiNi <sub>1/3</sub> Mn <sub>1/3</sub> Co <sub>1/3</sub> O <sub>2</sub> after reacting with FEC.....	65
Figure 3.4. SEM Images of a) pristine LiFePO <sub>4</sub> after reaction with FEC at room temperature for 30 min and b) delithiated LiFePO <sub>4</sub> after reaction with FEC at room temperature for 30 min. ....	66
Figure 3.5. Metal ion based Lewis acid catalyzed polymerization of FEC leading to the SEI.....	67

**LIST OF TABLES**

	Page
Table 1.1. Melting points of ammonium and pyrrolidinium bis(trifluoromethylsulfonyl)imide based ionic liquids <sup>20</sup> .....	6
Table 1.2. Comparison of viscosities of ionic liquids with different concentrations of chloride impurities at 20 °C <sup>29</sup> .....	10
Table 1.3. Comparison of viscosities and conductivities for a range of organic solvents and RTILs <sup>53</sup> .....	16
Table 2.1. Diffusion coefficient and solubility of O <sub>2</sub> in selected room temperature ionic liquids. ....	52

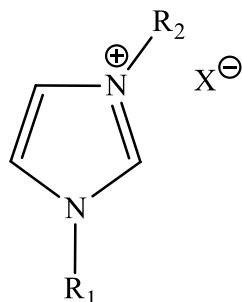
**NOMENCLATURE**

<u>Symbol</u>	<u>Description</u>
cP	Centipoise
[RMIM][PF <sub>6</sub> ]	N-alkyl-N-methylimidazolium hexafluorophosphate
[RMIM][TFSI]	N-alkyl-N-methylimidazolium bis(trifluoromethanesulfonyl)imide
MEOMIM-TFSI	N-methyl-N-ethoxymethylimidazolium bis(trifluoromethanesulfonyl)imide
MEOMIM-BF <sub>4</sub>	N-methyl-N-ethoxymethylimidazolium tetrafluoroborate
MFEIM-TFSI	N-methyl-N-fluoroethylimidazolium bis(trifluoromethanesulfonyl)imide
MFEPYR-TFSI	N-methyl-N-fluoroethylpyrrolidinium bis(trifluoromethanesulfonyl)imide
MEOMPYR-TFSI	N-methyl-N-ethoxymethyl pyrrolidinium bis(trifluoromethanesulfonyl)imide
MEOMPYR-BF <sub>4</sub>	N-methyl-N-ethoxymethylpyrrolidinium tetrafluoroborate
RTILs	Room temperature ionic liquids
TGA	Thermogravimetric analysis

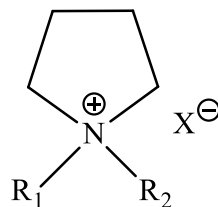
# 1. IONIC LIQUIDS

## 1.1. INTRODUCTION

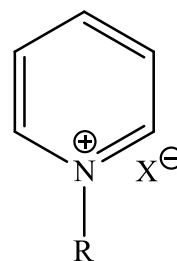
The term ionic liquid was originally used to describe molten salts consisting of various inorganic cations and anions<sup>1</sup>. Recently, the definition for ionic liquids has been extended to include salts that exist as liquids at or near room temperature, and are usually described as room temperature ionic liquids (RTILs). The composition of ionic liquids (that is, RTILs based on various anions and cations), has a major influence on the physicochemical properties of RTILs. A majority of the currently used RTILs are composed of organic cations and organic or inorganic anions (Figure 1.1).



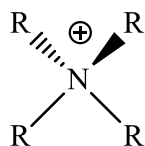
Imidazolium salts



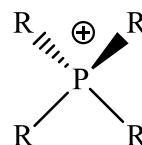
Pyrrolidinium salts



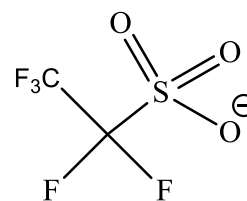
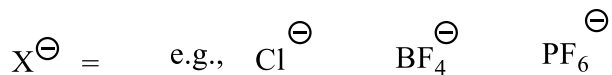
Pyridinium salts



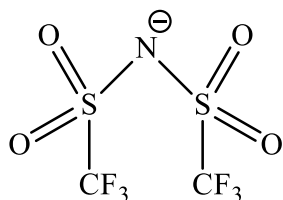
Tetraalkylammonium salts



Tetraalkylphosphonium salts



Pentafluoroethanesulfate



Bis(trifluoromethylsulfonyl)imide (TFSI)

Figure 1.1. Commonly used ionic liquids.

Conventional room temperature ionic liquids (RTILs) are generally those consisting of quaternary ammonium salts, such as tetraalkylammonium  $[\text{R}_4\text{N}]^+$  (cyclic and acyclic versions); the cyclic versions may be either saturated (e.g., piperidinium, pyrrolidinium) or aromatic (e.g., imidazolium, pyridinium). Thus, by modifying the nature of the cations and anions, the physical properties of ionic liquids can be optimized

for a given application. These properties include melting point, density, viscosity, solubility, and hydrophobicity. In recent years, ionic liquids have found a number of applications due to their unique physicochemical properties which differentiate them from other conventional organic solvents. The distinct physicochemical properties of ionic liquids include negligible low vapor pressures, melting points below room temperature, large electrochemical windows, low flammability, and high thermal stability.

## 1.2. HISTORY OF IONIC LIQUIDS

Ionic liquids have been known for a long time. The first reported ionic liquid ethylammonium nitrate was in 1914, with an observed melting point of 12 °C<sup>2,3</sup>. Recently, ionic liquids are being used extensively for various separation processes, in organo-catalysis, and as solvents in organic synthesis. In 1951, Hurley and Wier<sup>4</sup> developed the first chloroaluminate anion based RTIL for use in the low temperature plating of aluminum. The chloroaluminate based ionic liquids, however, were of limited use since they were moisture sensitive, and thereby, would decompose to form highly corrosive gas, HCl. During 1970-1980, ionic liquids, based on tetraalkylammonium cations and chloroaluminate anions, were used mostly for electrochemical applications<sup>5,6</sup>. Subsequently, RTILs were used as organic solvents in organic synthesis by Fry and Pienta<sup>7</sup>, and Boon and coworkers<sup>8</sup>. Hussey's landmark review on RTILs was published in 1983<sup>9</sup>. The early versions of room temperature ionic liquids were based on 1-ethyl-3-methylimidazolium cation and tetrafluoroborate and hexafluorophosphate anion; in general, these ionic liquids are air and water stable<sup>10</sup>. Based on these initial reports, a

large number of RTILs were subsequently synthesized that were air- and moisture tolerant. In 1998, novel ionic liquids, termed as “functionalized ionic liquids”, were reported by Davis and coworkers, based on organic cations that were extracted from the antifungal drug miconazole (**1**)<sup>11</sup> (Figure 1.2)

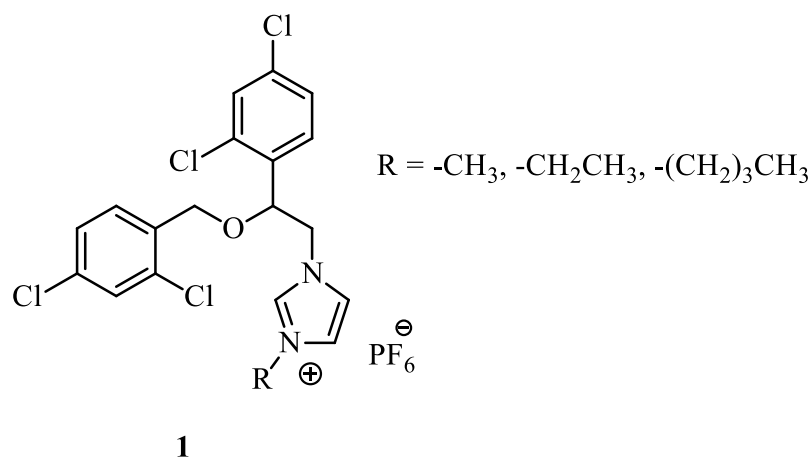


Figure 1.2. A “functionalized ionic liquid” based on the miconazole cation.

In “functionalized ionic liquids”, the functional groups are covalently bonded to either cations or anions. Thus, introduced functional groups can be used to optimize the physicochemical properties of the ionic liquids, which could be tailored to a specific application. The solvent properties of ionic liquids, including polarity, acidity, basicity, and polarizability<sup>12</sup> could be modulated by introducing these functional groups.

### 1.3. CHARACTERISTICS OF IONIC LIQUIDS

The physicochemical properties of RTILs are altered substantially based on the structures of the corresponding cations and anions. Thus, the purity of the ionic liquids is



an important issue, since the presence of even minute amounts of impurities such as water and halide anions could have deleterious effects on the properties of ionic liquids. The impact of the halide and aqueous impurities on the physical properties of RTILs was elegantly reviewed by Huddleston et al <sup>13</sup>, and Seddon et al <sup>14</sup>. It is therefore essential to carefully purify the ionic liquids, especially to remove water and halide impurities, in order to be able to measure reliable physicochemical properties.

**1.3.1. Melting Point.** Interestingly, ionic liquids with melting points up to 100 °C are often considered as RTILs. The structural features of the ionic liquids have a huge impact on the RTILs physical, physicochemical, and electrochemical properties; For example, both the nature of the cations and anions affect the melting point of the RTILs. The main factors that impact the melting points in ionic liquids are the charge distribution on the ions, hydrogen-bonding ability, the symmetry of the ions, and the van der Waals interactions with the neighboring molecules.

When comparing the melting point of ionic liquids with that of an inorganic salt (e.g., NaCl, mp 803 °C, 1-propyl-3-methylimidazolium chloride, mp 60 °C), it is clear that the substantial reduction in the melting point of the ionic liquids is due to the replacement of the small inorganic cation with large asymmetrical organic cations. This decrease in melting point due to the presence of sterically crowded asymmetric organic cations may be because the asymmetrical organic cations distort the effective packing of the ions in the crystal lattice<sup>15</sup>. However, the measured melting points of the ionic liquids are unreliable because they could undergo supercooling <sup>16,17</sup>. The melting point, in general, decreases from the methyl group to butyl and stays constant to the hexyl group, and then increases as the alkyl chain length increases<sup>18,19</sup>.

The effect of symmetry of the organic cation on the melting point of ionic liquids, based on ammonium and pyrrolidinium cations, was studied by Forsyth and coworkers (Table 1.1) <sup>20</sup>. The ionic liquid is usually a solid at room temperature, if the presence of the alkyl substituent leads to a symmetrical geometry. However, the ionic liquids remain as liquids at room temperature if the alkyl groups on cations results in an asymmetrical environment.

Table 1.1. Melting points of ammonium and pyrrolidinium bis(trifluoromethylsulfonyl)imide based ionic liquids<sup>20</sup>.

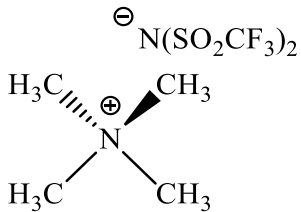
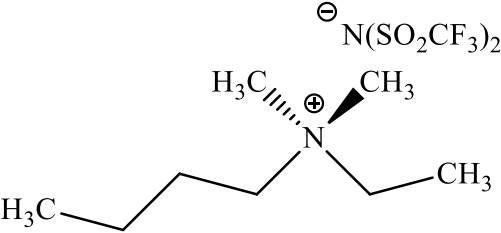
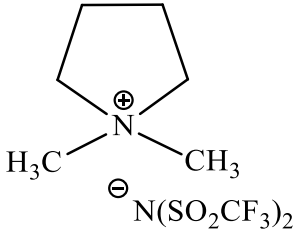
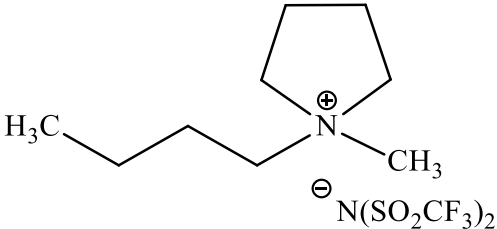
Structure	Melting Point (T <sub>m</sub> °C)
 <p>The structure shows a central nitrogen atom with a positive charge (⊕) bonded to four methyl groups (CH<sub>3</sub>). The methyl groups are arranged symmetrically: two are shown with wedged bonds (pointing up and right) and two with dashed bonds (pointing up and left). Above the nitrogen is a bis(trifluoromethylsulfonyl)imide anion (N(SO<sub>2</sub>CF<sub>3</sub>)<sub>2</sub>) with a negative charge (⊖).</p>	133
 <p>The structure shows a central nitrogen atom with a positive charge (⊕) bonded to a butyl group (H<sub>3</sub>C-CH<sub>2</sub>-CH<sub>2</sub>-CH<sub>2</sub>-), an ethyl group (-CH<sub>2</sub>-CH<sub>3</sub>), and two methyl groups (CH<sub>3</sub>). The methyl groups are shown with wedged bonds (pointing up and right). Above the nitrogen is a bis(trifluoromethylsulfonyl)imide anion (N(SO<sub>2</sub>CF<sub>3</sub>)<sub>2</sub>) with a negative charge (⊖).</p>	-8
 <p>The structure shows a five-membered pyrrolidinium ring with a positive charge (⊕) on the nitrogen atom. Two methyl groups (CH<sub>3</sub>) are attached to the nitrogen. Below the ring is a bis(trifluoromethylsulfonyl)imide anion (N(SO<sub>2</sub>CF<sub>3</sub>)<sub>2</sub>) with a negative charge (⊖).</p>	132

Table 1.1. Melting points of ammonium and pyrrolidinium bis(trifluoromethylsulfonyl)imide based ionic liquids (cont.).

 <p>The image shows the chemical structure of a pyrrolidinium cation. The nitrogen atom is positively charged and is bonded to a methyl group (CH<sub>3</sub>) and a butyl chain (H<sub>3</sub>C-CH<sub>2</sub>-CH<sub>2</sub>-CH<sub>2</sub>-CH<sub>2</sub>-). The pyrrolidinium ring is a five-membered ring containing the nitrogen atom. The counterion is a bis(trifluoromethylsulfonyl)imide anion, represented as N(SO<sub>2</sub>CF<sub>3</sub>)<sub>2</sub> with a negative charge.</p>	-18
---	-----

Similar behavior was observed in the phosphonium based ionic liquids. Thus, Seddon and coworkers synthesized a series of tetraalkylphosphonium ionic liquids with varying alkyl chain lengths, and found that tetra-*n*-hexylphosphonium hexafluorophosphate ([P<sub>6666</sub>][PF<sub>6</sub>]) ionic liquid has the highest melting point due to the presence of symmetric (C<sub>6</sub>H<sub>13</sub>)<sub>4</sub>P<sup>+</sup> cation with all substituents being *n*-hexyl groups. The melting points of the other ionic liquids in this series decrease when the alkyl chain is either increased or decreased <sup>21</sup>.

The melting points of ionic liquids can be modulated by various characteristics of anions such as charge delocalization and hydrogen bonding. Bulky anions with relatively more effective charge delocalization reduce the electrostatic attractive force between the ions and, thereby, lower the melting points. The intermolecular hydrogen bonding in the crystal lattice results in stronger packing and thus leads to an increase in melting point. RTILs with tetrafluoroborate [BF<sub>4</sub>]<sup>-</sup>, hexafluorophosphate [PF<sub>6</sub>]<sup>-</sup>, and bis(trifluoromethanesulfonyl)imide [TFSI]<sup>-</sup> anions, when compared with halogen based ionic liquids, have lower melting points due to the hydrogen bonding ability of halide anions <sup>22</sup>.

**1.3.2. Viscosity.** Viscosity of the RTILs are the largest barriers to the electrochemical application of RTILs because highly viscous RTILs will reduce the diffusion rate of the redox species; the high viscosity has a deleterious effect on the reaction rates of organic reactions. In comparison with water (1 cP at 20 °C), most of the RTILs have high viscosities, in the range of 20 cP to 30000 cP<sup>23</sup>. The selection of the anions and cations has a strong impact on the viscosity of RTILs, mostly due to the change in the intermolecular van der Waals attractions. Toduka and coworkers have analyzed the influence on the viscosity of imidazolium based ionic liquids by varying alkyl chain lengths on the anions<sup>24,25</sup>. The symmetry of the anion and its ability to form hydrogen bonds have a strong influence on the viscosity of RTILs. Hydrogen bonding between counteranions such as  $[\text{BF}_4]^-$  and  $[\text{PF}_6]^-$  lead to the formation of large complexes and an increase in viscosity.

The viscosity of RTILs also depends on the length of the alkyl groups on the cations. Viscosity of 3-alkyl-1-methylimidazolium hexafluorophosphate, bis(trifluoromethylsulfonyl)imide series ( $[\text{RMIM}][\text{PF}_6]$ , and  $[\text{RMIM}][\text{TFSI}]$ ) increase as the number of carbon atoms in the linear alkyl group increase<sup>26</sup>. Variations in viscosity of  $[\text{C}_n\text{MIM}][\text{BF}_4]$  ( $n = 2$  to  $n = 11$ ) vs increasing temperatures is shown in Figure 1.3.

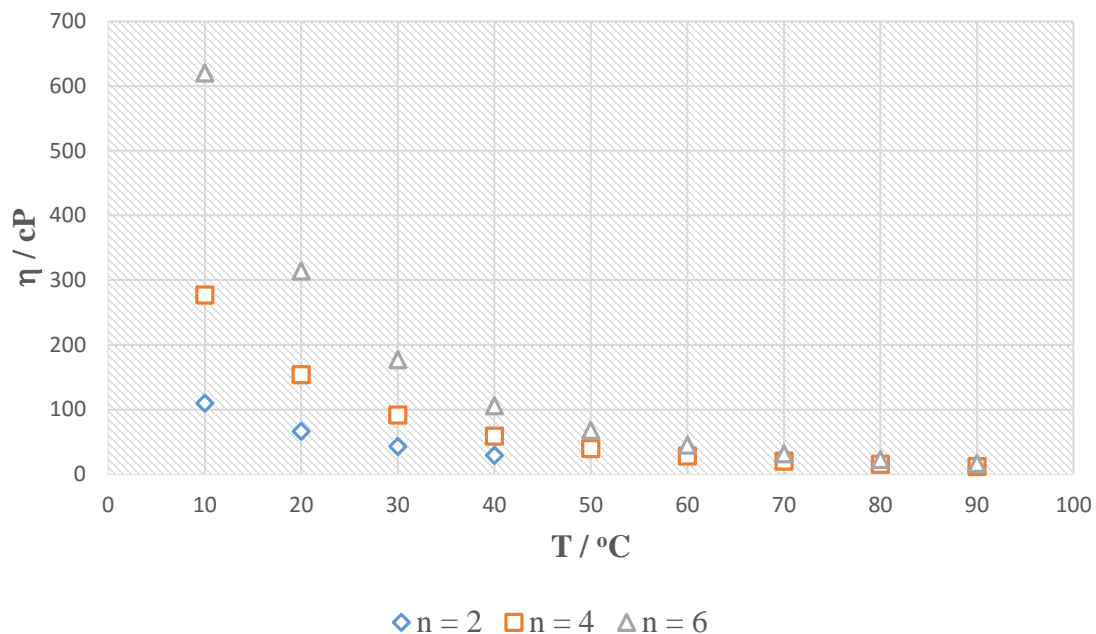
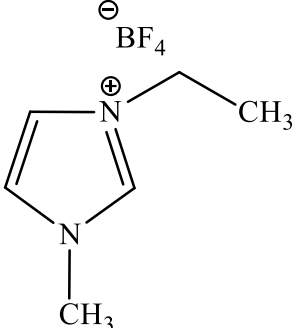
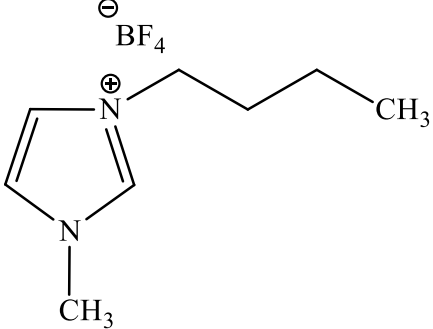
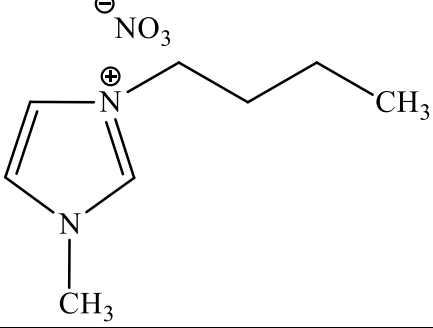
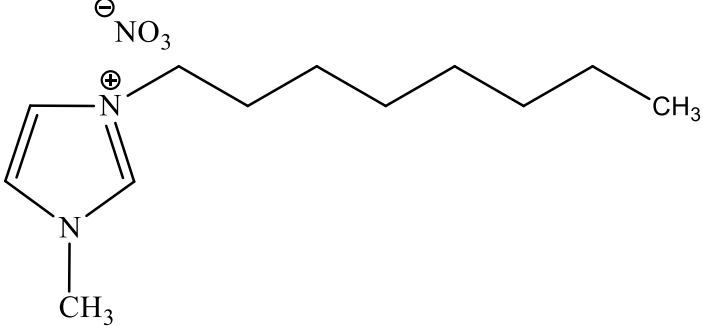


Figure 1.3. Viscosities of  $[C_nMIM][BF_4]$  ( $n = 2$  to  $n = 6$ ) vs temperature (data obtained from reference <sup>27</sup>).

Physical properties of ionic liquids are largely impacted by the presence of impurities. Marsh and coworkers studied the influence of impurities on different physicochemical properties of ionic liquids<sup>28</sup>. The influence of impurities, such as halides and water, on physicochemical properties was further investigated in detail by Seddon and coworkers<sup>29</sup>. Table 1.2 shows that even a low concentration of halides (chlorides) can increase the viscosity of the ionic liquids.

Table 1.2. Comparison of viscosities of ionic liquids with different concentrations of chloride impurities at 20 °C<sup>29</sup>.

Ionic liquid	[Cl]/mol kg <sup>-1</sup>	$\eta$ /mPa S
	0.01 1.8	66.5 92.4
	0.01 0.5	154 201
	0.02 1.7	67 222.7
	0.01 2.2	1238 8465

The high viscosity of ionic liquids imparts a major drawback to their applications. These shortcomings can be easily overcome by adding a small amount of organic solvent to drastically reduce the viscosity<sup>30</sup>.

**1.3.3. Density.** Density of the RTILs is the most measured feature and is essential for almost all applications of ionic liquids. In general ionic liquids are denser when compared with water. The molar mass of the anions have a dramatic impact on the density of ionic liquids. Thus, the bis(methanesulfonyl)amide  $[\text{Ms}_2\text{N}]^-$  based ionic liquids have lower densities, when compared with  $[\text{TFSI}]^-$  based ionic liquids<sup>31</sup>. Presence of longer alkyl chains on cation moiety leads to a decrease in the density of RTILs (Figure 1.4)<sup>28</sup>.

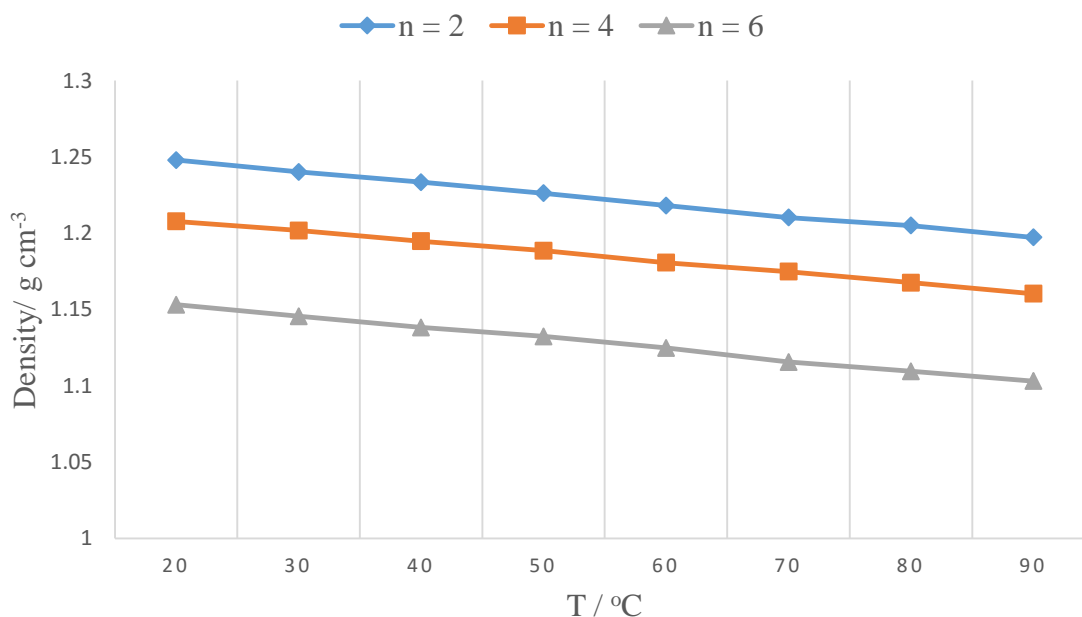


Figure 1.4. Density of  $[\text{C}_n\text{MIM}][\text{BF}_4]$  ( $n = 2-6$ ) vs temperature (data obtained from reference<sup>27</sup>).

The steric effect of longer alkyl chains prevents them from efficient close packing which, in turn, leads to lower density, whereas shorter alkyl chains pack more efficiently. As mentioned earlier, it is generally considered that the density of ionic liquids is higher than that of water, although Wilkes and coworkers demonstrated that density of some of the phosphonium based ionic liquids with various anions is lower when compared with water<sup>32</sup>. This also shows the importance of the anions on the density of ionic liquids.

Del Soto and coworkers observed that an increase in the water uptake in ionic liquids will lead to decrease in density<sup>32</sup>. Seddon and coworkers<sup>29</sup> showed that the presence of chloride impurities in the ionic liquid will lead to a nonlinear decrease in density.

**1.3.4. Thermal Stability.** Many ionic liquids have high thermal stability and the decomposition temperatures reported in the literature are about >400 °C, with minimal vapor pressure observed before the start of thermal decomposition. The thermal stability of ionic liquids relies upon the nature of the anions. Ionic liquids with highly nucleophilic and coordinating anions, such as halide anions, decompose at significantly lower temperatures. Ionic liquids with fewer nucleophilic anions such as [TFSI]<sup>-</sup>, are relatively more stable thermally<sup>33</sup>. The thermal stability of ionic liquids also depends on the type of cations. Most studies have shown that imidazolium, based ionic liquids<sup>34</sup>, are thermally more stable when compared with pyridinium<sup>25,35</sup> and tetraalkyl ammonium-based ionic liquids<sup>36,37</sup>. The methyl substitution at the C2 position on the imidazolium cation increases its thermal stability due to the absence of acidic hydrogen<sup>38-41</sup>. An increase in the alkyl chain length on cations doesn't seem to affect the thermal stability of the ionic liquids<sup>24</sup>. Phosphonium based ionic liquids have better thermal stability when compared



to ammonium based ionic liquids<sup>35,39</sup>. Two known thermal decomposition mechanisms of ionic liquids are the Hofmann elimination reaction and the reverse Menschutkin reaction. Figure 1.5 shows the scheme of a Hofmann elimination reaction.

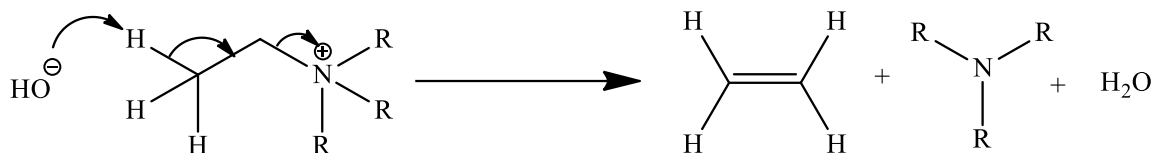


Figure 1.5. Schematic representation of Hofmann elimination.

A quaternary ammonium salt with a  $\beta$ -hydrogen atom will undergo Hofmann elimination at high temperature in the presence of a base. The imidazolium based ionic liquids with strong nucleophilic anions, such as halides, decompose by dealkylation of the relatively less sterically crowded alkyl group<sup>42,43</sup> via  $S_N2$  reaction (Figure 1.6).

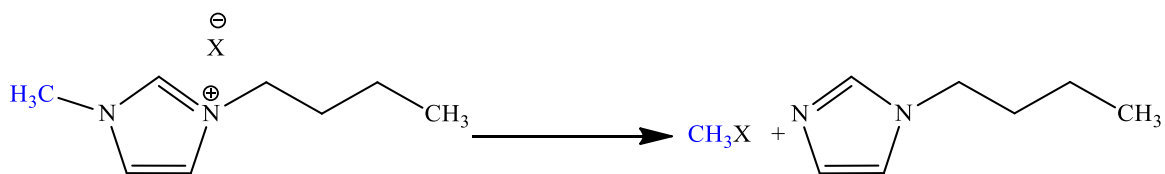


Figure 1.6. Scheme showing thermal decomposition of  $[C_4MIM][X]$ <sup>44</sup>.

Most of the thermal stability investigations of ionic liquids are performed using thermogravimetric analysis (TGA). Imidazolium based ionic liquids are found to be stable up to 450 °C<sup>45</sup>.

**1.3.5. Surface Tension.** The surface tension values (33.8 mNm<sup>-1</sup> for [C<sub>8</sub>MIM][Cl], 49.8 mNm<sup>-1</sup> for [C<sub>4</sub>MIM][PF<sub>6</sub>])<sup>46</sup> of ionic liquids were found to be higher than those for the conventional organic solvents such as methanol (22.07 mNm<sup>-1</sup>), acetone (23.5 mNm<sup>-1</sup>), and *n*-alkanes<sup>47-49</sup> (16.0 mNm<sup>-1</sup> for pentane, 25.6 mNm<sup>-1</sup> for dodecane), but lower when compared with water (71.98 mNm<sup>-1</sup>).

Freire and coworkers studied the effects of cations, anions, water, and temperature on the surface tension of ionic liquids<sup>49</sup>. They observed that both cations and anions have a dramatic influence on the surface tension of ionic liquids. An increase in the alkyl chain length for imidazolium based ionic liquids will decrease the surface tension. An increase in the size of the anion on RTILs means lower surface tension due to more effective charge dispersion and lower hydrogen bonding. The bulkier anions lead to more delocalization of the negative charge, and therefore, decrease the ability to form hydrogen bonds<sup>50</sup>. Accumulation of water in the ionic liquids leads to decreased electrostatic interactions between the ions and, thereby, results in lower surface tension.

As the temperature increases, the surface tension decreases linearly<sup>51</sup> (Figure 1.7).

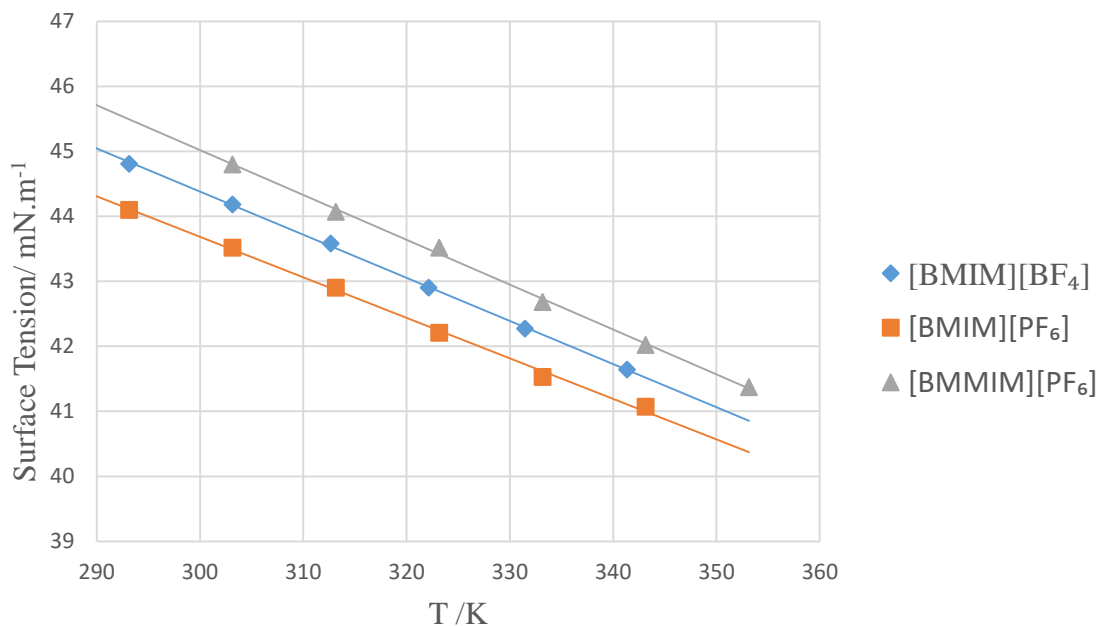


Figure 1.7. Variation in surface tension vs change in temperature for different ionic liquid (data obtained from reference <sup>46</sup>).

**1.3.6. Conductivity.** The conductivity of ionic liquids is an important property for their application as electrolytes in electrochemistry. Ionic liquids usually have large conductivities since they are mostly composed of charged ions. The room temperature ionic conductivities of ionic liquids are usually low and in the range of 0.1-18 mS/cm. The conductivity of any solution depends on the number of ions present but in case of the ionic liquids (due to the presence of the sterically crowded groups), results in lower ionic conductivities <sup>52</sup>. Table 1.3 lists conductivity values of ionic liquids compared to those of the conventional organic solvents in the presence of inorganic salt<sup>53</sup>.

Table 1.3. Comparison of viscosities and conductivities for a range of organic solvents and RTILs<sup>53</sup>.

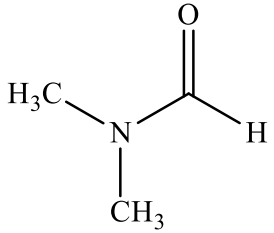
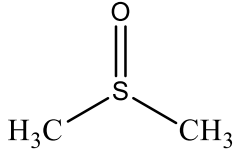
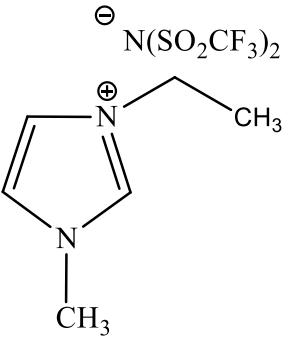
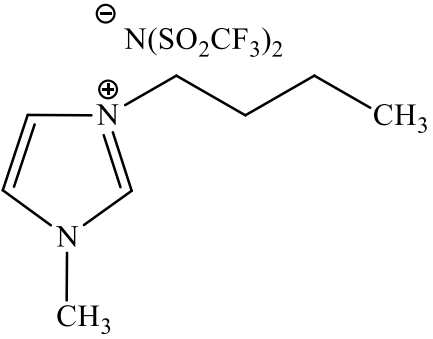
Solvent	Viscosity (mPs)	Conductivity (mΩ)
	0.794	4.0 <sup>a</sup>
CH <sub>3</sub> CN	0.345	7.6 <sup>a</sup>
CH <sub>3</sub> CH <sub>2</sub> OH	1.074	0.6 <sup>a</sup>
	1.987	2.7 <sup>a</sup>
	28	8.4
	44	3.9

Table 1.3. Comparison of viscosities and conductivities for a range of organic solvents and RTILs (cont.)

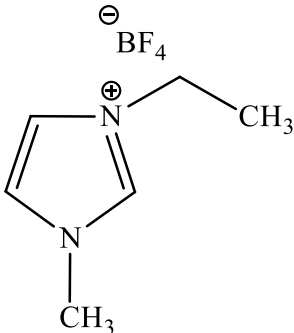
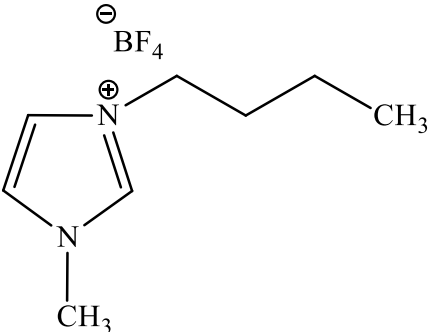
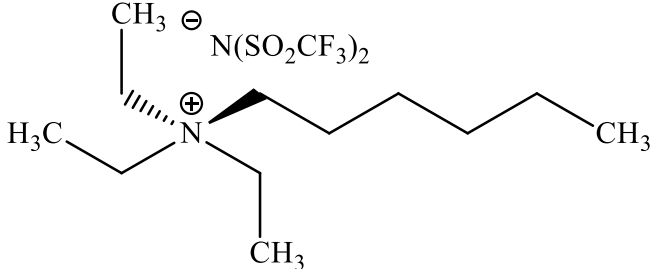
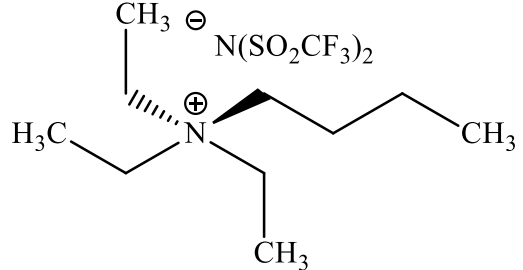
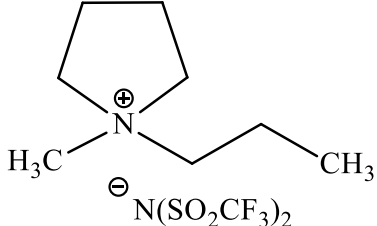
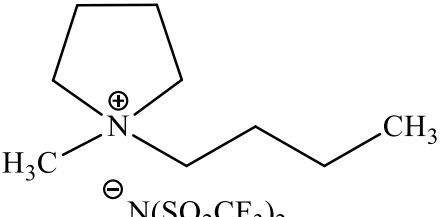
	43	13
	275	1.5
	167	0.67
	595	0.16
	63	1.4

Table 1.3. Comparison of viscosities and conductivities for a range of organic solvents and RTILs (cont.)

	85	2.2
---	----	-----

<sup>a</sup> Conductivity of organic solvent with 0.1 M tetrabutylammonium perchlorate at 22 °C.

The conductivity of most of the neat ionic liquids (i.e., without electrolyte salt) is lower when compared with conventional electrolytes (e.g., LiPF<sub>6</sub>) in organic solvents. The conductivity of ionic liquids having identical anions is found to decrease in the following order 1-alkyl-3-methylimidazolium > N,N-dialkylpyrrolidinium > tetraalkylammonium. The above conductivity order can be explained on the basis of change in cation symmetry; the planar imidazolium cation has higher conductivity than tetraalkylammonium cation, which has a tetrahedral geometry. The pyrrolidinium based ionic liquids have substituents present above and below the ring, and the nitrogen atom lies above the plane of four carbons which leads to lower conductivity values<sup>54</sup>. The conductivity of ionic liquids is highly temperature dependent and their conductivity values increase with an increase in temperature.

**1.3.7. Electrochemical Windows.** Electrochemical windows play an important role in the lithium ion batteries. Electrochemical window in lithium ion batteries is the potential range between which the electrolyte and the component electrolyte salts are neither oxidized nor reduced at the electrodes, and remain inert. Electrochemical windows of currently available common organic carbonate electrolytes have become a

limiting factor for high energy batteries. For example, currently used electrolyte in Li-ion batteries such as a mixture of ethylene carbonate (EC) and dimethyl carbonate (DMC) with  $\text{LiPF}_6$  can only support voltage up to approximately 5 V<sup>55</sup>. Ionic liquids as electrolyte solvents, have gained significant interest due to their wide electrochemical windows (5 – 6 V)<sup>56-58</sup>. Compton and coworkers reported that  $[\text{TFSI}]^-$  based ionic liquids have similar anodic limits and it is mostly due to the oxidation of the anion component of the ionic liquid<sup>59</sup>.  $[\text{TFSI}]^-$  based ionic liquids are known to have wide electrochemical windows than ionic liquids based on other anions, since ionic liquids based on  $[\text{TFSI}]^-$  anions are stable and are not susceptible to chemical or electrochemical reactions<sup>60</sup>.

The presence of impurities such as water and halides in ionic liquids has a dramatic impact on their electrochemical windows. Ionic liquids with halides ( $\text{Cl}^-$ ,  $\text{Br}^-$ ,  $\text{I}^-$ ) are more readily oxidized than  $[\text{TFSI}]^-$  based anions. Water in ionic liquids (as impurity) can be either reduced or oxidized and, hence, leads to decreases in both anodic and cathodic potential limits, which, in turn, reduces the overall electrochemical window<sup>61</sup>. Water also reacts with commonly used anions in ionic liquids such as  $[\text{BF}_4]^-$  or  $[\text{PF}_6]^-$  to form HF<sup>62</sup>.

**1.3.8. Water Miscibility.** The behavior of ionic liquids in the presence of water is of great importance since contact with water is easy and is too difficult to avoid. Ionic liquids based on  $[\text{BF}_4]^-$  and  $[\text{TFSI}]^-$  anions are insoluble in water at room temperature, whereas ionic liquids based on nitrate, ethanoate-, trifluoroacetate, and halide anions are completely miscible with water. For ionic liquids based on  $[\text{BF}_4]^-$  and  $[\text{CF}_3\text{SO}_3]^-$  anions the water miscibility depends on the chain lengths of the alkyl groups present on the cations.

Torres and coworkers showed that the water saturations of the hydrophobic ionic liquids such as [C<sub>4-8</sub>MIM][PF<sub>6</sub>] and [C<sub>6-10</sub>MIM][BF<sub>4</sub>], vary based on the sizes of the alkyl chain and the anion. They found that [PF<sub>6</sub>]<sup>-</sup> based ionic liquids dissolve less in water when compared with [BF<sub>4</sub>]<sup>-</sup> based ionic liquids and the solubility of water decreases with increasing alkyl chain length<sup>14</sup>.

Torres and coworkers further studied the hygroscopicity of different ionic liquids such as [C<sub>8</sub>MIM]Cl, [C<sub>8</sub>MIM][NO<sub>3</sub>], [C<sub>4</sub>MIM][BF<sub>4</sub>], and [C<sub>4</sub>MIM][PF<sub>6</sub>], by monitoring the absorption of water from atmospheric air at ambient room temperature as a function of time<sup>14</sup>. They found that ionic liquids based on nitrate and chloride anions absorbed more water when compared with [PF<sub>6</sub>]<sup>-</sup> anion-based ionic liquid. Hence, care must be taken when performing moisture sensitive reactions with ionic liquids by getting rid of moisture before a reaction.

**1.3.9. Flammability of Ionic Liquids.** RTILs, due to their low vapor pressure and high thermal stability are, in general, considered to be nonflammable. However, recently ionic liquids have been characterized as “combustible”, class IIIB liquids<sup>63</sup>. Smiglak and coworkers showed that a large number of commercially available RTILs are combustible. They analyzed the flammability of 20 different ionic liquids, which can be categorized into three main groups: protonated imidazolium nitrates and picrates; protonated C-nitro-substituted imidazolium nitrates and picrates; and 1-butyl-3-methylimidazolium azolates. In order to determine their combustibility, approximately 40 mg of samples were heated using a small torch flame for around 5-7 s. It was found that the rate of combustion depended on the amount of nitrogen and oxygen present. Most of the ionic liquids ignited under these conditions.<sup>63</sup>



The combustion was not complete for all of the ionic liquids; some of the tested ionic liquids burned for only a short period of time, whereas others burned rapidly.<sup>63</sup> The most rapid combustion was observed in the case of [C<sub>4</sub>MIM][4,5-dinitro-imidazolate]. RTILs have also been used as energetic materials and are being explored as hypergolic fuels<sup>64,65</sup>. Most of these energetic ionic liquids are synthesized by incorporating high energy density functional groups such as NO<sub>2</sub>, CN, and N<sub>3</sub>, in combination with high energy density anions such as [NO<sub>3</sub>]<sup>-</sup>, [ClO<sub>4</sub>]<sup>-</sup>, and [(N(CN)<sub>2</sub>)<sup>-</sup>. However, Fox and coworkers indicated that although ionic liquids are classified as flammable or nonflammable based on their flash points, it is generally accepted that the flammability hazard of a material should not be defined based on only a single flammability test<sup>66</sup>.

**1.3.10. Vapor Pressure.** RTILs have very low or even negligible vapor pressure due to the high intermolecular electrostatic interactions between the oppositely charged ions. Due to their low vapor pressure, they generate very low amounts of vapors and, hence, have very low impact on the environment. RTILs, such as [C<sub>4</sub>mim][PF<sub>6</sub>], have very low pressure (e.g., ca. 100 pPa)<sup>67</sup> at 298 K, when compared with water (3 kPa) at 298 K for H<sub>2</sub>O. Even though the RTILs have a negligibly small vapor pressure, it should not be considered as having a vapor pressure of near zero value. Earle and coworkers showed that a range of aprotic ionic liquids can be distilled and purified at 200-300 °C at low pressure (300 mbar)<sup>68</sup>.

## 1.4. IONIC LIQUID SYNTHESIS

The cation moiety of the ionic liquids is generated either by protonation of amines using an acid or through reaction of amines, phosphines, or sulfides with primary or

secondary alkyl halides. The  $S_N2$ -alkylation using the primary and secondary alkyl halides reaction is conveniently suited for the synthesis of ionic liquids due to the availability of a huge range of haloalkanes and also the reaction is irreversible at room temperature. Generally, an alkylation reaction is carried out using chloroalkanes, bromoalkanes and iodoalkanes and the reactivity of these haloalkanes follow the following order  $RI > RBr > RCl$ .

Generally, the first step (quaternization reaction) is carried out in a round bottom flask to obtain a colorless product under inert and reflux conditions. The product is then washed with either ethyl acetate or ether to remove any of the starting materials that remain. The first step is the formation of an imidazolium-based halide precursor, which undergoes either a metathesis reaction or reaction with an acid<sup>14</sup>. Both of these steps are performed at room temperature and, organic solvents are used for these reactions. These ionic liquids are either hydrophobic or hydrophilic, based on the nature of their anions. Ionic liquids with  $[PF_6]^-$  or  $[TFSI]^-$  as anions are hydrophobic and, for further purification after the final step, halide impurities are extracted using deionized water to obtain pure halide free ionic liquid. In the case of water miscible ionic liquids, the water is evaporated under high vacuum and the ionic liquid is mixed with dichloromethane and repeatedly cooled to 5 °C to obtain the desired ionic liquid. For water miscible ionic liquids formed by reaction based on the acid based method, the work-up includes the repetitive addition of water and removal of water/acid under high vacuum<sup>14</sup>.

## 1.5. RESEARCH GOALS

In the past few years, RTILs have been applied to an astounding number of areas, mainly as solvents and electrolytes. However, the main focus on the RTILs is in the energy sector. Lithium ion batteries are majorly used in the transportation industries, where safety is the main priority, and, therefore, RTILs are promising alternative electrolytes.

The goal of this work is to develop and synthesize RTILs that are stable over wide temperature range and can be used as electrochemical solvents. Focus is placed on four properties of RTILs, low viscosity, stable over wide temperature range, wide electrochemical stability, and high discharge capacities. This work also investigates the application of fluorinated ionic liquids as electrolytes in Li-O<sub>2</sub> batteries. Finally novel boron based anion receptors were synthesized and investigated for their application in Li-O<sub>2</sub> batteries.

## 2. SYNTHESIS AND ELECTROCHEMICAL PROPERTIES OF NOVEL IONIC LIQUIDS

### 2.1. INTRODUCTION

Li/CF<sub>x</sub> primary lithium batteries are composed of sub-fluorinated graphite as cathode materials and have high theoretical specific capacity and high energy density when compared with other primary lithium batteries, such as Li/MnO<sub>2</sub>, Li/SO<sub>2</sub>, or Li/SOCl<sub>2</sub><sup>69-71</sup>. The main limitation of the primary Li/CF<sub>x</sub> batteries is their low discharge performance at lower temperatures and the other common problem is the flammability of the electrolyte solvents, due to high temperatures during the discharge process which lead to explosions. The carbonate-based electrolytes that are used in these batteries are, mostly volatile and flammable and their electrochemical stability windows are relatively low<sup>72</sup>.

Room temperature ionic liquids (RTILs) have garnered a lot of interest in recent years as an alternative to carbonate based electrolytes in lithium/lithium ion batteries<sup>73-75</sup>, green synthesis<sup>76,77</sup>, and high energy density supercapacitors<sup>78-80</sup>, since they are relatively nonvolatile, less flammable or nonflammable, and have high thermal and electrochemical stabilities. Based on the favorable physicochemical and electrochemical properties of the imidazolium, piperidinium, and pyrrolidinium-based ionic liquids, they are frequently used as nonvolatile, nonflammable, and high voltage electrolyte materials for the primary lithium ion batteries<sup>74,81-83</sup>. However high viscosities and subpar low-temperature performance makes these substandard for use as a commercial solvent in batteries. The ionic liquids based on the alkoxyalkyl-side chain groups or fluoroalkyl substituents typically have relatively lower viscosities when compared to the dialkyl substituted ionic liquids<sup>84-86</sup>, while the molecular mass of the corresponding ionic liquids is slightly altered due to the presence of these substituents. Further, due to the electron

withdrawing capability of alkoxyalkyl and fluoroalkyl substituents, their HOMO-energy lowering effects<sup>55,87</sup> increase the oxidation potentials of the ionic liquid electrolytes, which complement the high voltage of the  $\text{CF}_x$  cathodes used in this study. Hence  $\beta$ -fluoroethyl- and ethoxymethyl substituents were selected, along with imidazolium and pyrrolidinium (compounds 1-6; Figure 2.1), for the synthesis of ionic liquid as electrolytes for lithium battery applications.

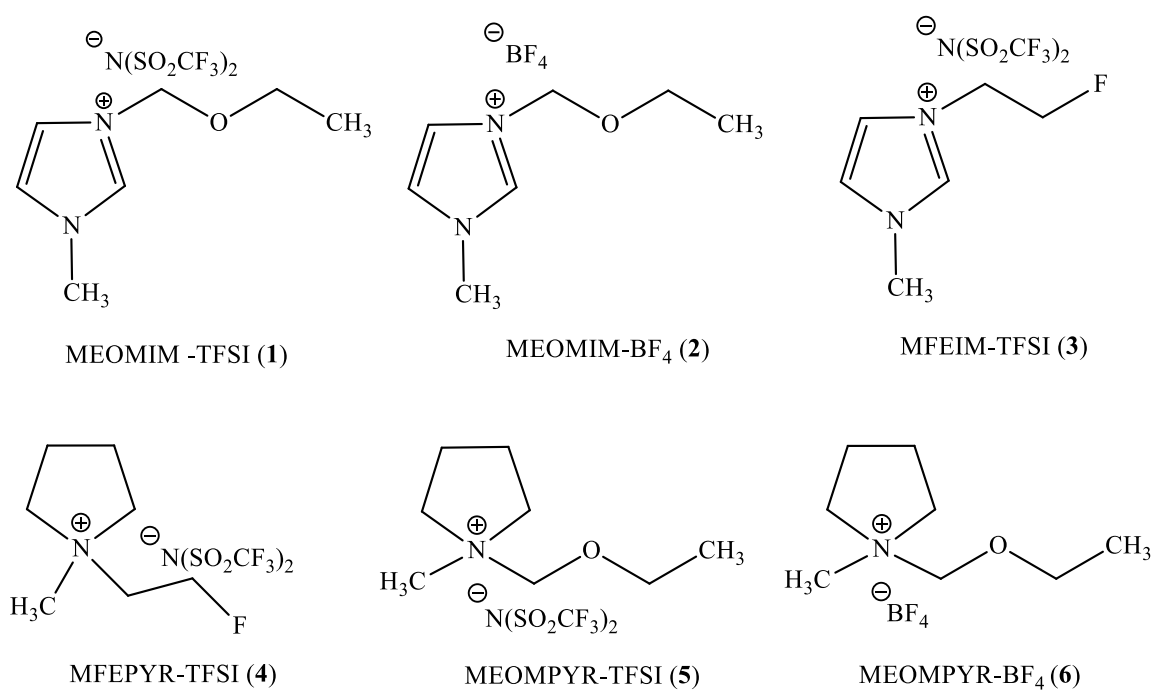


Figure 2.1. Alkoxyalkyl and fluoroalkyl-derived imidazolium and pyrrolidinium ionic liquids.

## 2.2. EXPERIMENTAL

**2.2.1. Materials and Methods.** Chloromethoxyethane (>96%) and LiTFSI (>98%) were purchased from TCI America. 4-chlorobutyronitrile (>97%) was purchased from Fisher Scientific. 3-Iodo-1,1,1-trifluoropropane (>99%) was obtained from Matrix Scientific. All other reagents, 1-methylpyrrolidine (>99%), 1-methylimidazole (>99%), diethyl ether (anhydrous, ACS certified) acetone (ACS certified, >99.5%), magnesium sulfate (anhydrous, 99.5%), silica gel (99%, 63-200 A° mesh size), acetone-*d*<sub>6</sub> were purchased from Sigma Aldrich and were used as received.

<sup>1</sup>H NMR, <sup>13</sup>C NMR, and <sup>19</sup>F NMR spectra were recorded on a INOVA-Varian 400 MHz spectrometer at 400 MHz, 100 MHz, and 376 MHz, respectively, in acetone-*d*<sub>6</sub> solvent. The chemical shifts for <sup>1</sup>H and <sup>13</sup>C NMR were referenced with respect to residual solvent signals or internal tetramethylsilane and the <sup>19</sup>F spectra were referenced to internal trichlorofluoromethane ( $\delta_{\text{CFCl}_3} = 0$ ). All the <sup>13</sup>C chemical shifts were assigned using proton coupled <sup>13</sup>C spectra. The ionic liquids with chloride or bromide counteranions are moisture sensitive and these reactions were done under an inert nitrogen atmosphere. The anion metathesis using LiTFSI was done in an aqueous solution, as the final products are insoluble in water.

Thermogravimetric analysis (TGA), using a TA Q500 instrument was conducted at a heating rate of 3 °C/min. Differential scanning calorimetry (DSC) analysis was performed using a TA Q200 instrument at a heating/cooling rate of 3 °C/min.

## 2.3. SYNTHESIS OF IONIC LIQUIDS

### 2.3.1. 1-Ethoxymethyl-3-methyl-imidazolium

**bis(trifluoromethanesulfonyl)imide (1).** To a stirred solution of chloromethoxyethane (11.2 g, 118 mmol) at 0 °C in a 50 mL round-bottom flask, 1-methylimidazole **8** (7.5 g, 91 mmol), was added drop wise under a nitrogen atmosphere, and stirred at 0 °C for 30 min, and at 50 °C for 1 h. The mixture was cooled to room temperature and washed with diethyl ether (28 mL). The product, 1-ethoxymethyl-3-methylimidazolium chloride (MEOMIM-Cl), was obtained as a light yellowish solid after filtration and drying in a high vacuum (14.73 g, 92%). The compound was used for the next step without further purification.

The above prepared 1-ethoxymethyl-3-methylimidazolium chloride **19** ((MEOMIM-Cl); 15.0g, 85 mmol) was dissolved in water and stirred with lithium bis (trifluoromethanesulfonyl) imide (23.3 g, 81 mmol) for 24 h. The product was extracted from the reaction mixture using dichloromethane and the organic layer was dried over MgSO<sub>4</sub>. The compound was eluted through a small column of silica gel for further purification. The solvent was then removed under high vacuum to give compound **1** (Figure 2.2) as an off-white viscous liquid (30.41 g, 85%); mp approximately -35 °C; *T<sub>d</sub>* ~ 405 °C; <sup>1</sup>H NMR (400 MHz, acetone-*d*<sub>6</sub>): δ 9.13 (s, 1 H imidazole-C<sub>2</sub>H), 7.81 (bs, 1 H) and 7.73 (bs, 1H) imidazole-C<sub>4,5</sub>-H, 5.69 (s, 2H, N-CH<sub>2</sub>), 4.07 (s, 3H,-N-methyl), 3.64 (q, J = 7 Hz, 2H, O-CH<sub>2</sub>), 1.16 (t, J = 7 Hz, 3H, methyl); <sup>13</sup>C (100 MHz, acetone-*d*<sub>6</sub>; <sup>1</sup>H, <sup>19</sup>F-coupled): δ 137.6 (d, J<sub>CH</sub> = 201 Hz), 123.8 (d, J<sub>CH</sub> = 205 Hz) and 121.9 (d, J<sub>CH</sub> = 203 Hz), 119.2 (q, J<sub>CF</sub> = 320 Hz), 79.6 (t, J<sub>CH</sub> = 163 Hz), 66.2 (t, J<sub>CH</sub> = 144 Hz), 36.7 (q, J<sub>CH</sub> = 143 Hz), 14.2 (q, J<sub>CH</sub> = 126 Hz); <sup>19</sup>F NMR (376 MHz, acetone-*d*<sub>6</sub>) δ -78.91(s).

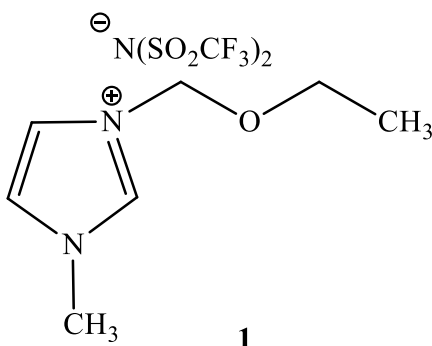


Figure 2.2. Structure of 1-Ethoxymethyl-3-methyl-imidazolium bis(trifluoromethanesulfonyl)imide.

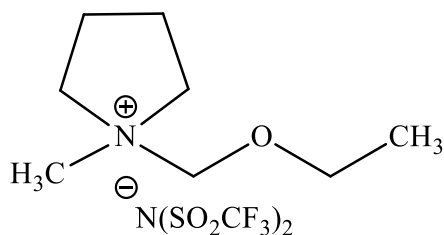
### 2.3.2. 1-Ethoxymethyl-1-methyl-pyrrolidinium

**bis(trifluoromethanesulfonyl)imide (5).** To a stirred solution of chloromethoxyethane (5.64 g, 59.7 mmol) at 0 °C in a 50 mL round bottom flask, 1-methylpyrrolidine **12** (5.0 g, 58.7 mmol) was added dropwise under a nitrogen atmosphere, and stirred at 0 °C for 30 min. The yellowish white solid obtained after 30 min was mixed with 10 mL of diethyl ether and stirred for 10 min. The 1-ethoxymethyl-1-methylpyrrolidine chloride, obtained as a yellow solid after filtration, was washed with diethyl ether (50 mL) and dried in a high vacuum (10.01 g, 95%).

The above prepared 1-ethoxymethyl-1-methyl-pyrrolidinium chloride **18** ((MEOMPYR-Cl); 6.56 g, 36.5 mmol) was dissolved in 20 mL of water and stirred with lithium bis(trifluoromethanesulfonyl)imide (10.47 g, 36.5 mmol) for 24 h at room temperature. The ionic liquid formed was extracted using dichloromethane and the organic layer was dried over MgSO<sub>4</sub>. The solvent was then removed in the presence of high vacuum to give compound **5** (Figure 2.3) as a brown viscous liquid (15.1 g, 97%);



$^1\text{H-NMR}$  (400 MHz, acetone- $d_6$ ): 4.87 (s, 2H, N-CH<sub>2</sub>-O), 3.96 (q,  $J_{\text{CH}} = 8$  Hz, 2H, O-CH<sub>2</sub>), 3.77 (m, 2H), 3.63 (m, 2H), 3.27 (s, 3H, N-CH<sub>3</sub>), 2.31 (broad d,  $J = 8$  Hz, 4H, ring -CH<sub>2</sub>-CH<sub>2</sub>),  $\delta$  1.27 (t,  $J = 8$  Hz, 3H, -CH<sub>3</sub>);  $^{13}\text{C NMR}$  (100 MHz, acetone- $d_6$ ;  $^1\text{H}$ -coupled)  $\delta$  116.0 (q,  $J_{\text{CF}} = 320$  Hz), 90.3 (t,  $J_{\text{CH}} = 165$  Hz), 69.3 (t,  $J_{\text{CH}} = 143$  Hz), 61.8 (t,  $J_{\text{CH}} = 146$  Hz), 47.5 (quartet,  $J_{\text{CH}} = 152$  Hz), 22.6 (t,  $J_{\text{CH}} = 137$  Hz), 14.4 (q,  $J_{\text{CH}} = 126$  Hz), ;  $^{19}\text{F NMR}$  (376 MHz, acetone- $d_6$ )  $\delta$  -78.83 (s).



5

Figure 2.3. Structure of 1-Ethoxymethyl-1-methyl-pyrrolidinium bis(trifluoromethanesulfonyl)imide.

### 2.3.3. 1-(3-cyanopropyl)-3-methylimidazolium

**bis(trifluoromethanesulfonyl)imide (7).** 4-chlorobutyronitrile (5.0 g, 48 mmol) was added to a stirred solution of 1-methylimidazole **8** (4g, 48 mmol) in toluene (20 mL) at room temperature. The reaction mixture was stirred for 24 h at 80 °C. The product formed in the bottom layer was removed using a Pasteur pipette and washed with ether (2 x 20 mL) to remove any starting material. The ether was then removed under vacuum using a rotary evaporator to obtain the product (4.7 g, 50%).

The above prepared 1-(3-cyanopropyl)-3-methylimidazolium chloride (4.7 g, 25 mmol) was dissolved in 30 mL of water and stirred with lithium bis(trifluoromethylsulfonyl)imide (7.2 g, 25 mmol) for 24 h at room temperature. The ionic liquid was extracted using dichloromethane, and washed with water and dried over  $\text{MgSO}_4$ . The solvent was then removed in the presence of a high vacuum to give compound **7** (9.67 g, 90%, Figure 2.4);  $^1\text{H}$  NMR (400 MHz, acetone- $d_6$ )  $\delta$  9.03 (s, 1 H), 7.77 (s, 1 H), 7.70 (s, 1 H), 4.48 (t,  $J_{\text{CH}} = 7$  Hz, 2 H), 4.03 (s, 3 H), 2.62 (t,  $J_{\text{CH}} = 7$  Hz, 2 H), 2.34 (quintet,  $J_{\text{CH}} = 7$  Hz);  $^{13}\text{C}$  NMR (100 MHz, acetone- $d_6$ ;  $^1\text{H}$ -coupled)  $\delta$  137.1 (d,  $J_{\text{CH}} = 220$  Hz), 124.4 (d,  $J_{\text{CH}} = 210$  Hz), 122.8 (d,  $J_{\text{CH}} = 210$  Hz), 120.3 (quartet,  $J_{\text{CF}} = 313$  Hz), 118.8 (s), 48.5 (t,  $J_{\text{CH}} = 144$  Hz), 36.06 (quartet,  $J_{\text{CH}} = 144$  Hz), 26.0 (t,  $J_{\text{CH}} = 133$  Hz), 13.8 (m);  $^{19}\text{F}$  NMR (376 MHz, acetone- $d_6$ )  $\delta$  -74.69(s).

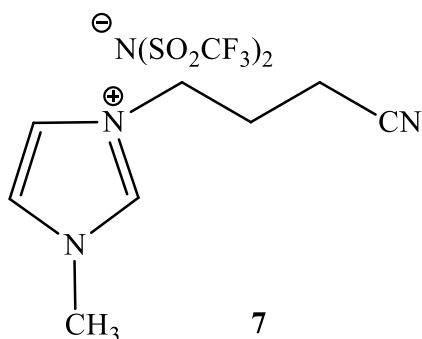


Figure 2.4. Structure of 1-(3-cyanopropyl)-3-methylimidazolium bis(trifluoromethanesulfonyl)imide.

### 2.3.4. 1-(3,3,3-trifluoropropyl)-3-methylimidazolium

**bis(trifluoromethanesulfonyl)imide (11).** 1,1,1-trifluoro-3-iodopropane (7.4 g, 33 mmol) was added to 1-methylimidazole **8** (2.7 g, 33 mmol) and the reaction mixture was stirred at 70 °C for 4 h. The resulting solid was filtered and washed with anhydrous ether to remove any unreacted starting materials. <sup>1</sup>H NMR analysis of the product indicated that it was a 1:1 mixture of compounds **9** and **10** (Figure 2.5). Recrystallization of the crude mixture from acetone/ether (10 mL), gave compound **9** as a pale yellow solid (5.0 g, 50%).

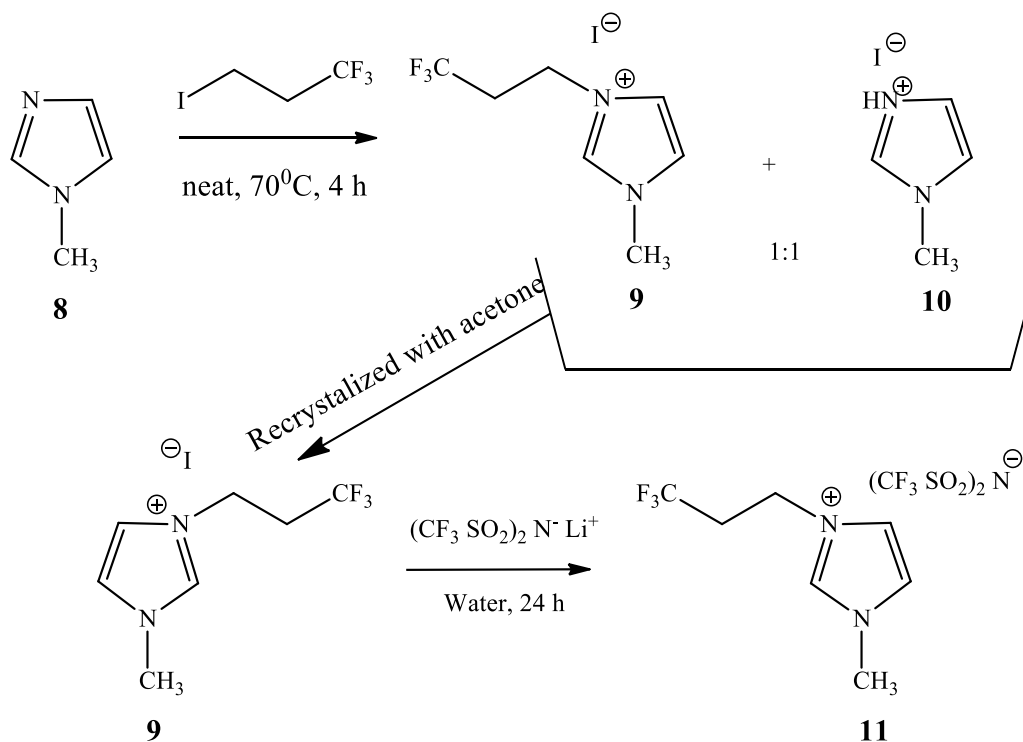


Figure 2.5. Synthesis of 1-(3,3,3-trifluoropropyl)-3-methylimidazolium bis(trifluoromethanesulfonyl) imide.

The above prepared 1-(3,3,3-trifluoropropyl)-3-methylimidazolium iodide **9** was dissolved in 20 mL of water and stirred with lithium bis(trifluoromethylsulfonyl) imide (4.7 g, 16 mmol) for 24 h at room temperature. The ionic liquid formed was extracted using dichloromethane and the organic layer was washed with water (2 x 50 mL). The organic layer was dried using MgSO<sub>4</sub>, and solvent was removed under reduced pressure using a rotary evaporator. Removal of the residual solvent in a high vacuum (4 h) gave product **11** as a yellow viscous liquid: (7 g, 93%); <sup>1</sup>H NMR (400 MHz, acetone-*d*<sub>6</sub>) δ 9.13 (s, 1 H), 7.87 (s, 1 H), 7.74 (s, 1 H), 4.73 (t, J<sub>CH</sub> = 7.0 Hz, 2 H), 4.07 (s, 3 H); <sup>13</sup>C NMR 100 MHz, acetone-*d*<sub>6</sub>; <sup>1</sup>H, <sup>19</sup>F-coupled) δ 138.0 (d, J<sub>CH</sub> = 220 Hz), 126.8 (quartet, <sup>1</sup>J<sub>CF</sub> = 275 Hz), 125.1 (d, J<sub>CH</sub> = 203 Hz), 123.7 (d, J<sub>CH</sub> = 200 Hz), 121.0 (d, J<sub>CF</sub> = 319 Hz), 43.8 (dt, J<sub>CH</sub> = 149 Hz, <sup>3</sup>J<sub>CF</sub> = 8 Hz), 36.8 (quartet, J<sub>CH</sub> = 144 Hz), 34.5 (overlapping doublets, <sup>2</sup>J<sub>CF</sub> = 29 Hz, <sup>2</sup>J<sub>CH</sub> = 4 Hz); <sup>19</sup>F NMR (376 MHz, acetone-*d*<sub>6</sub>) δ -64.85 (t, J<sub>HF</sub> = 10 Hz), -78.75(s).

### 2.3.5. 1-(3,3,3-trifluoropropyl)-1-methylpyrrolidinium

**bis(trifluoromethanesulfonyl)imide (14).** 1,1,1-trifluoro-3-iodopropane (2.6 g, 1.2 mmol) was added to 1-methylpyrrolidine **12** (1 g, 1.2 mmol) and the reaction mixture was stirred at room temperature for 1 h. The resulting pale yellow solid was filtered and washed with anhydrous ether. <sup>1</sup>H NMR analysis of the product indicated that it exclusively formed 1-H-1-methylpyrrolidinium iodide **13** instead of the expected product, 1-(3,3,3-trifluoropropyl)-1-methylpyrrolidinium iodide **14** (Figure 2.6). <sup>1</sup>H NMR (400 MHz, acetone-*d*<sub>6</sub>) δ 3.4 (broad s, 4 H), 2.9 (s, 3 H), 2.15 (m, 4H); <sup>13</sup>C NMR 100 MHz, acetone-*d*<sub>6</sub>; <sup>1</sup>H-coupled) δ 54.9 (t, J<sub>CH</sub> = 145 Hz), 39.7 (quartet, J<sub>CH</sub> = 142 Hz), 23.5 (t, J<sub>CH</sub> = 136 Hz).

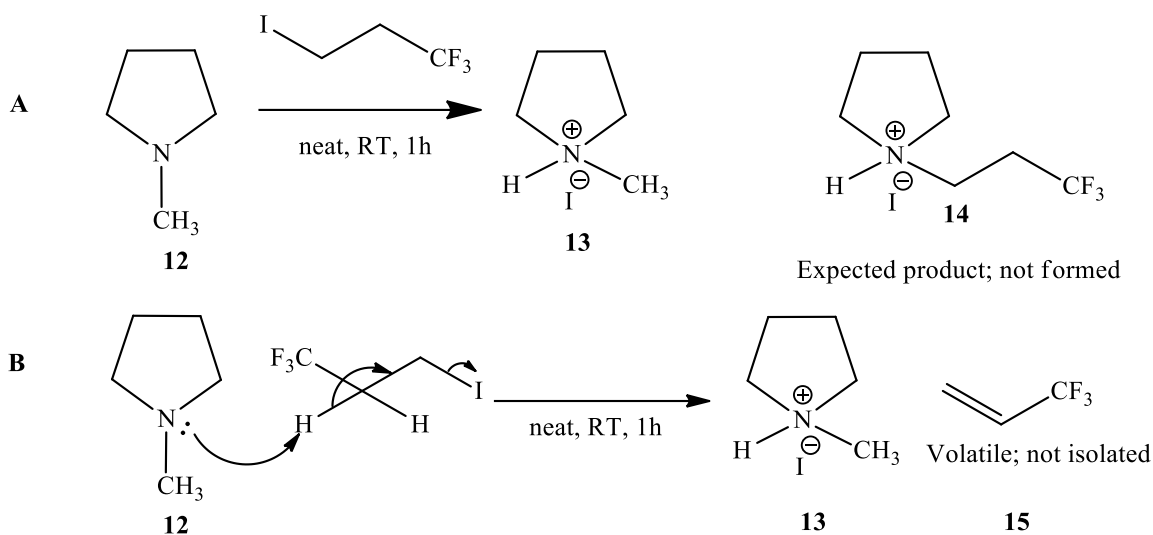


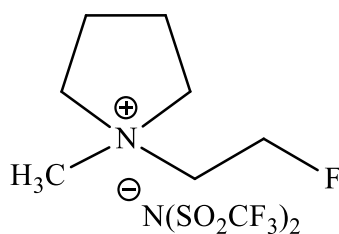
Figure 2.6. A) Synthesis of 1-(3,3,3-trifluoropropyl)-1-methylpyrrolidinium bis(trifluoromethanesulfonyl)imide, B) Predicted mechanism of formation of the unexpected elimination product.

### 2.3.6. 1-(2-fluoroethyl)-1-methylpyrrolidinium

**bis(trifluoromethanesulfonyl)imide (4).** 1-bromo-2-fluoroethane (6.55 g, 51.61 mmol) was added dropwise, in 30 min, to a stirred solution of 1-methylpyrrolidine **12** (4.37 g, 51.41 mmol) at 0 °C, in an inert atmosphere. To the white solid obtained, diethyl ether (10 mL) was added and stirred for 10 min. The 1-(2-fluoroethyl)-1-methylpyrrolidinium bromide **16**, obtained as a white solid after filtration, was washed with diethyl ether (50 mL) and dried in a high vacuum (yield 8.74 g, 81.18%).

Lithium bis(trifluoromethanesulfonyl)imide (11.90 g, 41.45 mmol) was dissolved in 20 mL of water and added drop wise to an aqueous solution of 1-(2-fluoroethyl)-1-methylpyrrolidinium bromide **4** (8.75 g, 41.23 mmol). The product layer was washed with water and extracted using dichloromethane solvent and dried ( $\text{MgSO}_4$ ). Removal of solvent in a high vacuum gave product **4** (Figure 2.7) as a viscous liquid (14.0 g, 82.2%);

$^1\text{H}$  NMR (400 MHz, acetone- $d_6$ ):  $\delta$  5.15 (m,  $J = 3.2$  Hz 1H -CH<sub>2</sub>-F) 5.03 (m,  $J = 3.2$  Hz 1H -CH<sub>2</sub>-F), 3.98 (t,  $J = 4$  Hz 1H-N-CH<sub>2</sub>-), 4.05 (t,  $J = 4$  Hz 1H-N-CH<sub>2</sub>-), 3.8 (m, 4H ring -CH<sub>2</sub>-N-), 3.3 (s, 3H-N-CH<sub>3</sub>), 2.35 (m, 4H ring-CH<sub>2</sub>-CH<sub>2</sub>-).  $^{13}\text{C}$ -NMR ( $^1\text{H}$  coupled) (100 MHz, acetone- $d_6$ ;  $^1\text{H}$ ,  $^{19}\text{F}$ -coupled)  $\delta$  120.33 (q,  $J_{\text{CF}} = 320$  Hz), 78.5 (qm,  $J_{\text{CH}} = 154$  Hz), 65.46 (t,  $J_{\text{CH}} = 148$  Hz), 64.12 (t,  $J_{\text{CH}} = 125$  Hz), 48.89 (tm,  $J_{\text{CH}} = 145$  Hz), 21.47 (t,  $J_{\text{CH}} = 134$  Hz).  $^{19}\text{F}$  NMR (376 MHz, acetone- $d_6$ )  $\delta$  -218.37 (m,  $J = 26.32$  Hz, F-CH<sub>2</sub>), -78.85 (s, TFSI)



4

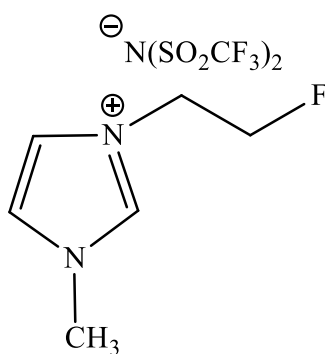
Figure 2.7. Structure of 1-(2-fluoroethyl)-1-methylpyrrolidinium bis(trifluoromethanesulfonyl)imide.

### 2.3.7. 1-(2-fluoroethyl)-3-methylimidazolium

**bis(trifluoromethanesulfonyl)imide (3).** To a stirred solution of 1-bromo-2-fluoroethane (10.85 g, 85 mmol) at 0 °C in a 50 mL round bottom flask, 1-methylimidazole.**8** (7 g, 85 mmol), was added drop wise in an inert atmosphere. The reaction mixture was stirred at 0 °C for 30 min, and at 50 °C in a water bath for 15 h. The reaction mixture was cooled to room temperature and washed with diethyl ether (28 mL).

Compound **17** was obtained as a light yellow solid after filtration, purification, and drying in high vacuum (15.33 g, 86.3%).

The yellow solid was dissolved in water and stirred with lithium bis(trifluoromethanesulfonyl)imide (23.30 g, 81 mmol) for 15 h. The product was extracted from the reaction mixture using dichloromethane. The organic layer was dried ( $\text{MgSO}_4$ ), and the solvent removed in high vacuum to give compound **3** (Figure 2.8) as an off-white viscous liquid (69%, 58.4 mmol).  $^1\text{H}$  NMR (400 MHz, acetone- $d_6$ ):  $\delta$  9.07 (s, 1H-imidazole), 7.77 (apparent dd, 1H-imidazole), 4.97 (dd,  $J = 80$  Hz, F-  $\text{CH}_2$ ), 4.85 (dd,  $J = 80$  Hz, F-  $\text{CH}_2$ ), 4.79 (dd,  $J = 80$  Hz, N-  $\text{CH}_2$ ), 4.72 (dd,  $J = 80$  Hz, N-  $\text{CH}_2$ ), 4.10 (s, -N-methyl);  $^{13}\text{C}$ -NMR (100 MHz, acetone- $d_6$ ;  $^1\text{H}$ ,  $^{19}\text{F}$ -coupled)  $\delta$  137.80 (d,  $J_{\text{CH}} = 223$  Hz), 124.26 (d,  $J_{\text{CH}} = 199$  Hz), 123.2 (d,  $J_{\text{CH}} = 200$  Hz), 120.33 (q,  $J_{\text{CF}} = 320$  Hz) 82.31 (qd,  $J_{\text{CH}} = 152$  Hz, 16 Hz), 50.85 (dt,  $J_{\text{CH}} = 142$  Hz, 31 Hz), 36.66 (qt,  $J_{\text{CH}} = 143$  Hz);  $^{19}\text{F}$  NMR (376 MHz, acetone- $d_6$ )  $\delta$ -223.29 (m,  $J = 45$  Hz, F-  $\text{CH}_2$ ), 78.91 (s, TFSI),



**3**

Figure 2.8. Structure of 1-(2-fluoroethyl)-3-methylimidazolium bis(trifluoromethanesulfonyl)imide.

### 2.3.8. 1-Ethoxymethyl-3-methyl-imidazolium tetrafluoroborate (2).

To a stirred solution of chloromethoxyethane (7.7 g, 81 mmol) at 0 °C in a 50 mL round bottom flask, 1-methylimidazole **8** (5 g, 61 mmol), was added drop wise in an inert atmosphere. The reaction mixture was continuously stirred, at 0 °C for 30 min. The solid precipitated was stirred at 50 °C in a water bath for 1 h. The mixture was cooled to room temperature and washed with diethyl ether (28 ml). A light yellowish solid was obtained after filtration, purification, and drying in high vacuum (10.11 g, 94%). The yellowish solid (10 g, 56 mmol) was dissolved in acetone and stirred with NaBF<sub>4</sub> (6.91 g, 63 mmol) for 48 h. The reaction mixture was filtered and filtrate was passed through magnesium sulfate to remove water. The compound was then passed through a silica gel column and concentrated using a rotary evaporator and high vacuum. Compound **2** (Figure 2.9) was obtained as a yellowish viscous liquid (95%, 14.12 g)

<sup>1</sup>H NMR (400 MHz, acetone- *d*<sub>6</sub>): δ 8.9 (s, 1H-imidazole), 7.7 ( apparent dd, 1H-imidazole), 7.7 (apparent dd, 1H-imidazole), 5.6 (s, 2H, N- CH<sub>2</sub>), 4.0 (s, 3H-N-methyl), 3.6 (q, J = 7.0 Hz , 2H, O-CH<sub>2</sub>), 1.1 (t, J = 7.0 Hz, 3H, methyl ) ; <sup>13</sup>C-NMR (<sup>1</sup>H coupled) (100 MHz, acetone- *d*<sub>6</sub>; <sup>1</sup>H-coupled) δ 137.6 (d, J<sub>CH</sub> = 216 Hz), 124.9 (d, J<sub>CH</sub> = 216 Hz), 122.5 ( dm, J<sub>CH</sub> = 209 Hz), 79.4 (t, J<sub>CH</sub> = 165 Hz), 66 .1 ( tq, J<sub>CH</sub> = 147 Hz, 6 Hz), 36.6 (q, J<sub>CH</sub> = 143 Hz), 14.9 (qt, J<sub>CH</sub> = 126 Hz, 3 Hz); <sup>19</sup>F NMR (376 MHz, acetone- *d*<sub>6</sub>) δ -149.7.



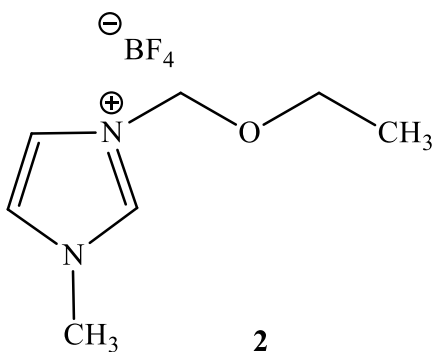


Figure 2.9. Structure of 1-ethoxymethyl-3-methyl-imidazolium tetrafluoroborate.

### 2.3.9. 1-Ethoxymethyl-1-methyl-pyrrolidinium tetrafluoroborate (**6**).

Chloromethoxyethane (5.64 g, 59.7 mmol) was added drop wise, in 30 minutes, to a stirred solution of 1-methylpyrrolidine **12** (5.0 g, 58.7 mmol) at 0 °C, under inert atmosphere. To the yellowish white solid immediately obtained on mixing the reagents, diethyl ether (10 mL) was added and stirred for 10 min. The 1-ethoxymethyl-1-methylpyrrolidine chloride was obtained as a yellow solid after filtration, was washed with diethyl ether (50 mL), and dried in high vacuum (10.25 g, 97.6%).

The 1-ethoxymethyl-1-methylpyrrolidine chloride **18** (55.7 mmol, 10.01 g) was dissolved in acetone (10 mL) in a 50 mL round bottom flask and a solution of NaBF<sub>4</sub> (58.7 mmol, 6.44 g) in acetone (10 mL) was added. This mixture was stirred at room temperature for 14 h. The reaction mixture was filtered and the filtrate was dried using anhydrous magnesium sulfate. The solution was again filtered to remove magnesium sulfate and excess solvent was removed using a rotary evaporator. The residual oil obtained was washed with ether three times (3 x 25 mL) and dried under high vacuum. Compound **6** (Figure 2.10) was obtained as a yellowish viscous liquid (86 %).

$^1\text{H-NMR}$  (400 MHz, acetone- $d_6$ )  $\delta$  4.8 (s, 2H, N-CH<sub>2</sub>-O),  $\delta$  3.9 (q, 2H, O-CH<sub>2</sub>,  $J_{\text{CH}} = 8$  Hz),  $\delta$  3.75 (m, 2H, diastereotopic H),  $\delta$  3.64 (m, diastereotopic 2H),  $\delta$  3.25 (s, N-CH<sub>3</sub>, 3H),  $\delta$  2.3 (apparent dd, 4H, ring -CH<sub>2</sub>-CH<sub>2</sub>-,  $J_{\text{CH}} = 10$  Hz, 8 Hz),  $\delta$  1.24 (t, 3H,  $J = 4$  Hz);  $^{13}\text{C NMR}$  (100 MHz, acetone- $d_6$ ;  $^1\text{H}$ -coupled)  $\delta$  90.1 (t,  $J_{\text{CH}} = 162$  Hz), 69.2 (tq,  $J_{\text{CH}} = 144$  Hz, 5 Hz), 61.4 (t,  $J_{\text{CH}} = 146$  Hz), 47.5 (q,  $J_{\text{CH}} = 143$  Hz), 22.6 (t,  $J_{\text{CH}} = 135$  Hz), 15.1 (qt,  $J_{\text{CH}} = 126$  Hz, 3 Hz);  $^{19}\text{F NMR}$  (376 MHz, acetone- $d_6$ )  $\delta$  -150 Hz (BF<sub>4</sub>).

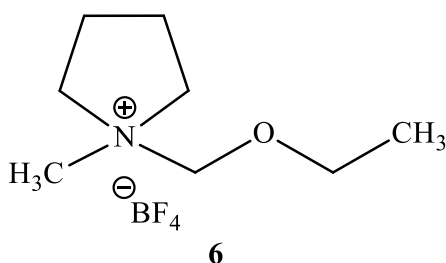


Figure 2.10. Structure of 1-ethoxymethyl-1-methyl-pyrrolidinium tetrafluoroborate.

## 2.4. RESULTS AND DISCUSSION

**2.4.1. Synthesis.** A series of imidazolium and pyrrolidinium based ionic liquids containing monofluoroethyl, ethoxymethyl, 1-cyanopropyl, and 3,3,3-trifluoropropyl substituents were synthesized. 1-Methylimidazole and 1-methylpyrrolidine were reacted with corresponding alkyl, fluoroalkyl, cyanoalkyl, and alkoxy halides and the resulting halide salts were metathesized with lithium bis(trifluoromethylsulfonyl)imide (LiTFSI) and sodium tetrafluoroborate (NaBF<sub>4</sub>) to give TFSI and tetrafluoroborate based salts, respectively (Figures 2.11 and 2.12), using a modified procedure<sup>88,89</sup>. These ionic liquids were obtained as liquids at room

temperature after silica gel purification and drying in vacuum, and were characterized by  $^1\text{H}$ ,  $^{13}\text{C}$ , and  $^{19}\text{F}$  NMR spectroscopy.

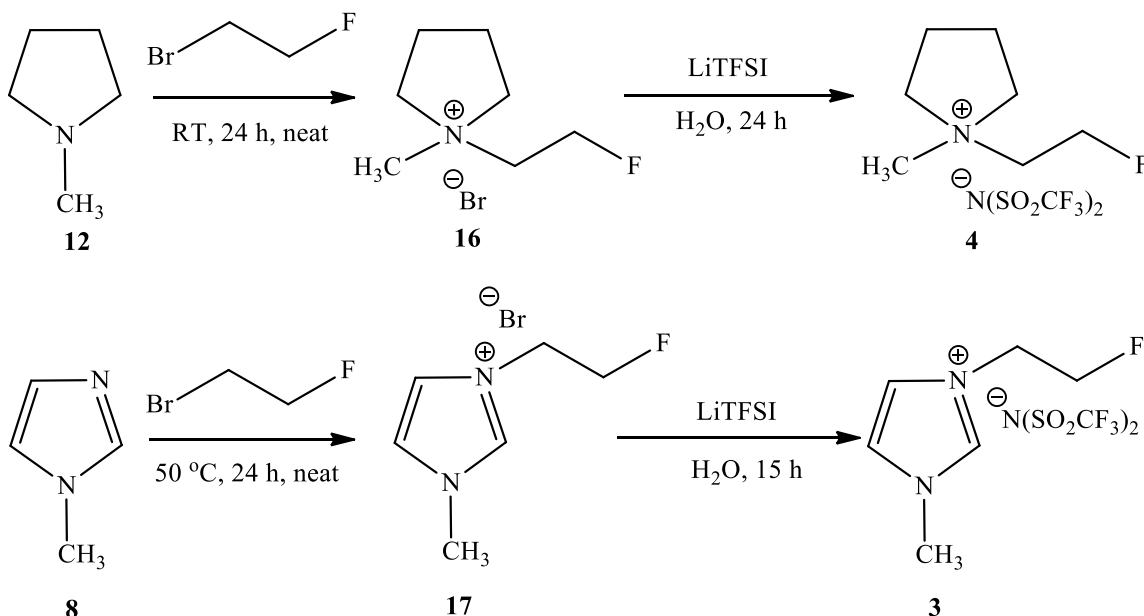


Figure 2.11. Synthesis of 1-methyl-1-fluoroethylpyrrolidinium and 1-methyl-3-fluoroethylimidazolium bis(trifluoromethylsulfonyl)imide ionic liquids.

The melting points of these ionic liquids were dependent on the nature of the counter-anions; bis(trifluoromethanesulfonyl)imide [TFSI]<sup>-</sup> anions were lower when compared with their tetrafluoroborate [BF<sub>4</sub>]<sup>-</sup> analogues. Differential scanning calorimetry (DSC) analysis was done in collaboration with Contour energy systems for these ionic liquids showing a wide liquid range for these materials.

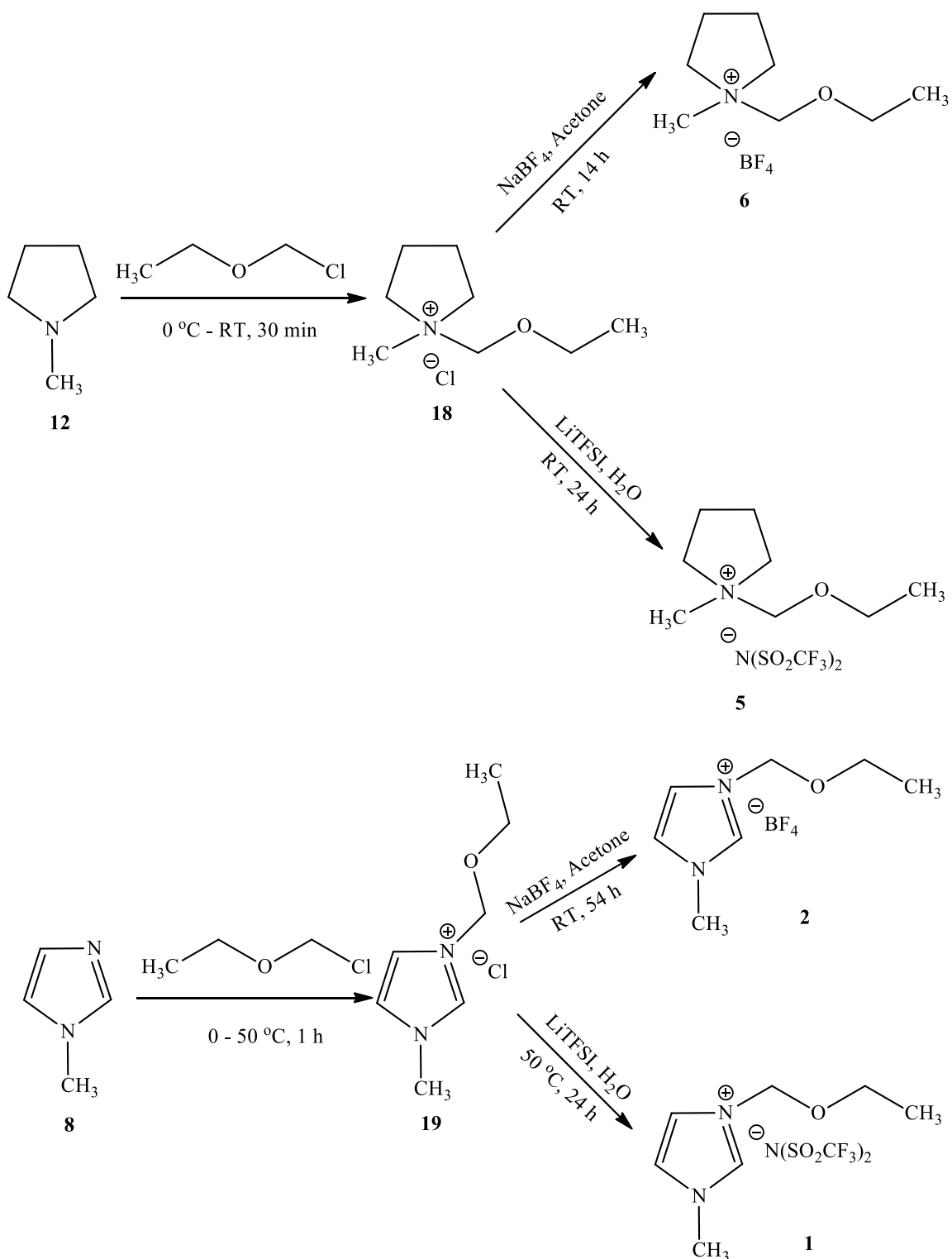


Figure 2.12. Synthesis of 1-methyl-1-ethoxymethylpyrrolidinium and 1-methyl-3-ethoxymethylimidazolium bis(trifluoromethylsulfonate) ionic liquids.

**2.4.2. Thermal Stability.** Figure 2.13 shows the Thermogravimetric analysis (TGA) plot of 1-trifluoropropyl-3-methylimidazolium bis(trifluoromethanesulfonyl)imide. In general, [TFSI]<sup>-</sup> based ionic liquids are found to be thermally more stable when compared with their corresponding [BF<sub>4</sub>]<sup>-</sup> analogues. MEOMIM-BF<sub>4</sub> is stable up to 200 °C, while MEOMPYR-BF<sub>4</sub> starts to decompose at 50 °C. When comparing [TFSI]<sup>-</sup> anion containing ionic liquids, alkoxyalkyl-derived ionic liquids (MEOMIM-TFSI and MEOMPYR) are stable up to 200 °C, while the fluoroalkyl derived ionic liquids (MFEIM-TFSI and MFEPYR-TFSI) have a greater thermal stability up to 350 °C. In general, the ether-functionalized imidazolium-based ionic liquids have relatively lower thermal stabilities when compared with their alkyl-side chain derived ionic liquids. These high thermal stabilities and nonvolatile characteristics of ionic liquids are favorable for the batteries to operate under high temperatures.

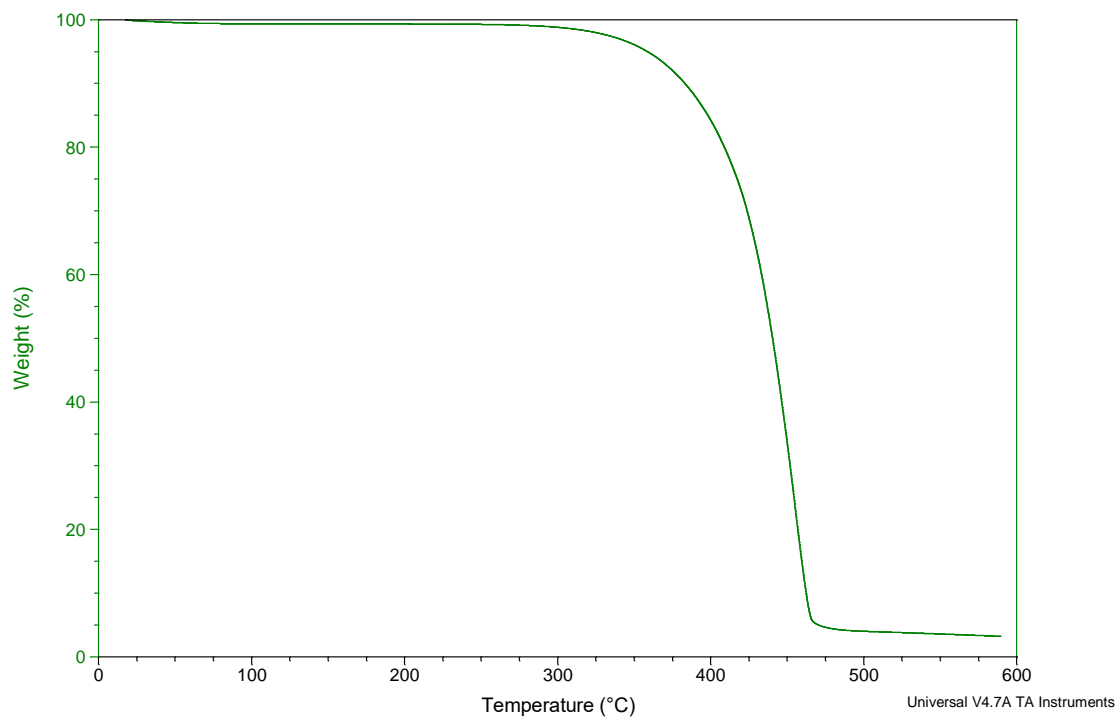


Figure 2.13. Thermogravimetric analysis of 1-trifluoropropyl-3-methylimidazolium bis(trifluoromethanesulfonyl)imide ( $T_d = 423$  °C).

Further DSC studies were done at contour energy systems by Dr. T.A. Arunkumar and Dr. Simon C. Jones for these ionic liquids (compound **1-6**) and their corresponding Li salts mixtures which showed no melting/freezing behavior up to  $-60$  °C <sup>45</sup>.

**2.4.3. Electrochemical Studies.** Electrochemical studies, such as ionic conductivity, electrochemical stability, and cell discharge studies, were done in collaboration with Dr. T.A.Arunkumar and Dr. Simon C. Jones at Contour energy systems<sup>45</sup>. The ionic conductivity for these RTILs (compound **1-6**) was in the range of 3-5 mScm<sup>-1</sup>. The ionic liquids (compound **1-6**) mixed with their corresponding Li-salt have lower ionic conductivities due to the increase in viscosity. Electrochemical stabilities of the neat ionic liquids (compound **1-6**) were analyzed using voltammetry in collaboration

with Contour energy systems<sup>45</sup>. Among ionic liquids with [TFSI]<sup>-</sup> anions, the pyrroldinium based have most electrochemical stability windows than their imidazolium based analogues. Among the alkoxyalkyl group based ionic liquids, MEOMPYR-TFSI has the widest stability window of 6.2 V and for the fluoroalkyl-derived ionic liquid, MFEPYR-TFSI, has the highest electrochemical window of 5.7 V.

Cell performance studies were done in Li/CF<sub>x</sub> primary battery system using 2016 coin cells in collaboration with Contour energy systems<sup>45</sup>. Most of these ionic liquids showed high discharge capacities (>700 mAh g<sup>-1</sup>), even at low discharge rates (~C/100) and were comparable to the conventional carbonate-based electrolytes<sup>45</sup>.

These ionic liquids (compound **1-6**) were further analyzed by our group member Ninu Madria for their toxicity to human health and were found to be relatively non-toxic when compared with the corresponding lithium salt, LiTFSI<sup>45</sup>.

## **2.5. FLUORINATED IONIC LIQUID IN LITHIUM/OXYGEN BATTERY**

**2.5.1. Introduction.** Lithium (Li) air batteries were first reported in the year 1996<sup>90</sup>, but due to various limitations related to lithium air batteries they were of limited interest. In the last decade, due to increased demand for batteries with high energy density for application in electric vehicles, as well as the development of new electrode materials and electrolytes, have intensified the research interest in this area.

Although the term Li-air battery is commonly used, most of the laboratories use a pure oxygen environment since the presence of H<sub>2</sub>O and CO<sub>2</sub> might degrade the performance of a battery. However, the long term goal is to develop a true Li-air battery which is only possible if a selective membrane is developed which only allows permeation of oxygen.

In a Li-O<sub>2</sub> battery the oxidation of lithium at a metal electrode and reduction of oxygen at the air electrode, generates current flow. The main advantage of the Li-O<sub>2</sub> battery is its high energy density when compared with currently used energy alternatives such as a Li-ion battery and gasoline power. This advantage in energy density (compared with others) is mainly due to the use of oxygen from the air, avoiding the need to store oxygen at the air electrode. As shown in Figure 2.14, the theoretical energy density of

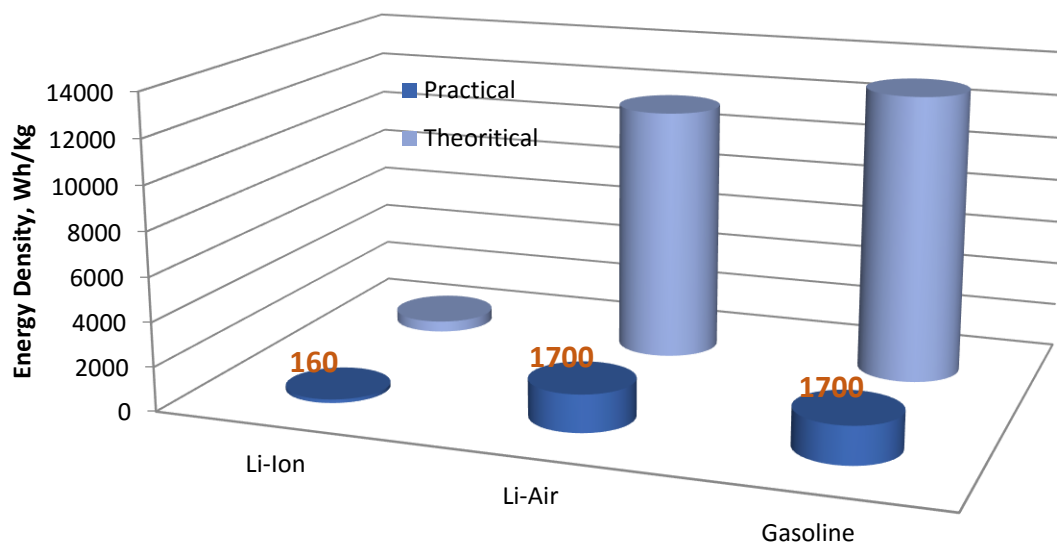


Figure 2.14. Gravimetric energy densities (W·h/kg) for various types of rechargeable batteries compared to gasoline. For Li-air, the practical value is just an estimate <sup>91</sup>.

gasoline is almost comparable with that of the Li-O<sub>2</sub> battery. Although the practical energy densities of the Li-O<sub>2</sub> battery and gasoline are same, the energy density of Li-O<sub>2</sub> battery depends on the porosity of the air electrode and the electrolytes used on the air



electrode side <sup>92</sup>. The discharge reaction at the cathode leads to formation of Li<sub>2</sub>O<sub>2</sub> or Li<sub>2</sub>O as depositions on the carbon surface and the pores of the electrode. Electrolyte formulation has a large influence on oxygen solubility, oxygen transport, and the deposition process of carbon electrodes and thus, in turn, affects the discharge capacity and mAh/mL O<sub>2</sub> ratio. J Read and coauthors showed that increasing the oxygen concentration in electrolytes would mean an increase in discharge capacity and, also, decreasing the electrolyte viscosity would lead to an increase in discharge capacity <sup>93</sup>. Perfluorochemicals are well known as oxygen carriers in the fields of medicine and biotechnology due to the high solubility of oxygen <sup>94</sup>. Hence, based on the above facts, perfluorohexyl and perfluoroethyl groups were selected with imidazole to synthesize ionic liquids for their application as electrolytes for Li-O<sub>2</sub> batteries.

**2.5.2. Materials and Methods.** 1-Iodo-1H,1H,2H,2H-perfluorooctane (>95 %), 1,1,1,2,2-pentafluoro-4-iodobutane (>97%) and LiTFSI (>95%) were purchased from Oakwood products, Inc. All other reagents, 1-bromobutane (>98%), 1-methylimidazole (>99%), magnesium sulfate (anhydrous, 99.5%), alumina (neutral, 80-200 mesh), dichloromethane (ACS certified, >99.8%), ethyl acetate (ACS certified), toluene (ACS certified), and acetone-*d*<sub>6</sub> were purchased from Sigma Aldrich and were used as received.

<sup>1</sup>H NMR, <sup>13</sup>C NMR, and <sup>19</sup>F NMR spectra were recorded on a INOVA-Varian 400 MHz spectrometer at 400 MHz, 100 MHz, and 376 MHz, respectively in acetone-*d*<sub>6</sub> solvent. The chemical shifts for <sup>1</sup>H and <sup>13</sup>C NMR were referenced with respect to residual solvent signals or internal tetramethylsilane, and the <sup>19</sup>F spectra were referenced to internal trichlorofluoromethane ( $\delta_{\text{CFCl}_3} = 0$ ). All <sup>13</sup>C chemical shifts were assigned using

proton coupled  $^{13}\text{C}$  spectra. The ionic liquids with iodide or bromide counteranions are moisture sensitive and these reactions were done in an inert nitrogen atmosphere. The anion metathesis using LiTFSI was done in an aqueous solution, as the final products are insoluble in water.

### 2.5.3. Synthesis of Fluorinated Ionic Liquids.

**2.5.3.1 1-Methyl-3-(3,3,4,4,5,5,6,6,7,7,8,8,8-tridecafluorooctyl)-imidazolium bis(trifluoromethanesulfonyl)imide (21).** 1-Iodo-1H,1H,2H,2H-perfluorooctane (34.38 g, 72.5 mmol) was dissolved in toluene (60 mL) and 1-methyl imidazole **8** (5.95 g, 72.5 mmol) was added to the round bottom flask in an nitrogen atmosphere and stirred for 16 h under reflux conditions (110 °C). After 16 h, the product was obtained as a yellow crude solid at the bottom of the flask. Upon cooling the toluene reaction mixture to 0 °C, the solidified product was separated from the reaction mixture by simply decanting the toluene. The rest of the solid product was filtered under a vacuum and washed with diethyl ether (150 mL) to remove any starting materials. The crude product was then placed under the vacuum for 2 h to obtain an off white solid **20** (yield: 75%).

The solid crude product (29.30 g, 52 mmol) obtained was dissolved in deionized water at 65 °C and LiTFSI (14.92 g, 52 mmol) was then added to the solution and stirred at room temperature for 6 h. The ionic liquid being insoluble formed a separate layer at the bottom, which was extracted using ethyl acetate (150 mL). The ethyl acetate was then washed with deionized water (3 x 100 mL) to remove the iodide impurities.  $\text{AgNO}_3$  was added to the separated deionized water layer after the last wash to confirm that the iodide ions were completely removed during the wash. The organic ethyl acetate layer was then dried over  $\text{MgSO}_4$ , then activated carbon was added to remove any colored impurities. The organic layer was then passed through the bed of alumina to remove the impurities.

The organic solvent was then removed using a rotary evaporator and kept under a direct vacuum at 65 °C for 6 h to remove trace amounts of ethyl acetate to obtain compound **21** (Figure 2.15).

$^1\text{H}$  NMR (400 MHz, acetone- $d_6$ ):  $\delta$  9.19 (s, 1 H imidazole-C<sub>2</sub>H), 7.92 (bs, 1 H) and 7.76 (bs, 1H) Imidazole-C<sub>4,5</sub>-H, 4.84 (t, 2H, -N-CH<sub>2</sub>), 4.09 (s, 3H,-N-methyl), 3.11 (m, 2H, -CH<sub>2</sub>-CF<sub>2</sub>);  $^{13}\text{C}$  (100 MHz, acetone-  $d_6$ ;  $^1\text{H}$ ,  $^{19}\text{F}$ -coupled):  $\delta$  138.32 (d, J = 221 Hz ) 125.19 (dm, J = 205 Hz), 123.86 (dm, J = 203 Hz), 121.06 (qt, J = 319 Hz ), 121.39-109.35 (multiplets), 42.91 (t, J = 146 Hz ), 36.91 (qt, J = 143 Hz ), 32.08 (tt, J = 133 Hz ).  $^{19}\text{F}$  NMR (376 MHz, acetone- $d_6$ )  $\delta$  - 79 Hz (s, 3F, CF<sub>3</sub>), - 80.8 Hz (tt, 3F, CF<sub>3</sub>-CF<sub>2</sub>), - 113.42 (m, CF<sub>2</sub>-CH<sub>2</sub>-), -121.37 Hz (m, 2F, CF<sub>2</sub>), -122.40 Hz (m, 2F, CF<sub>2</sub>), -123.10 Hz (m, 2F, CF<sub>2</sub>), -125.80 Hz (m, -CF<sub>2</sub>-CF<sub>3</sub>).

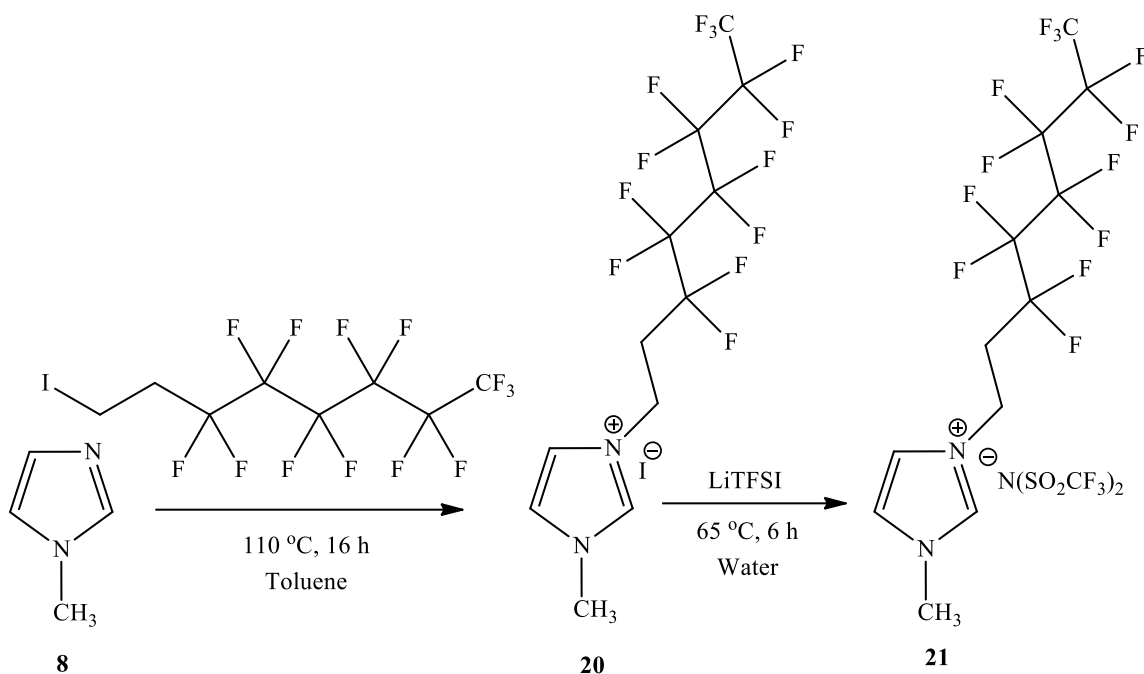


Figure 2.15. Synthesis of 1-Methyl-3-(3,3,4,4,5,5,6,6,7,7,8,8,8-tridecafluorooctyl)-imidazolium bis(trifluoromethanesulfonyl)imide.

### 2.5.3.2 1-Methyl-3-(3,3,4,4,4-pentafluorobutyl)-imidazolium

**bis(trifluoromethanesulfonyl)imide (23).** To a stirred solution of 1-iodo1H,1H,2H,2H-perfluorobutane (19.3 g, 70.44 mmol) in 70 mL toluene at room temperature, 1-methylimidazole **8** (5.79 g, 70.44 mmol) was added in an inert atmosphere and stirred for 16 h at reflux temperature (110 °C). After 16 h, the crude product formed a separate layer at the bottom which, upon cooling to 0 °C, formed a solid layer. The remaining toluene was decanted and the crude solid product was washed with 150 mL diethyl ether and the product **22** was kept under high vacuum for 6 h to remove any remaining solvent (yield: 86%).

The solid crude product (21.57 g, 60.57 mmol) obtained was dissolved in deionized water at 65 °C and LiTFSI (17.39 g, 60.57 mmol) was added to the solution

and stirred at room temperature for 6 h. The ionic liquid that formed a separate layer at the bottom of flask, was then extracted using ethyl acetate (150 mL). The organic layer was washed with deionized water (4 x 150 mL). AgNO<sub>3</sub> was added to the separated deionized water after the fourth wash to confirm the complete removal of iodide impurities. The organic layer was then dried over MgSO<sub>4</sub> and filtered. The organic layer was then mixed with activated charcoal and heated slightly to remove the colored impurities. The organic layer was then passed through a short alumina column to remove any impurities. Further ethyl acetate was removed using a rotary evaporator and the ionic liquid **23** (Figure 2.16) was then kept under vacuum at 65 °C for 6 h to remove any remaining solvents. <sup>1</sup>H NMR (400 MHz, acetone-*d*<sub>6</sub>): δ 9.16 (s, 1 H imidazole-C<sub>2</sub>H), 7.89 (bs, 1H), 7.74 (bs, 1H), imidazole-C<sub>4,5</sub>-H, 4.80 (t, 2H, N-CH<sub>2</sub>), 4.07 (s, 3H,-N-methyl), 3.03 (m, 2H, -CH<sub>2</sub>-CF<sub>2</sub>-).

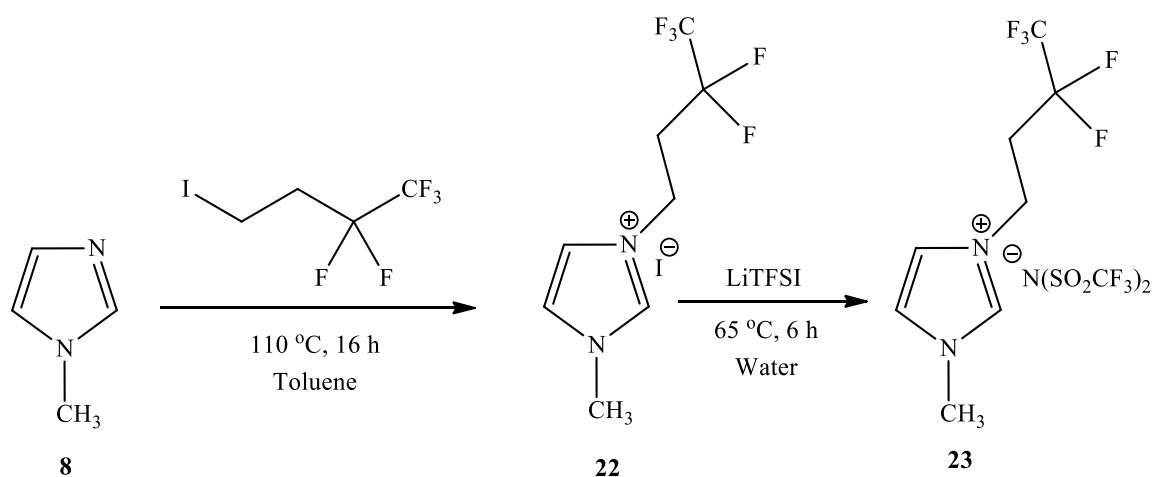


Figure.2.16. Synthesis of 1-methyl-3-(3,3,4,4,4-pentafluorobutyl)-imidazolium bis(trifluoromethanesulfonyl)imide.

### 2.5.3.3 1-Methyl-3-butylimidazolium bis(trifluoromethanesulfonyl)imide (**25**)

1-Methyl imidazole **8** (7.4 g, 90 mmol) was added to 100 mL of toluene and mixed with a slight excess of 1-bromobutane (14.8 g, 108 mmol) in an inert atmosphere and kept at reflux condition (110 °C) for 24 h. After 24 h, the reaction mixture was kept at -20 °C for 3 h. The top toluene layer was decanted and the remaining viscous semi-solids were washed with hot ethyl acetate several times. The liquid obtained was then placed under vacuum for 6 h at 80 °C to remove the starting materials and ethyl acetate (Yield: 81 %).

The above prepared 1-methyl-3-butylimidazolium bromide **24** (18 g, 82 mmol) was then dissolved in deionized water (100 mL) at 65 °C and then mixed with LiTFSI (22.50 g, 82 mmol) and stirred at 65 °C for 24 h. After 24 h, the liquid suspension formed at the bottom was extracted using dichloromethane and the organic layer was washed with the deionized water (3 x 100 mL). The final separated deionized water layer was tested to confirm the removal of all bromide impurities by adding AgNO<sub>3</sub>. The organic layer was then dried over MgSO<sub>4</sub> and mixed with activated charcoal and stirred overnight to remove colored impurities. The organic layer was then passed through a plug of alumina to remove any remaining impurities. Further the organic layer was concentrated using a rotary evaporator and ionic liquid **25** (Figure 2.17) was kept under high vacuum at 65 °C for 6 h to remove any remaining solvents.

<sup>1</sup>H-NMR (400 MHz, acetone-*d*<sub>6</sub>): δ 9.05 (s, 1H imidazole-C<sub>2</sub>H), 7.83 (bs, 1H) and 7.77 (bs, 1H) imidazole-C<sub>4,5</sub>-H, 4.45 (t, 2H, N-CH<sub>2</sub>-), 4.15(s, 3H,-N-methyl), 1.50 (m, 4H, -CH<sub>2</sub>-CH<sub>2</sub>-), 1.07 (t, 3H, -CH<sub>3</sub>); <sup>13</sup>C (100 MHz, acetone- *d*<sub>6</sub>; <sup>1</sup>H, <sup>19</sup>F-coupled) δ 137.3 (d, J = 220 Hz, imidazole-C<sub>2</sub>), 124.8 (dm, J = 200 Hz, 4 Hz) and 123.4 (dm, J = 200 Hz, 4 Hz), 124.1 (q, J<sub>CF</sub> = 319 Hz ), 50.30 (t, J = 143 Hz ), 36.6 (q, J = 143 Hz ), 32.72 (tm, J

= 128 Hz, 5 Hz ), 19.9 (tm, J = 126 Hz, 4 Hz), 13.6 (qm, J = 124 Hz, 4 Hz).  $^{19}\text{F}$  NMR (376 MHz, acetone- $d_6$ )  $\delta$  -78.94.

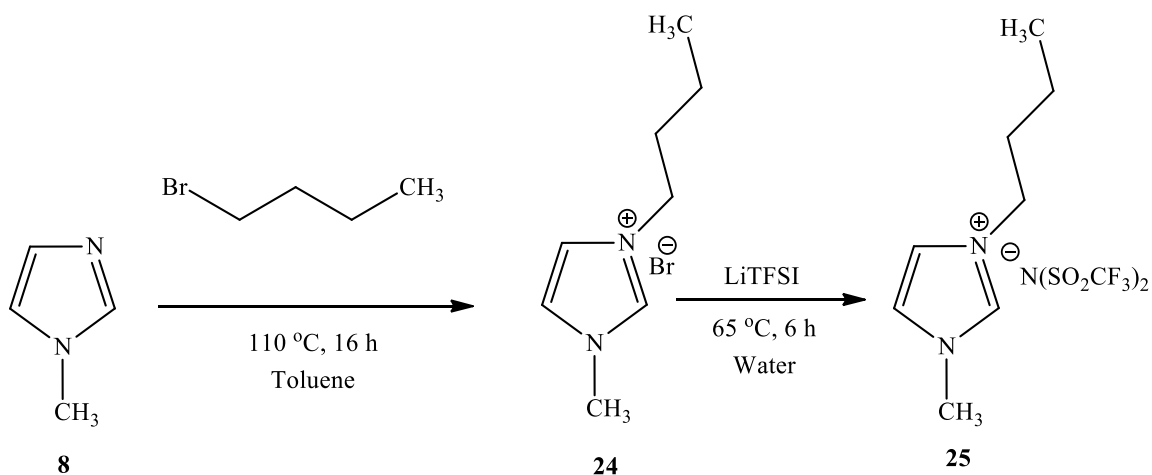


Figure 2.17. Synthesis of 1-methyl-3-butylimidazolium bis(trifluoromethanesulfonyl)imide.

**2.5.4. Preliminary Results.** As seen from Table 2.1, the diffusion coefficient of  $\text{O}_2$  for fluorinated ionic liquids is very low due to their high viscosity when compared with ethyl methylimidazolium bis(trifluoromethanesulfonyl)imide and butyl methylpyrrolidinium bis(trifluoromethanesulfonyl)imide. The solubility of  $\text{O}_2$  (as expected), in fluorinated ionic liquids is very high when compared with other ionic liquids. The problem with viscosity of fluorinated ionic liquid can be solved by mixing the ionic liquid with other solvents; this is currently being tested.

Table 2.1. Diffusion coefficient and solubility of O<sub>2</sub> in selected room temperature ionic liquids.

<b>Ionic Liquid</b>	<b>Diffusion coefficient 10<sup>6</sup> x D<sub>O<sub>2</sub></sub>( cm<sup>2</sup>s<sup>-1</sup>)</b>	<b>Solubility of O<sub>2</sub> mmol dm<sup>-3</sup></b>
<b>Polyfluorinated EMIM-TFSI (21)</b>	0.61	15.4
<b>EMIM-TFSI</b>	9.7	1.38
<b>N-methyl-N-butyl-PyrrolidiniumTFSI (25)</b>	8.77	1.09

## 2.6. BORON BASED ANION RECEPTORS

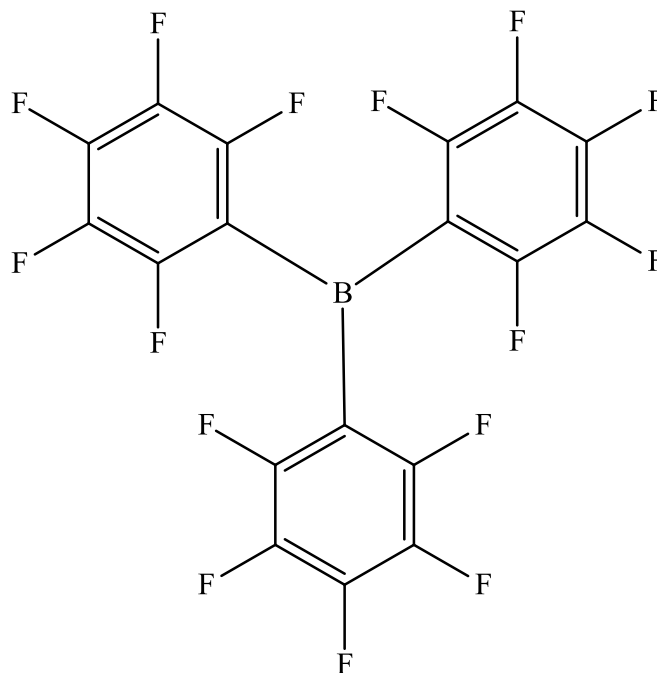
**2.6.1. Introduction.** Anion receptors that selectively bind to specific anions have already been applied to various biological <sup>95</sup> and environmental applications <sup>96</sup>. An anion receptor can bind with various anions through hydrogen bonding <sup>97</sup>, covalent bonding <sup>98</sup> or Lewis acid-base interactions <sup>99</sup>. The boron based anion receptors bind through Lewis acid-based interactions. Binding ability of these anion receptors is applied towards the bio- and chemosensors due to the change in color or fluorescence properties. The boron atom present in the trisubstituted compounds such as BX<sub>3</sub> (where X is halogen) has a sp<sup>3</sup> trigonal symmetry with an empty p-orbital, which has the ability to accept lone pair of electrons from nucleophiles. The boron atom acts as an anion receptor due to its weak Lewis acidity.

Most of the research related to anion receptors is focused towards bio- and chemosensors <sup>100</sup>, although recently some are being applied towards development of novel anion receptors which help in dissolving lithium salts such as LiO<sub>2</sub> and Li<sub>2</sub>O<sub>2</sub>. During the discharge process the oxidation reaction at the anode leads to formation of Li<sup>+</sup>



ions. These  $\text{Li}^+$  ions then undergo reduction reaction with oxygen to form  $\text{Li}_2\text{O}_2$  and  $\text{LiO}_2$  salts. These lithium salts precipitate during the operation of the Li-air batteries and in turn block the pores present at the surface of the anode. These lithium salts, however, are insoluble and seals the pores of the anode, eventually making the anode surface inaccessible for the  $\text{O}_2$  reduction reaction<sup>91</sup>. Anion receptors also help in the dissociation of lithium salts such as  $\text{LiF}$ , which increases the lithium and fluoride ion transference numbers and ionic conductivity<sup>101</sup>.

Recently Kyu Tae Lee and coworkers synthesized tris(pentafluorophenyl) borane **26** (TPFPB, Figure 2.18). TPFPB forms a thermodynamically stable species by binding as an anion receptor with peroxide. TPFPB could be electrochemically oxidized with improved kinetics than the oxidation of solid  $\text{Li}_2\text{O}_2$  on carbon powder microelectrode. The superoxide radical binds with TPFPB to form TPFPB-peroxide anion complex through disproportionation mechanism. The first discharge capacities for  $\text{Li}_2\text{O}_2$ /super P/PVDF electrodes are substantially increased in the presence of the TPFPB (814 mAh  $\text{g}^{-1}$ ) when compared to one without the anion receptor additive (277 mAh  $\text{g}^{-1}$ )<sup>102</sup>.

**26**Figure 2.18. Structure of tris(pentafluorophenyl)borane (TPFPB) <sup>102</sup>.

Michel Armand and coworkers<sup>103</sup> synthesized novel borate based anion receptors (Figure 2.19) whose binding ability can be tuned. These borate esters were found to bind reversibly and form multiple complexes with anions. Further these anion receptors can be modified by substituting with electron withdrawing or releasing groups to get expected binding conditions. These triol borate esters were also stable for wide voltage window of 1-5 V vs Li/Li<sup>+</sup>. Even though these borate esters have wide electrochemical stability, due to the presence of high ring strain, they undergo ring opening as seen during NMR studies <sup>103</sup>.

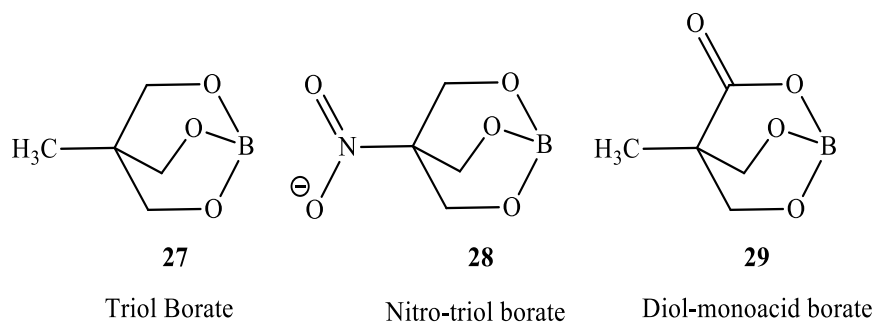


Figure 2.19. Structure of borate ester based anion receptors <sup>103</sup>.

Although the TPFPB acts as an appropriate boron-based anion receptor, its binding ability cannot be modified. An appropriate anion receptor should have moderately strong binding affinity. Hence a series of boron-based anion receptors **30** (Figure 2.20) were synthesized with phenyl moiety in collaboration with our research group member Jatin Mehta.

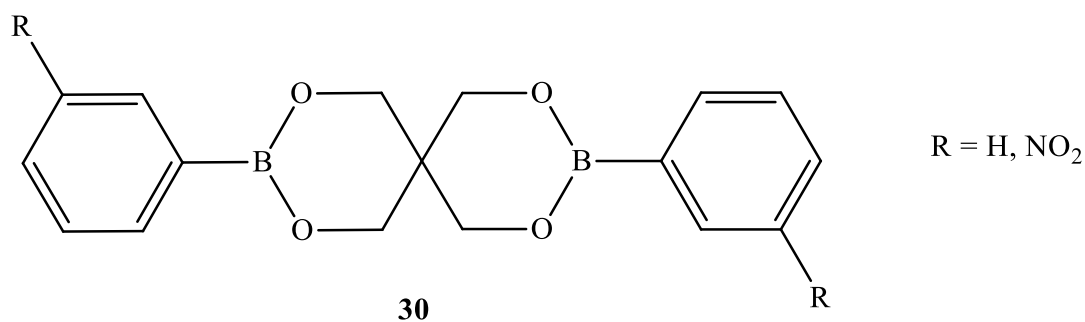


Figure 2.20. Structure of boron based anion receptor.

**2.6.2. Materials and Methods.** All the reagents were obtained from commercial sources and used as received unless otherwise noted. <sup>1</sup>H NMR and <sup>13</sup>C NMR spectra were recorded on a INOVA-Varian 400 MHz spectrometer at 400 MHz and 100 MHz

respectively in acetone- $d_6$  solvent. The chemical shifts for  $^1\text{H}$  and  $^{13}\text{C}$  NMR were referenced with respect to residual solvent signals. All the  $^{13}\text{C}$  chemical shifts were assigned using proton coupled  $^{13}\text{C}$  spectra.

### 2.6.3. Synthesis of Boron Based Anion Receptors.

#### 2.6.3.1 3,9-diphenyl-2,4,8,10-tetraoxa-3,9-diborasp[5.5]undecane (**33**).

Phenylboronic acid **31** (4.92 g, 40.5 mmol) and pentaerythritol **32** (2.2 g, 16.2 mmol) were added to 50 mL of acetone in a round bottom flask at room temperature. To this mixture, finely powdered molecular sieves (size 4 Å) and 1 mL of conc.  $\text{H}_2\text{SO}_4$  were added and refluxed for 4 h. After 4 h, the mixture was cooled to room temperature and filtered through silica to remove the molecular sieves and inorganic impurities. The resulting organic layer was evaporated under vacuum to obtain yellowish solid crude product which was then washed with absolute ethanol to remove any unreacted phenylboronic acid. The product **33** (Figure 2.21) was obtained as an off white colored solid. (2.0 g, 40.8%).  $^1\text{H}$  NMR (400 MHz, acetone- $d_6$ ):  $\delta$  4.15 (s,  $-\text{CH}_2-\text{O}-\text{B}$ ),  $\delta$  7.32-7.73 (m, aromatic protons);  $^{13}\text{C}$ -NMR (100 MHz, acetone- $d_6$ ;  $^1\text{H}$ -coupled)  $\delta$  65.44 (tm,  $J_{\text{CH}} = 150$  Hz),  $\delta$  128.46 (dd,  $J_{\text{CH}} = 166$  Hz),  $\delta$  131.81 (dm,  $J_{\text{CH}} = 150$  Hz),  $\delta$  134.82 (dm,  $J_{\text{CH}} = 157$  Hz).

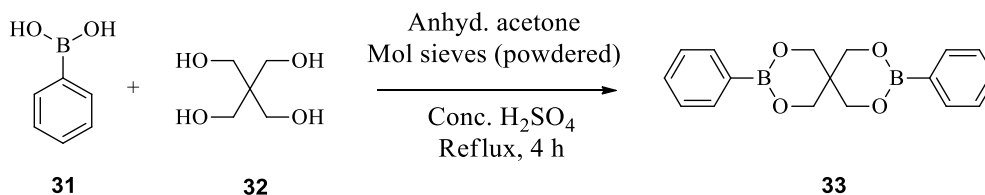


Figure 2.21. Synthesis of 3,9-diphenyl-2,4,8,10-tetraoxa-3,9-diborasp[5.5]undecane.

**2.6.3.2 3,9-bis(3-nitrophenyl)-2,4,8,10-tetraoxa-3,9-diborasp[5.5]undecane (35).** 3-Nitrophenylboronic acid **34** (5.0 g, 30 mmol) and pentaerythritol **32** (1.6 g, 12 mmol) were added to 50 mL of acetone in a round bottom flask at room temperature. To this mixture, finely powdered molecular sieves (size 4 Å) and 1 mL of conc. H<sub>2</sub>SO<sub>4</sub> were added and refluxed for 4 h. After 4 h, the mixture was cooled to room temperature and filtered through silica to remove the molecular sieves and inorganic impurities. The resulting organic layer was evaporated under vacuum to obtain yellowish solid crude product which was then washed with absolute ethanol to remove any unreacted phenylboronic acid. The product **35** (Figure 2.22) was obtained as an off white colored solid. (2.2 g, 46.8%). <sup>1</sup>H NMR (400 MHz, acetone-*d*<sub>6</sub>): δ 4.26 (s, -CH<sub>2</sub>-O-B), δ 7.68-8.53 (aromatic protons); <sup>13</sup>C-NMR (100 MHz, acetone-*d*<sub>6</sub>; <sup>1</sup>H-coupled) δ 65.61 (tm, J<sub>CH</sub> = 148 Hz), δ 126.42 (dd, J<sub>CH</sub> = 159 Hz), δ 128.91 (dm, J<sub>CH</sub> = 168 Hz), δ 130.10 (dm, J<sub>CH</sub> = 164 Hz), δ 140.80 (dm, J<sub>CH</sub> = 160 Hz).

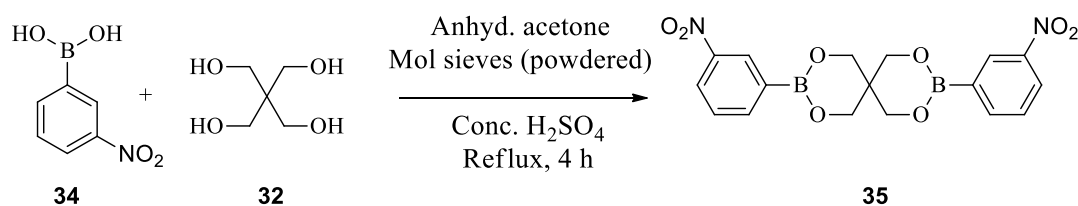


Figure 2.22. Synthesis of 3,9-bis(3-nitrophenyl)-2,4,8,10-tetraoxa-3,9-diborasp[5.5]undecane.

## 2.7. CONCLUSION

In summary, a series of ionic liquids with imidazole and pyrrolidine as backbone, and bis(trifluoromethanesulfonyl)imide [TFSI]<sup>-</sup> and tetrafluoroborate [BF<sub>4</sub>]<sup>-</sup> anions were

synthesized and evaluated for their potential as electrolytes using 2016 coin cells for primary Li/CFx batteries. Most of the ionic liquid and their Li-salt mixtures showed no freezing/melting behavior up to -60 °C and are thermally stable up to at least 200 °C, as seen by TGA analysis. In general, the fluoroalkyl-derived ionic liquids have superior thermal stability ( $T_d > 350$  °C) than their alkoxyalkyl-derived analogues, the [TFSI]<sup>-</sup> anion-based ionic liquids are thermally and electrochemically more stable than the [BF<sub>4</sub>]<sup>-</sup> anion-based electrolytes. Some of these ionic liquid electrolytes exhibit high discharge capacities ( $>700$  mAh g<sup>-1</sup>) at low rates of discharge ( $\sim C/100$ ), comparable to those of the state of the art carbonate-based electrolytes <sup>71</sup>. However, at higher current rates and for fluoroalkyl-derived ionic liquids, the discharge capacity is limited.

### 3. CHEMICAL DELITHIATION OF $\text{LiFePO}_4$ ; EFFECT ON THE SOLID ELECTROLYTE INTERFACE

#### 3.1. INTRODUCTION

In recent years, lithium-ion batteries have been widely used for energy storage due to their high power, environmental friendliness, and a long life cycle<sup>104-106</sup>. After the commercialization of lithium-ion batteries most of the focus has been on developing cathode materials<sup>107-109</sup> since they determine the energy density, rate capability, and the cost of lithium-ion batteries. The current research on the lithium-ion battery is focused on the high voltage cathode materials that are mainly focused on layered transition metal oxides  $\text{LiMO}_2$  ( $M = \text{Ni, Mn, Co}$ ) and spinel structures  $\text{LiM}_2\text{O}_4$  ( $M = \text{Mn, Ni}$ )<sup>110-113</sup>. Among the above mentioned cathode materials,  $\text{LiCoO}_2$  (LCO) is very toxic<sup>114</sup> and very expensive;  $\text{LiNiO}_2$ , even though is isostructural with  $\text{LiCoO}_2$ , cannot be commercialized due to its tendency to block Li diffusion pathways<sup>115</sup>. They are also thermally unstable since  $\text{Ni}^{3+}$  can be easily reduced when compared with  $\text{Co}^{3+}$ <sup>116</sup>. Since Goodenough's group in 1997 first reported that lithium iron phosphate ( $\text{LiFePO}_4$ ) can display the intercalation/de-intercalation of lithium ions reversibly, it has been used as cathode material for powering electric vehicles (EVs) and hybrid electric vehicles (HEVs).  $\text{LiFePO}_4$  has also been considered as a favorable candidate for cathode material in the lithium-ion battery due to its nontoxicity, low cost, and high thermal stability characteristics,<sup>117-124</sup> and a theoretical capacity of  $170 \text{ mAh g}^{-1}$  (Figure 3.1)<sup>111</sup>. However, due to poor electrical and ionic conductivity of  $\text{LiFePO}_4$  results to lower rate capacity, and low utilization to overcome this drawback, continuous research efforts have resulted

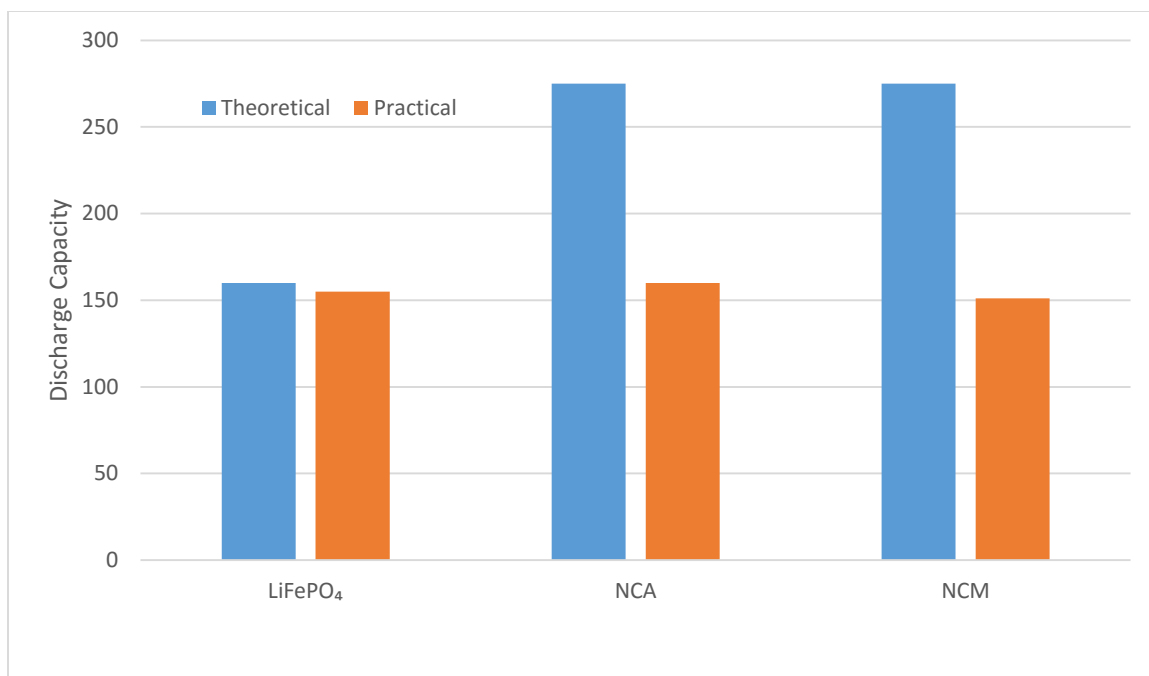


Figure 3.1. A range of lithium-ion battery electrodes either currently available or under development and comparison of their theoretical and practical capacity (NCA:  $\text{LiNi}_{0.8}\text{Co}_{0.15}\text{Al}_{0.05}\text{O}_2$ , NCM:  $\text{LiNi}_{1/3}\text{Mn}_{1/3}\text{Co}_{1/3}\text{O}_2$ )<sup>125</sup>.

in the development of new cathode materials such as  $\text{LiNi}_{0.8}\text{Co}_{0.15}\text{Al}_{0.05}\text{O}_2$ , and  $\text{LiNi}_{1/3}\text{Mn}_{1/3}\text{Co}_{1/3}\text{O}_2$ .  $\text{LiNi}_x\text{Co}_y\text{Mn}_z\text{O}_2$  (NMC) has higher specific capacity when compared with both LCO and  $\text{LiFePO}_4$ , but almost similar operating voltage.

$\text{LiNi}_{1/3}\text{Mn}_{1/3}\text{Co}_{1/3}\text{O}_2$  is the most common form of NMC that is used in the commercial battery market. NMCs are considered as perfect candidates for cathode materials in lithium-ion batteries due to their high capacity, better capacity retention, and excellent high temperature stability in the presence of electrolyte<sup>126-128</sup>. In addition to the above property of high specific capacity, NMCs also have fast lithiation/delithiation kinetics due to their layered structure<sup>129</sup>. In addition to the development of new cathode materials, the last decade has also seen development of new formulations of electrolytes



which also include the designing and understanding of the formation of a solid electrolyte interphase (SEI)<sup>130-132</sup>.

SEI is formed when the electrolyte undergoes decomposition at the electrode and mostly consists of organic and inorganic electrolyte decomposition products. This layer, under ideal conditions, prevents further decomposition of electrolyte at the electrode surface by blocking electron transport while simultaneously allowing the Li ions to pass through during the cycling process. Although, when the development of a solid electrolyte interphase (SEI) is non-uniform on the surface of Li metal, it results in poor cycle retention capability and even, in the worst case, a short circuit between two electrodes<sup>133-135</sup>. In recent years, many attempts have been made to overcome these serious problems, such as modification of Li metal anodes<sup>133,136,137</sup>, introduction of modified separators<sup>138</sup>, structural modification of Li metal anodes,<sup>133,139,140</sup> and use of functionalized electrolyte additives<sup>141-143</sup>. The use of electrolytes as additives seems to be the most cost effective and easier method for stabilizing the Li metal anodes to obtain the desired enhanced cycle performance, as well as being safe for commercialization and use in the Li-ion battery.

## 3.2. EXPERIMENTAL

**3.2.1. Material and Methods.**  $\text{LiNi}_{1/3}\text{Mn}_{1/3}\text{Co}_{1/3}\text{O}_2$ , nitronium tetrafluoroborate ( $\text{NO}_2\text{BF}_4$ ), disodium peroxydisulfate ( $\text{Na}_2\text{S}_2\text{O}_8$ ) and lithium iron phosphate ( $\text{LiFePO}_4$ ) were purchased from Sigma Aldrich and used as received. Acetonitrile (>99% ACS Certified) was purchased from Fisher Scientific. Fluoroethylene carbonate (FEC) and trifluorotoluene ( $\text{PhCF}_3$ ) were purchased from TCI America.

$^{19}\text{F}$  NMR spectra were recorded on an INOVA-Varian 400 MHz spectrometer at 376 MHz, in acetone- $d_6$  solvent. The  $^{19}\text{F}$  NMR spectra were referenced to the internal standard trichlorofluoromethane ( $\delta\text{CFCl}_3 = 0$ ).

X-ray photoelectron Spectrometer (XPS) studies were done using KRATOS AXIS 165 X-ray Photoelectron Spectrometer at Material Research Centre, Missouri University of Science and Technology, using monochromated Aluminium X-ray source.

### **3.2.2. Chemical Delithiation of Cathode Materials.**

**3.2.2.1 Delithiation using  $\text{Na}_2\text{S}_2\text{O}_8$ .**  $\text{LiFePO}_4$  was mixed with  $\text{Na}_2\text{S}_2\text{O}_8$  in 10 mL of deionized water and stirred using a magnetic stirrer under nitrogen atmosphere for 48 h. The delithiated  $\text{LiFePO}_4$  being insoluble in water was filtered whereas as the rest of the products such as  $\text{Na}_2\text{SO}_4$  and  $\text{Li}_2\text{SO}_4$  are soluble in water. The delithiated  $\text{LiFePO}_4$  was then washed several time with distilled water to remove the impurities and dried in an oven at 110 °C. Similar procedure was used for the delithiation of  $\text{LiNi}_{1/3}\text{Mn}_{1/3}\text{Co}_{1/3}\text{O}_2$ .

**3.2.2.2 Delithiation using  $\text{NO}_2\text{BF}_4$ .**  $\text{LiNi}_{1/3}\text{Mn}_{1/3}\text{Co}_{1/3}\text{O}_2$  was mixed with  $\text{NO}_2\text{BF}_4$  in 10 mL acetonitrile and stirred using a magnetic stirrer under inert atmosphere for 48 h. The extent of delithiation in  $\text{Li}_{1-x}\text{Ni}_{1/3}\text{Mn}_{1/3}\text{Co}_{1/3}\text{O}_2$  could be controlled by changing the ratio of the  $\text{LiNi}_{1/3}\text{Mn}_{1/3}\text{Co}_{1/3}\text{O}_2$  and  $\text{NO}_2\text{BF}_4$ . These experiments required a slight excess of  $\text{NO}_2\text{BF}_4$ , due to the high reactivity of  $\text{NO}_2\text{BF}_4$  and also the formation of side products, and it decomposition even before the reaction started. The delithiated  $\text{LiNi}_{1/3}\text{Mn}_{1/3}\text{Co}_{1/3}\text{O}_2$  was then washed three times with acetonitrile to remove the soluble impurities under nitrogen atmosphere and dried at room temperature under vacuum.

These delithiated materials were reacted with fluoroethylene carbonate (FEC) at room temperature for 30 min, in acetonitrile as solvent, and trifluorotoluene ( $\text{PhCF}_3$ ) as an internal standard.

### 3.3. RESULTS AND DISCUSSION

**3.3.1.  $^{19}\text{F}$  NMR Studies.** To investigate the formation of a solid electrolyte interface (SEI) on the surfaces of delithiated materials that were reacted with FEC, NMR experiments were performed. Figure 3.2 displays the reaction mixture of fluoroethylene carbonate (FEC) and delithiated  $\text{LiFePO}_4$  at various time intervals, with trifluorotoluene as an internal standard. The NMR spectrum showed that around 5% of the FEC disappeared to form the SEI during the first 15 min, and remained constant over time. The other delithiated cathode material,  $\text{LiNi}_{1/3}\text{Mn}_{1/3}\text{Co}_{1/3}\text{O}_2$ , when treated with FEC also showed no soluble degradation of products and the disappearance of FEC to form the SEI. Formation of SEI on these delithiated cathode materials was mostly due to Lewis acid catalyzed ring-opening polymerization, and not through oxidative mechanism since the oxidation potential of FEC is  $> 4.5 \text{ V vs Li/Li}^+$ , whereas the maximum  $E_{\text{ox}}$  of the delithiated  $\text{LiFePO}_4$  is  $\sim 3.55 \text{ V vs Li/Li}^+$ .

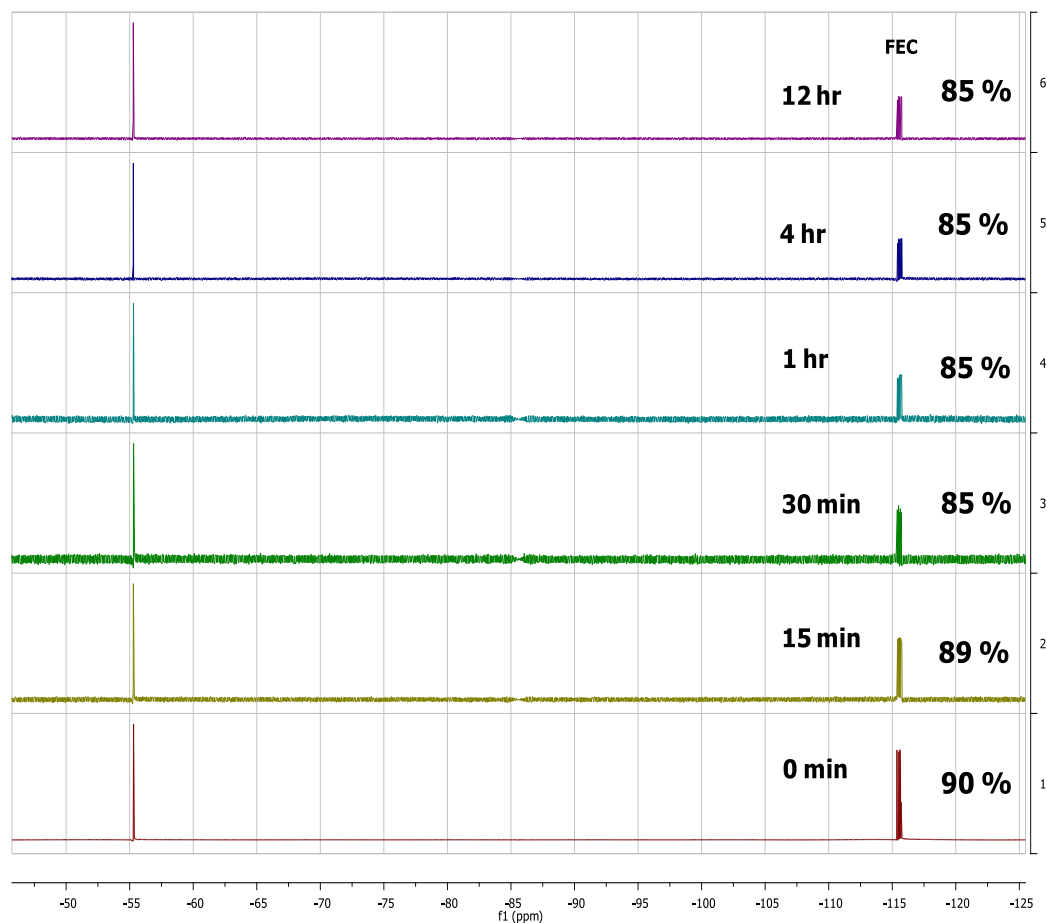


Figure 3.2. The reaction mixture of fluoroethylene carbonate (FEC) and delithiated  $\text{LiFePO}_4$  at various time intervals with trifluorotoluene as an internal standard.

**3.3.2. X-ray Photoelectron Spectrometry Studies (XPS).** To determine the formation of SEI on the surface of delithiated cathode materials, XPS measurements were made. The XPS was performed and the analysis of C 1s, O 1s, Li 1s and F 1s (Figure 3.3) were done since the composition of SEI was mostly carbonate based polymers.

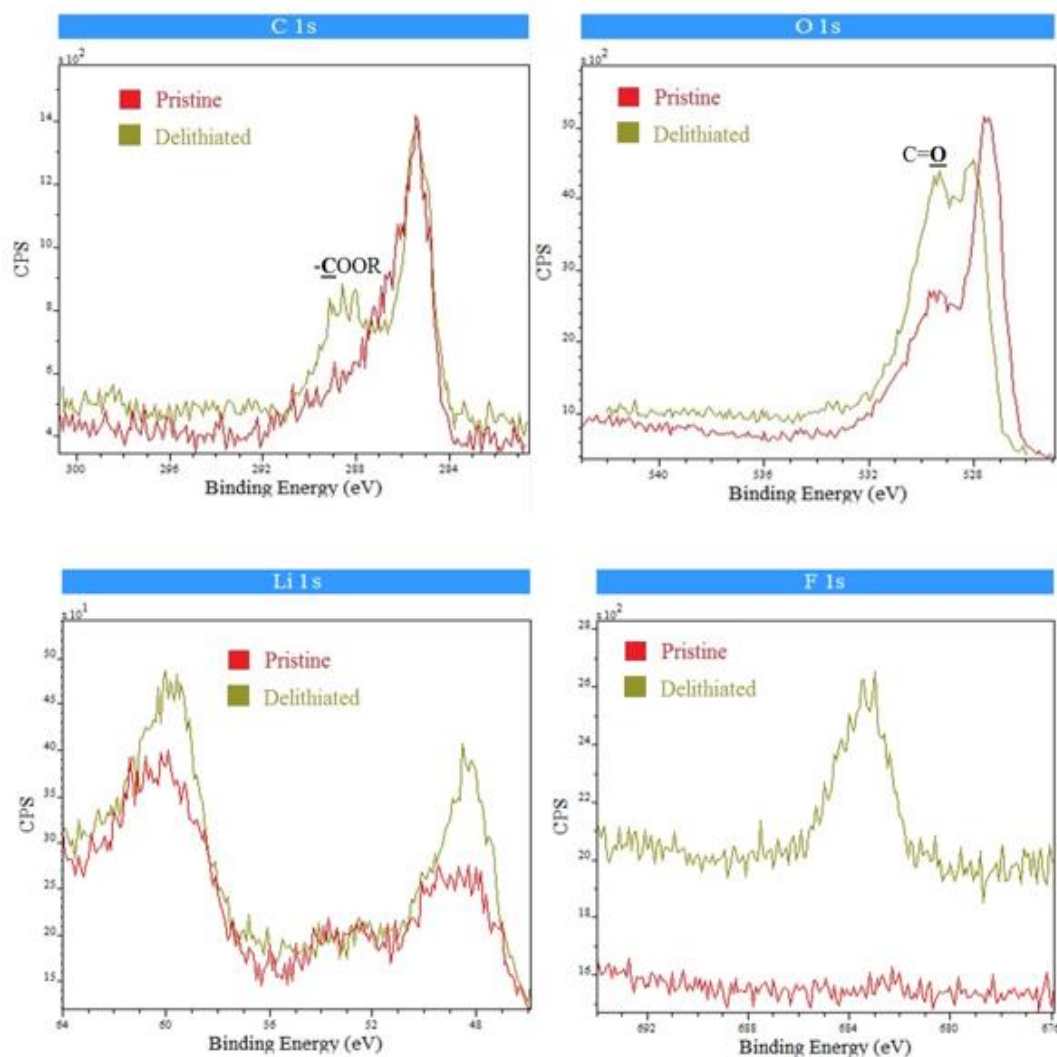


Figure 3.3. C 1s, O 1s, Li 1s and F 1s XPS spectra of the pristine and delithiated  $\text{LiNi}_{1/3}\text{Mn}_{1/3}\text{Co}_{1/3}\text{O}_2$  after reacting with FEC.

F 1s spectrum was also recorded due to the presence of fluoroethylene carbonate. The formation of SEI was apparent from the XPS Spectra (Figure 3.3) of the FEC treated cathode materials; C 1s spectra shows an extra peak corresponding to the presence of -COOR group and this is further confirmed by the presence of the C=O peak seen in the O 1s spectra. F 1s spectra also shows a peak for the fluorine, indicating the formation of a SEI layer consisting of poly(fluoroethylene carbonate).

**3.3.3. Scanning Electron Microscopy Studies (SEM).** Figure 3.4. shows the different surface morphologies of  $\text{LiFePO}_4$  and delithiated  $\text{LiFePO}_4$  after reaction with FEC at room temperature for 30 min.

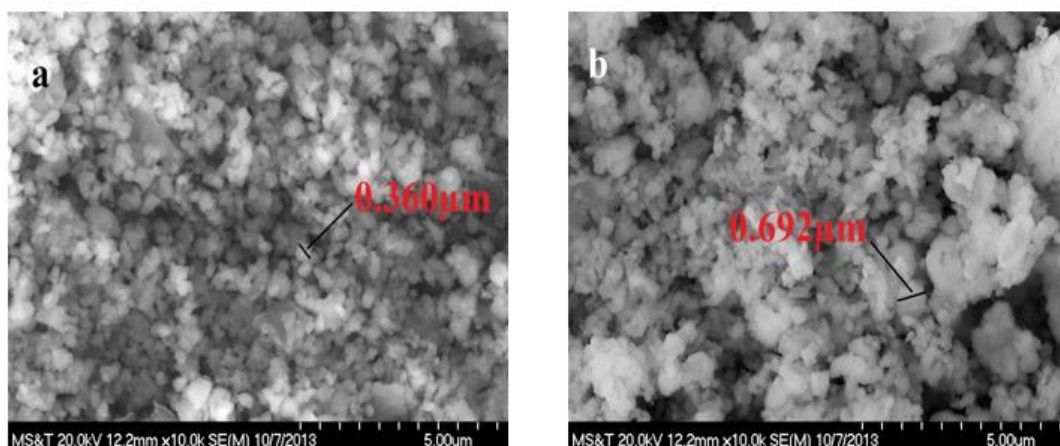


Figure 3.4. SEM Images of a) pristine  $\text{LiFePO}_4$  after reaction with FEC at room temperature for 30 min and b) delithiated  $\text{LiFePO}_4$  after reaction with FEC at room temperature for 30 min.

The surface of the pristine  $\text{LiFePO}_4$  after the reaction with FEC was smoother and smaller, whereas the surface of the delithiated  $\text{LiFePO}_4$ , after reaction with FEC at room temperature for 30 min had a compact layer with lots of white particles that were attached or dispersed on the surface.

### 3.4. PROBABLE SEI FORMATION MECHANISM.

The metal acted as a lewis acid and was reduced (as shown in Figure 3.5) which led to the ring opening of fluoroethylene carbonate. This process was then continued when

another molecule of fluoroethylene carbonate underwent the same reduction process, and this finally led to the polymerization of fluoroethylene carbonate, leading to the formation of a Solid Electrolyte Interface.

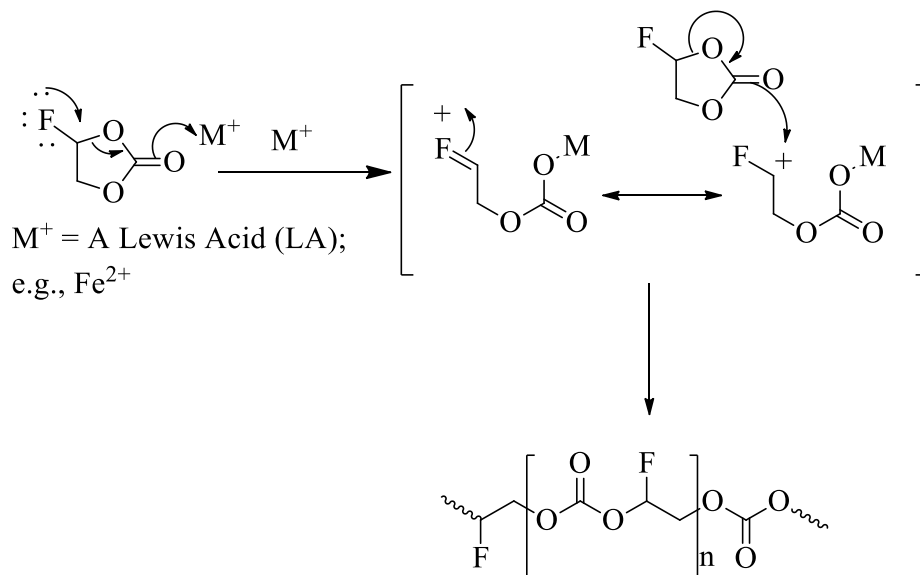


Figure 3.5. Metal ion based Lewis acid catalyzed polymerization of FEC leading to the SEI.

### 3.5. CONCLUSION

In summary, cathode materials  $\text{LiFePO}_4$  and  $\text{LiNi}_{1/3}\text{Mn}_{1/3}\text{Co}_{1/3}\text{O}_2$  were delithiated using  $\text{NO}_2\text{BF}_4$  and  $\text{Na}_2\text{S}_2\text{O}_8$  as oxidizers. The formation of SEI on the cathode surface was monitored using fluoroethylene carbonate as an electrolyte additive and monitored by  $^{19}\text{F}$  NMR, XPS and SEM.  $^{19}\text{F}$  NMR clearly showed a decrease in the peak corresponding to FEC when compared with the internal standard trifluorotoluene. XPS spectra of F 1s showed new peaks when compared with the pristine  $\text{LiFePO}_4$ , indicating the formation of SEI. Lastly, SEM images of the pristine and delithiated samples, after

reaction with FEC, showed obvious changes in the morphology, confirming the formation of SEI.



## APPENDIX

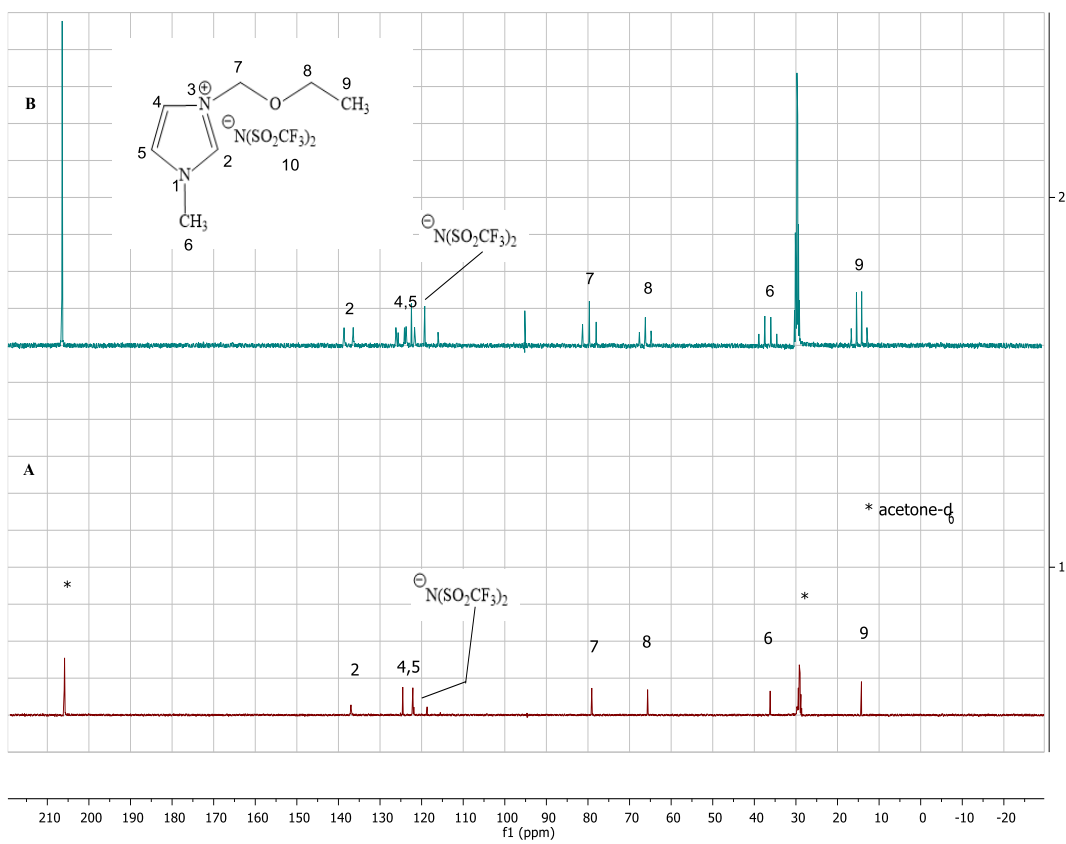


Figure A.1.  $^{13}\text{C}$  NMR (A, proton decoupled; B, proton coupled) spectra of 1-ethoxymethyl-3-methylimidazolium bis(trifluoromethanesulfonyl)imide<sup>45</sup>.

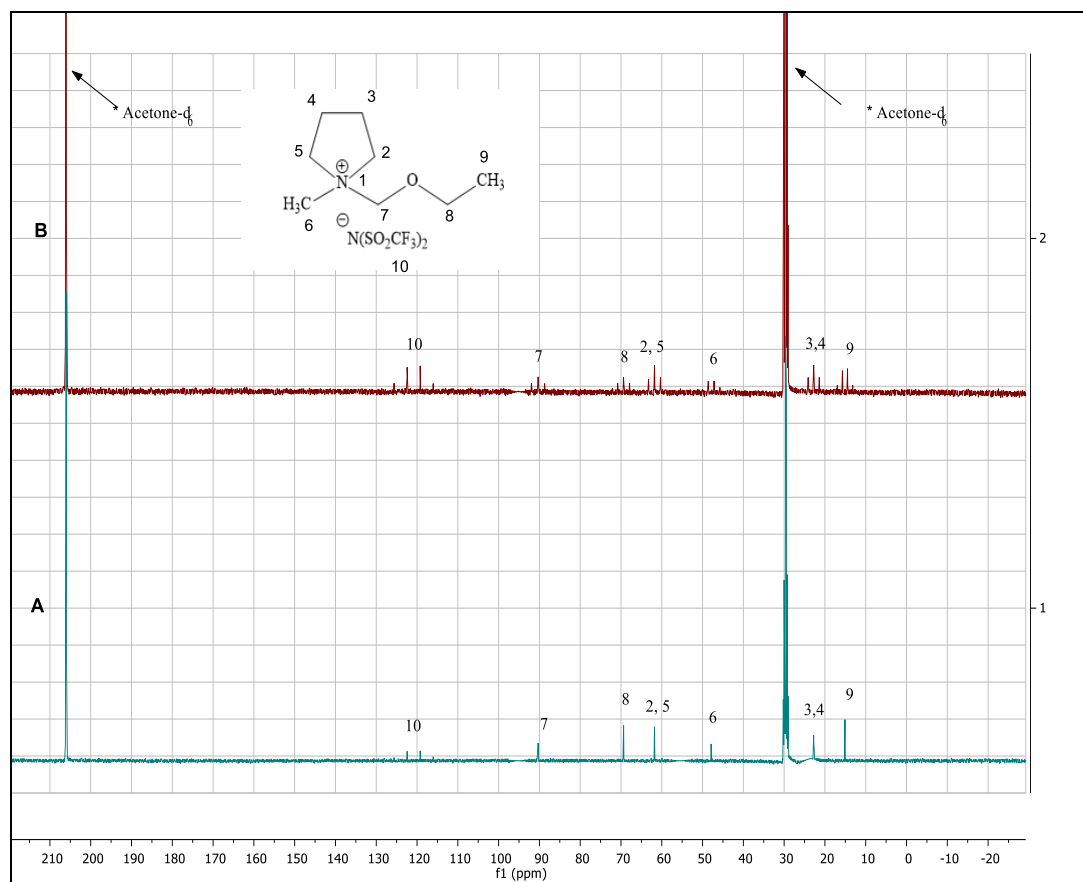


Figure A.2.  $^{13}\text{C}$  NMR (**A**, proton decoupled; **B**, proton coupled) spectra of 1-ethoxymethyl-1-methyl-pyrrolidinium bis(trifluoromethanesulfonyl)imide (**4**)<sup>45</sup>.

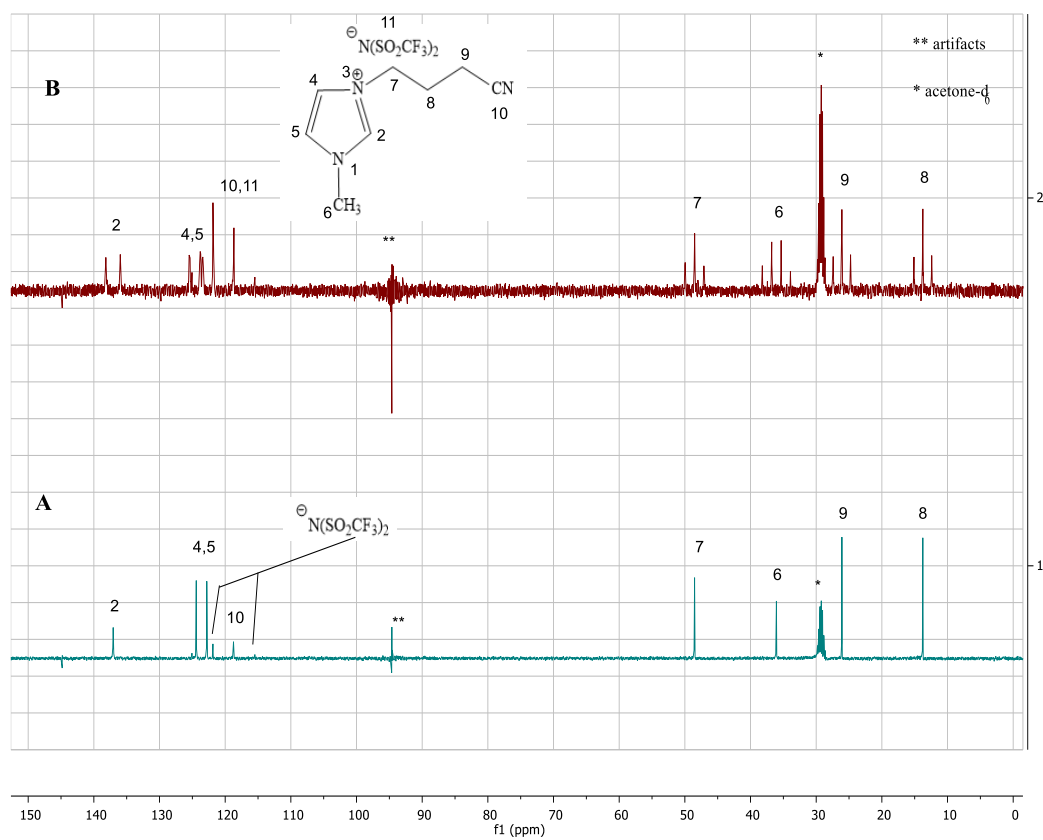


Figure A.3.  $^{13}\text{C}$  NMR (100 MHz, **A**, proton decoupled; **B**, proton coupled) spectra of 1-cyanopropyl-3-methylimidazolium bis(trifluoromethanesulfonyl)imide.

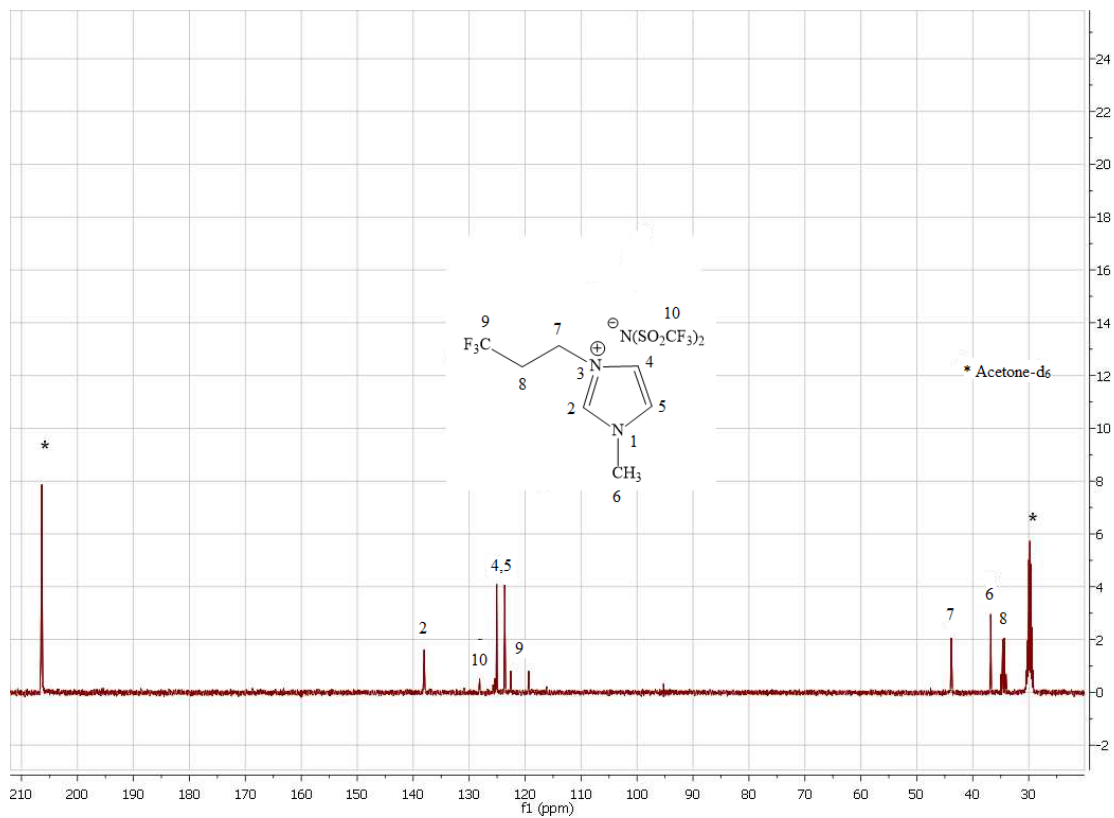


Figure A.4.  $^{13}\text{C}$  NMR spectrum (100 MHz) of 1-(3,3,3-trifluoropropyl)-3-methylimidazolium bis(trifluoromethanesulfonyl)imide.

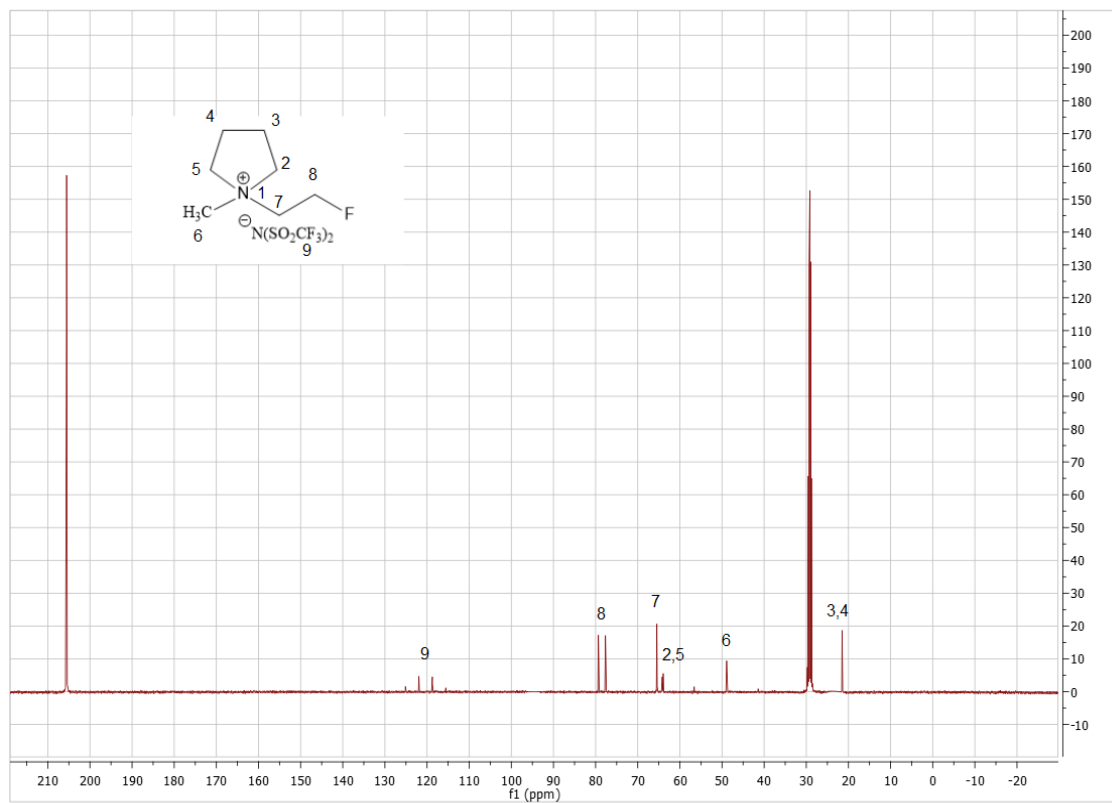


Figure A.5.  $^{13}\text{C}$  NMR decoupled (100 MHz, acetone- $d_6$ ) spectrum of (2-fluoroethyl)-1-methylpyrrolidinium bis(trifluoromethanesulfonyl)imide.

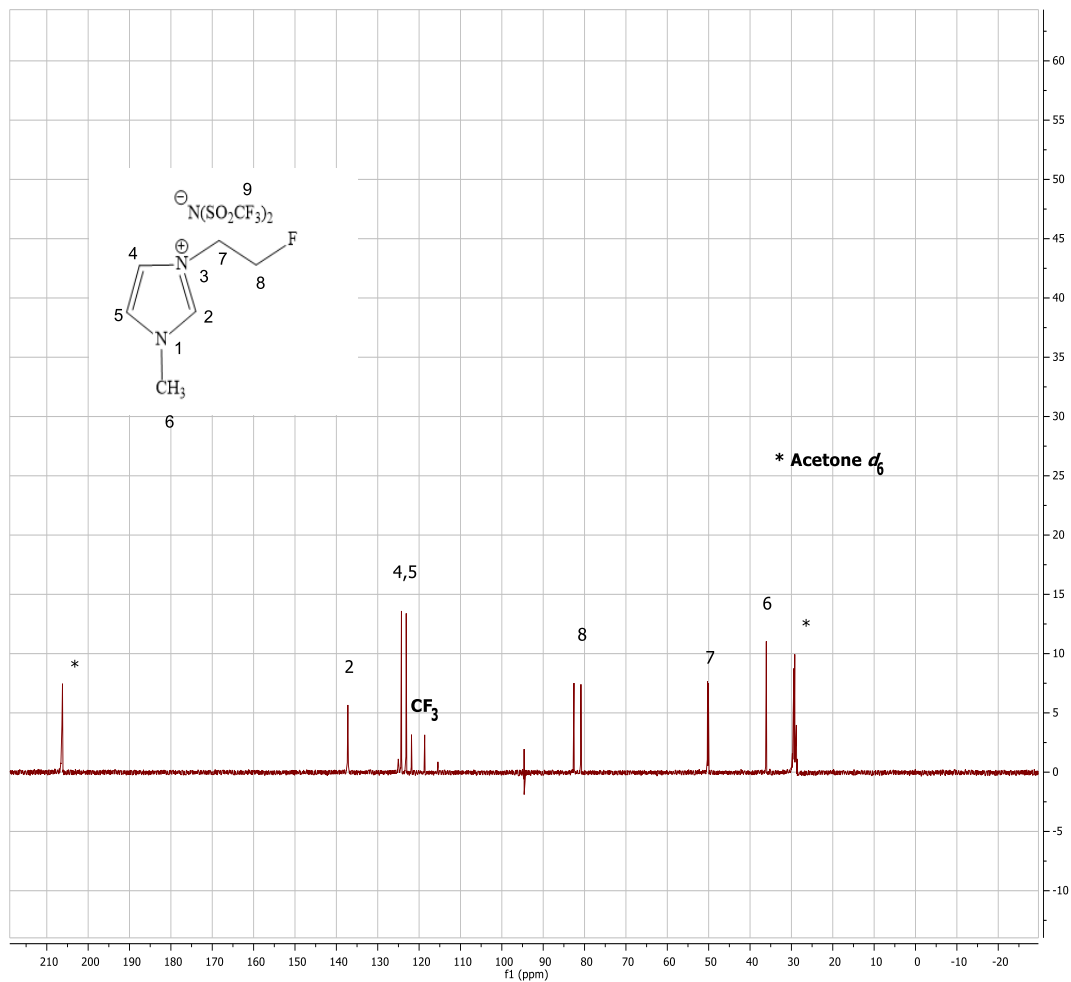


Figure A.6.  $^{13}\text{C}$  NMR decoupled (100 MHz, acetone- $d_6$ ) spectrum of 1-(2-fluoroethyl)-3-methylimidazolium bis(trifluoromethanesulfonyl)imide.

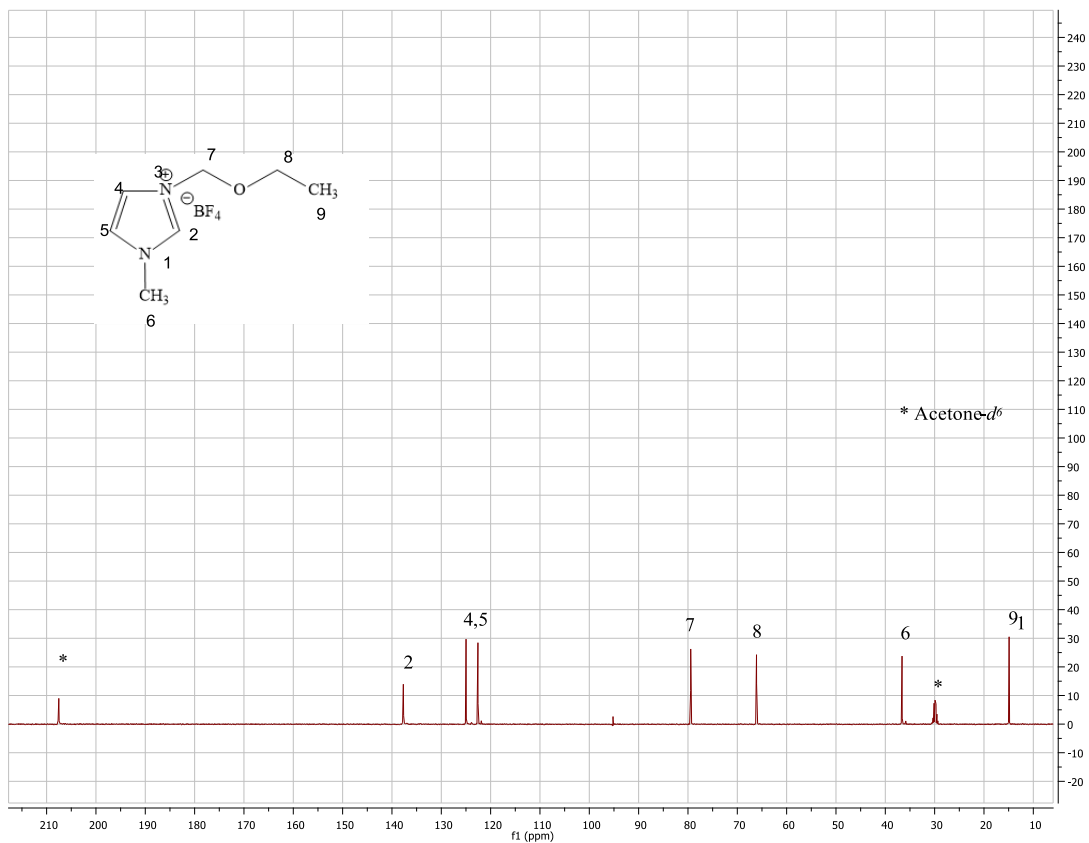


Figure A.7.  $^{13}\text{C}$  NMR decoupled (100 MHz, acetone- $d_6$ ) spectrum of 1-methyl-3-ethoxymethylimidazolium tetrafluoroborate <sup>45</sup>.

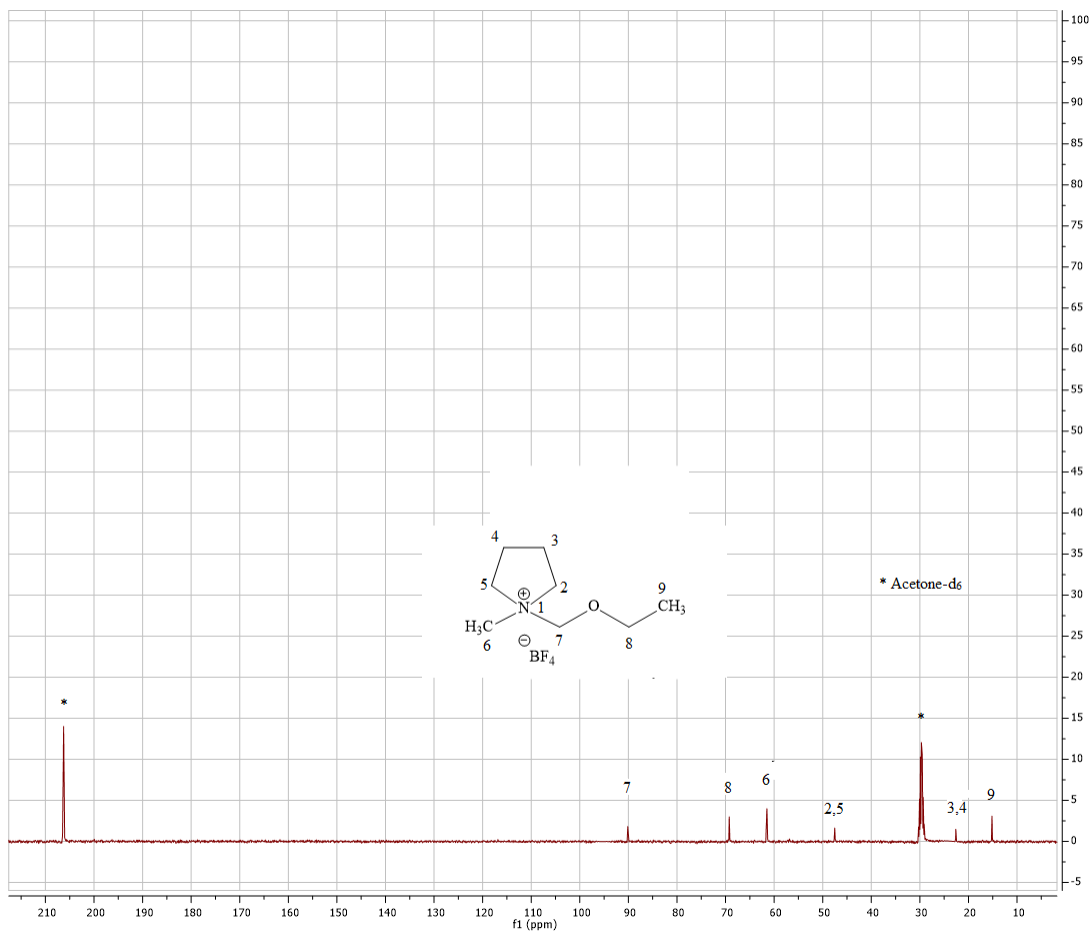


Figure A.8.  $^{13}\text{C}$  NMR decoupled (100 MHz, acetone- $d_6$ ) spectra of 1-ethoxymethyl-1-methyl-pyrrolidinium tetrafluoroborate <sup>45</sup>.



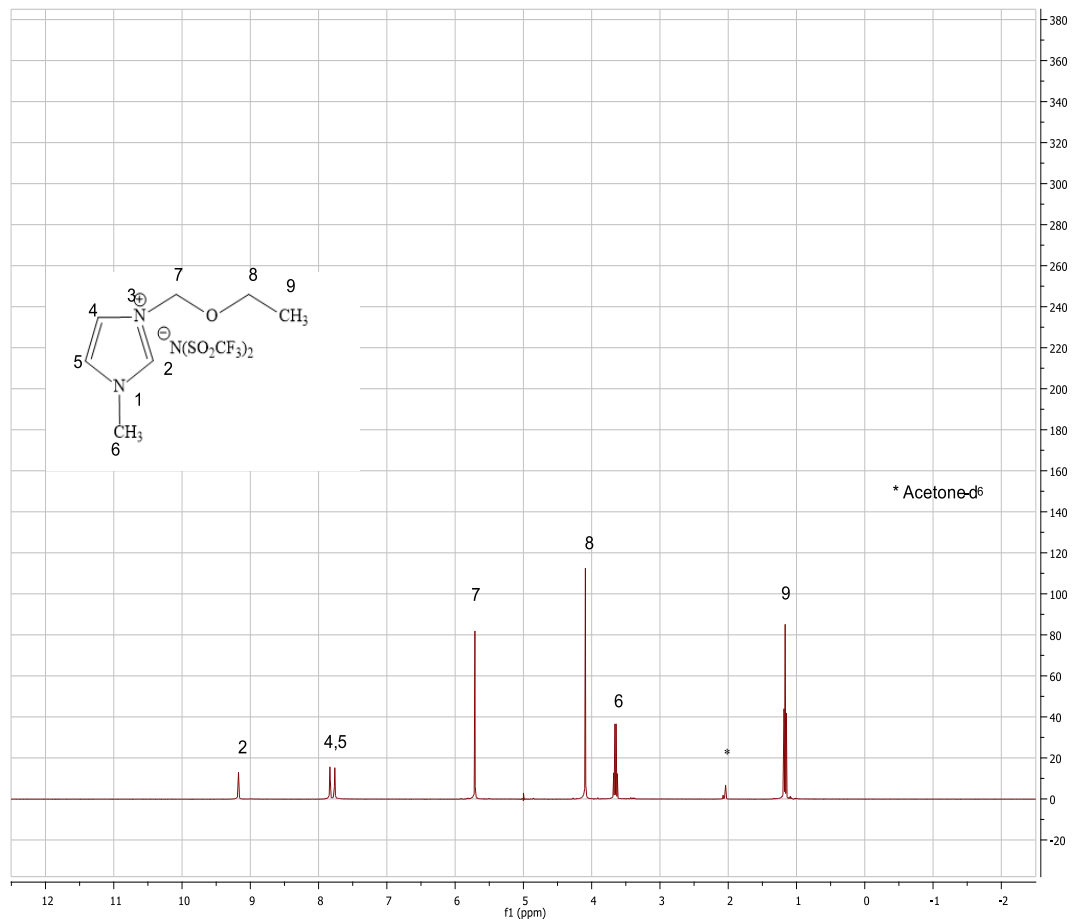


Figure A.9.  $^1\text{H}$  NMR spectrum (400 MHz) of 1-ethoxymethyl-3-methylimidazolium - bis(trifluoromethanesulfonyl)imide <sup>45</sup>.

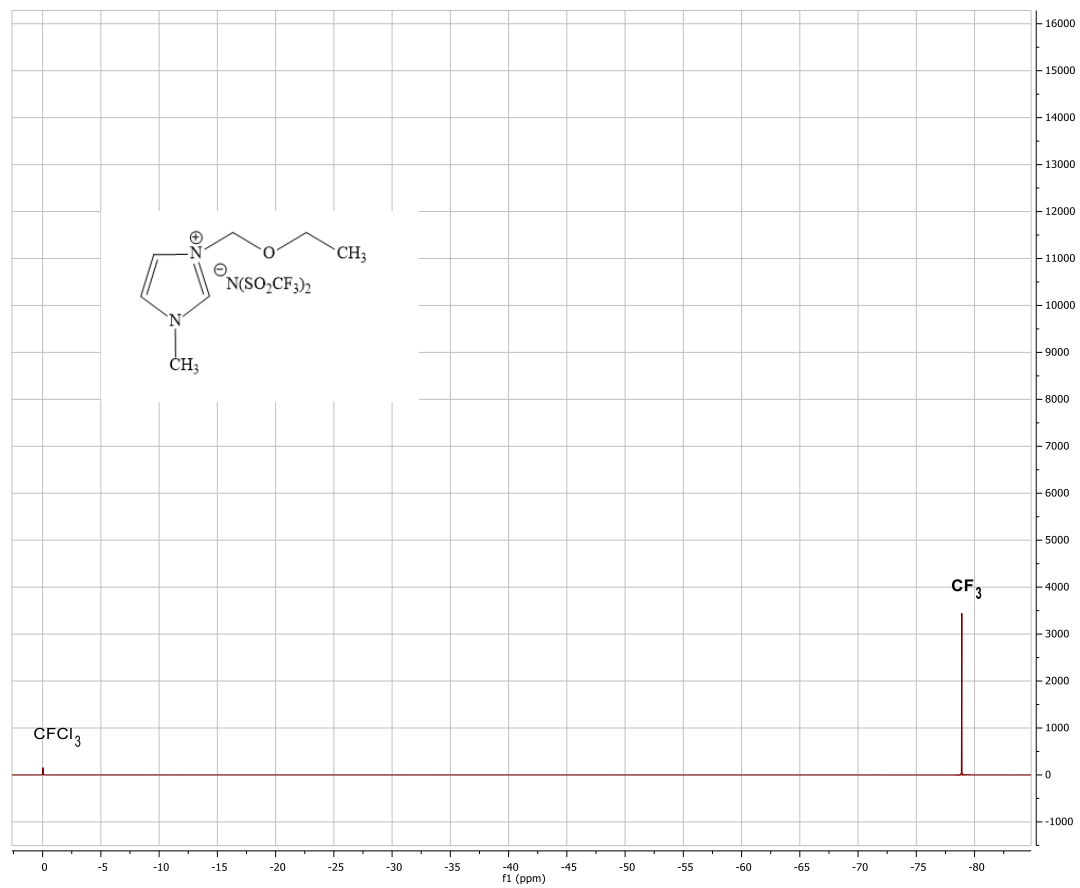


Figure A.10.  $^{19}\text{F}$  NMR spectrum (376 MHz) of 1-ethoxymethyl-3-methylimidazolium bis(trifluoromethanesulfonyl)imide <sup>45</sup>.

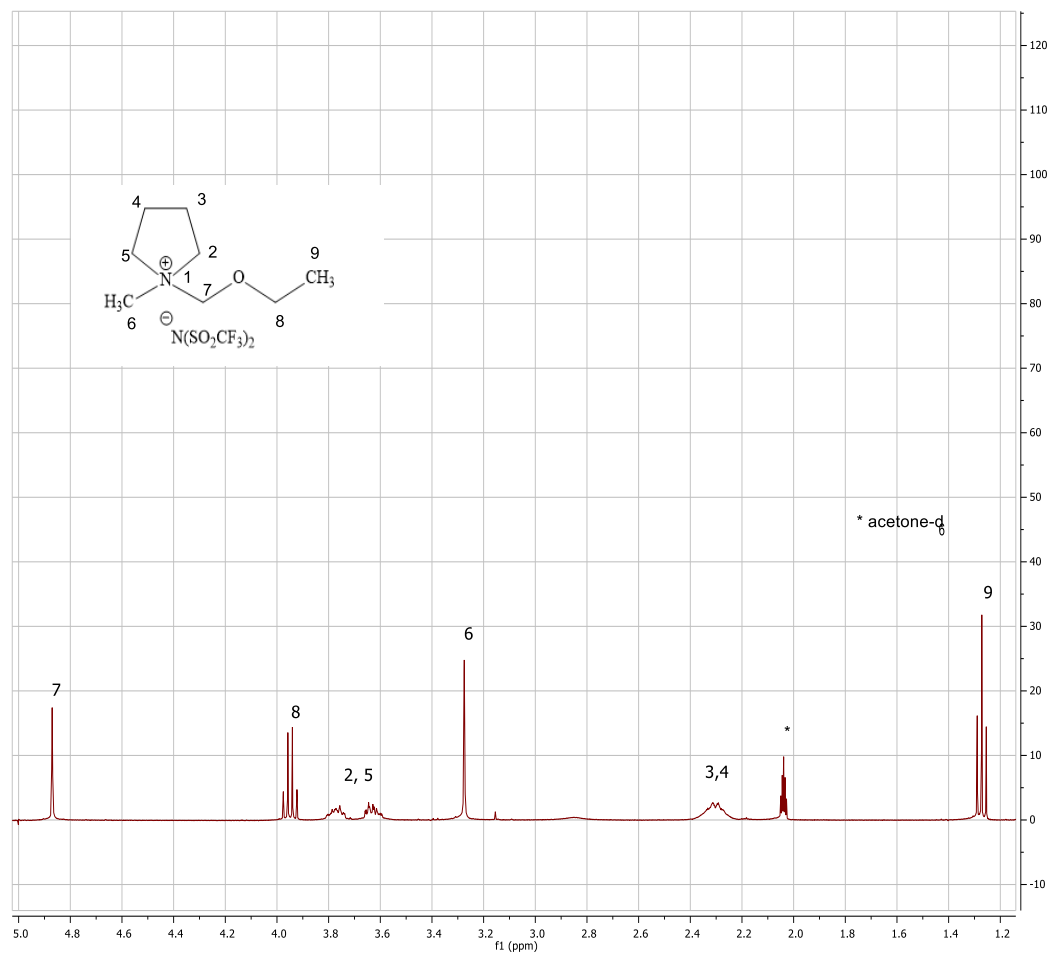


Figure A.11.  $^1\text{H}$  NMR spectrum (400 MHz) of 1-ethoxymethyl-1-methylpyrrolidinium bis(trifluoromethanesulfonyl)imide<sup>45</sup>.

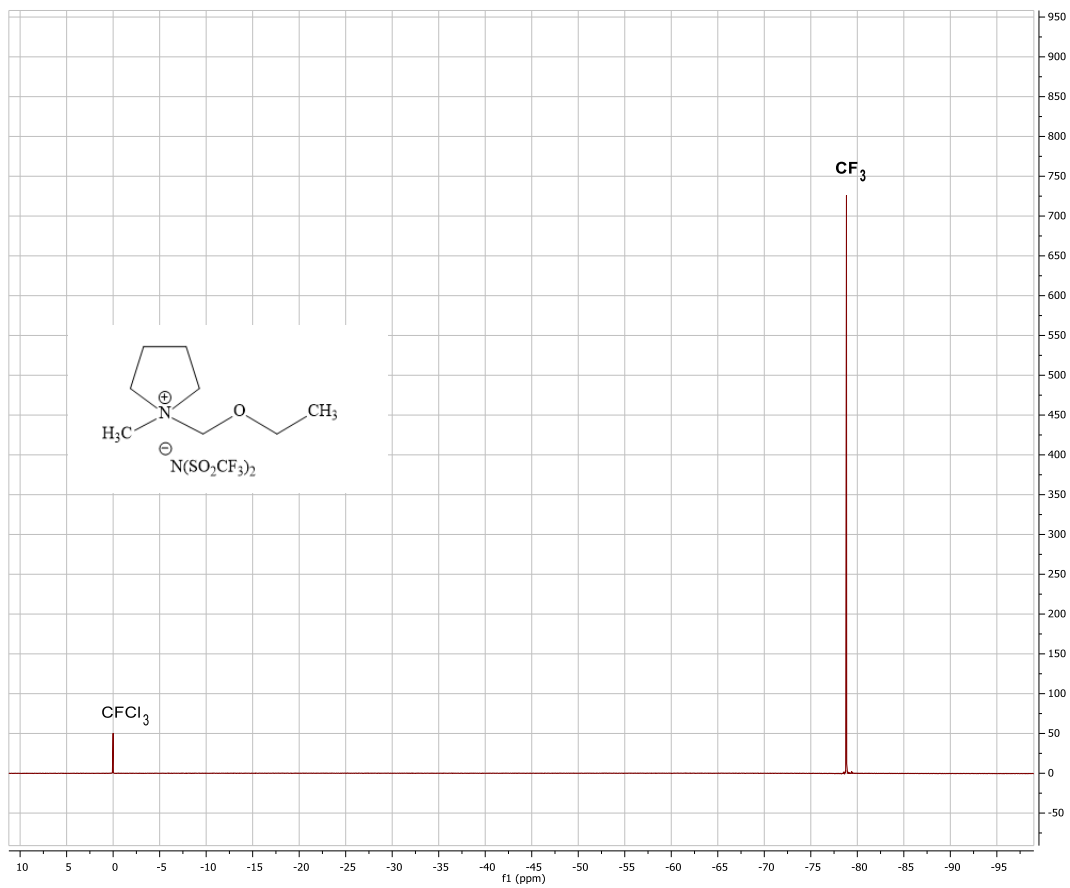


Figure A.12.  $^{19}\text{F}$  NMR (376 MHz) spectrum of 1-ethoxymethyl-1-methylpyrrolidinium bis(trifluoromethanesulfonyl)imide <sup>45</sup>.

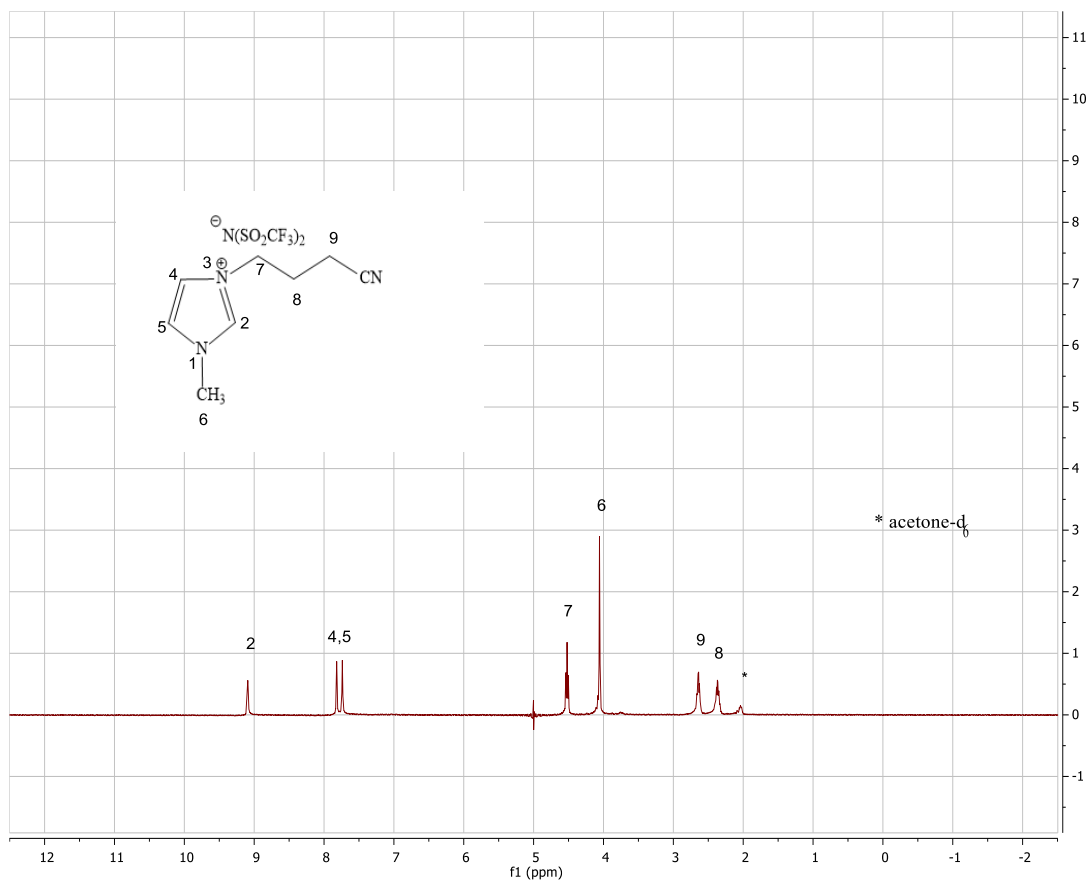


Figure A.13.  $^1\text{H}$  NMR spectrum (400 MHz) of 1-cyanopropyl-3-methylimidazolium bis(trifluoromethanesulfonyl)imide.

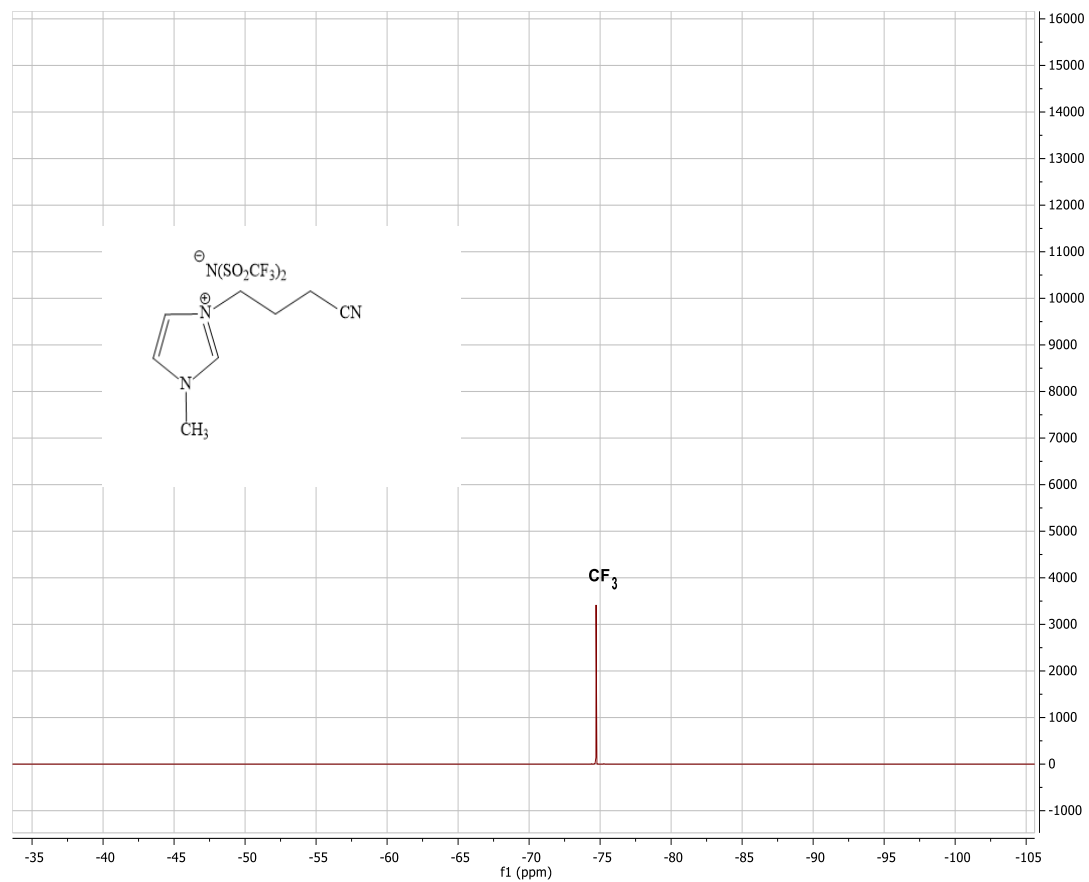


Figure A.14.  $^{19}\text{F}$  NMR (376 MHz) spectrum of 1-cyanopropyl-3-methylimidazolium bis(trifluoromethanesulfonyl)imide.

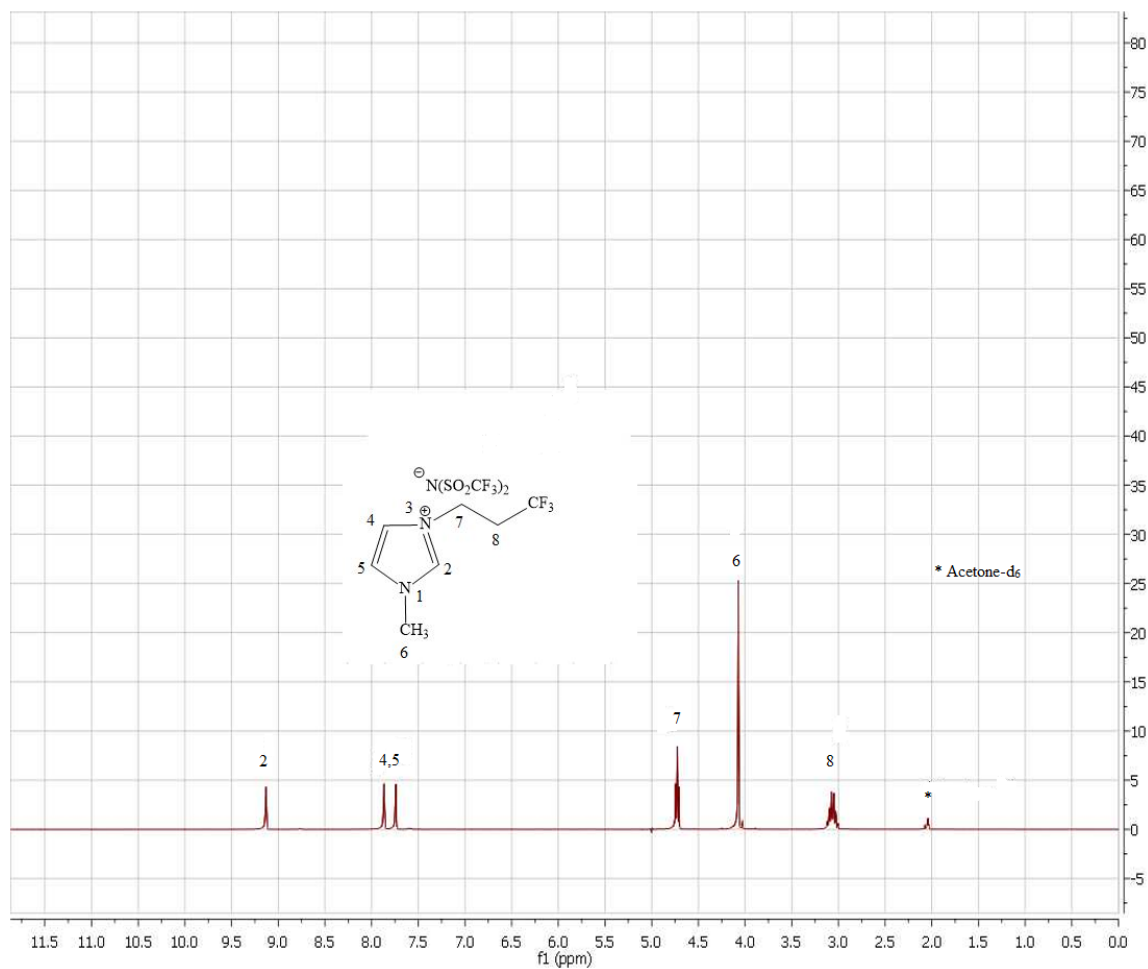


Figure A.15.  $^1\text{H}$  NMR spectrum of 1-trifluoropropyl-3-methyl-imidazolium bis(trifluoromethanesulfonyl)imide.

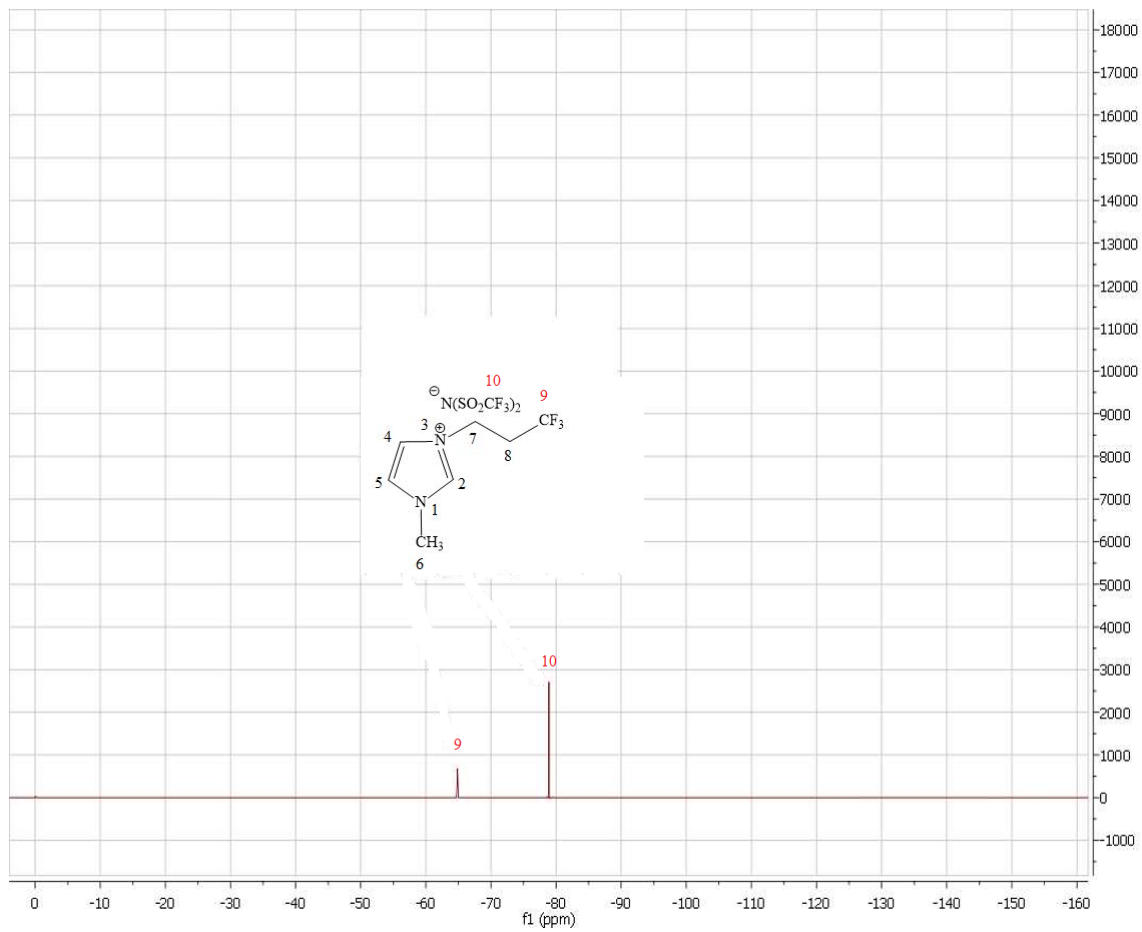


Figure A.16.  $^{19}\text{F}$  NMR (376 MHz) spectrum of 1-trifluoropropyl-3-methylimidazolium bis(trifluoromethanesulfonyl)imide.



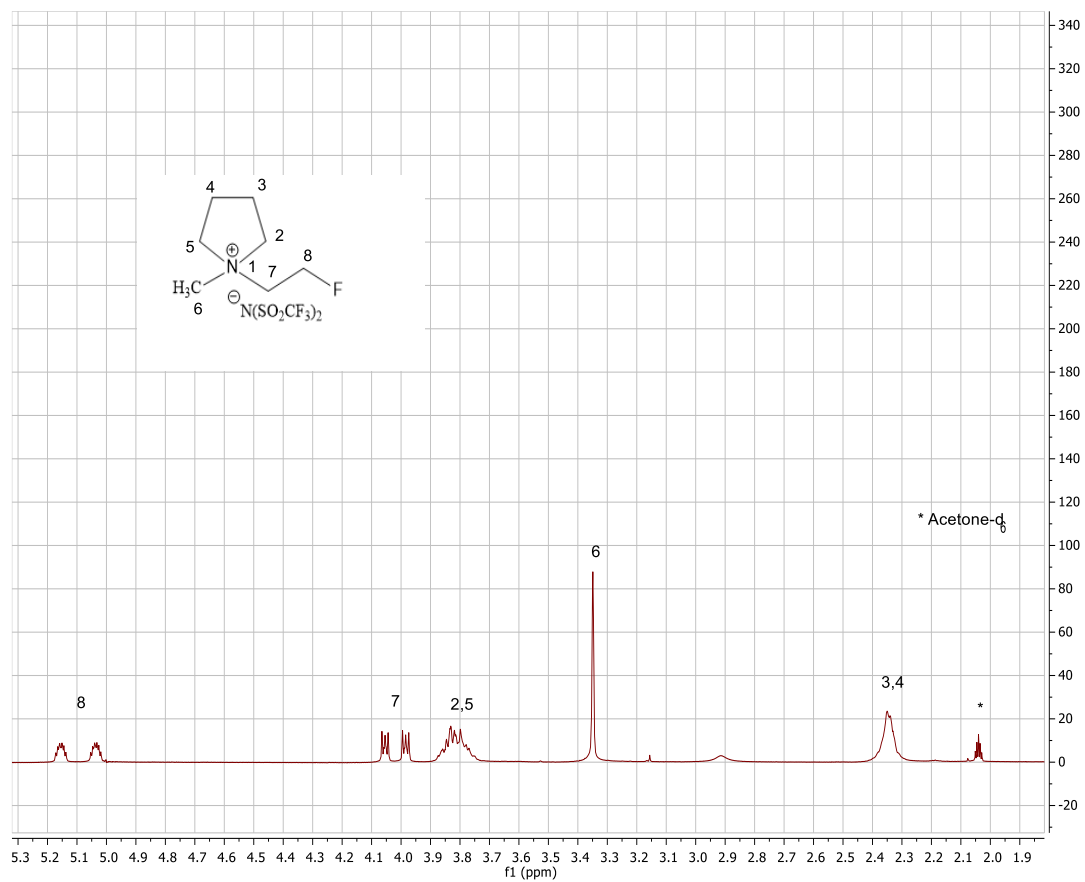


Figure A.17.  $^1\text{H}$  NMR (400 MHz, acetone- $d_6$ ) spectrum of (2-fluoroethyl)-1-methylpyrrolidinium bis(trifluoromethanesulfonyl)imide<sup>45</sup>.

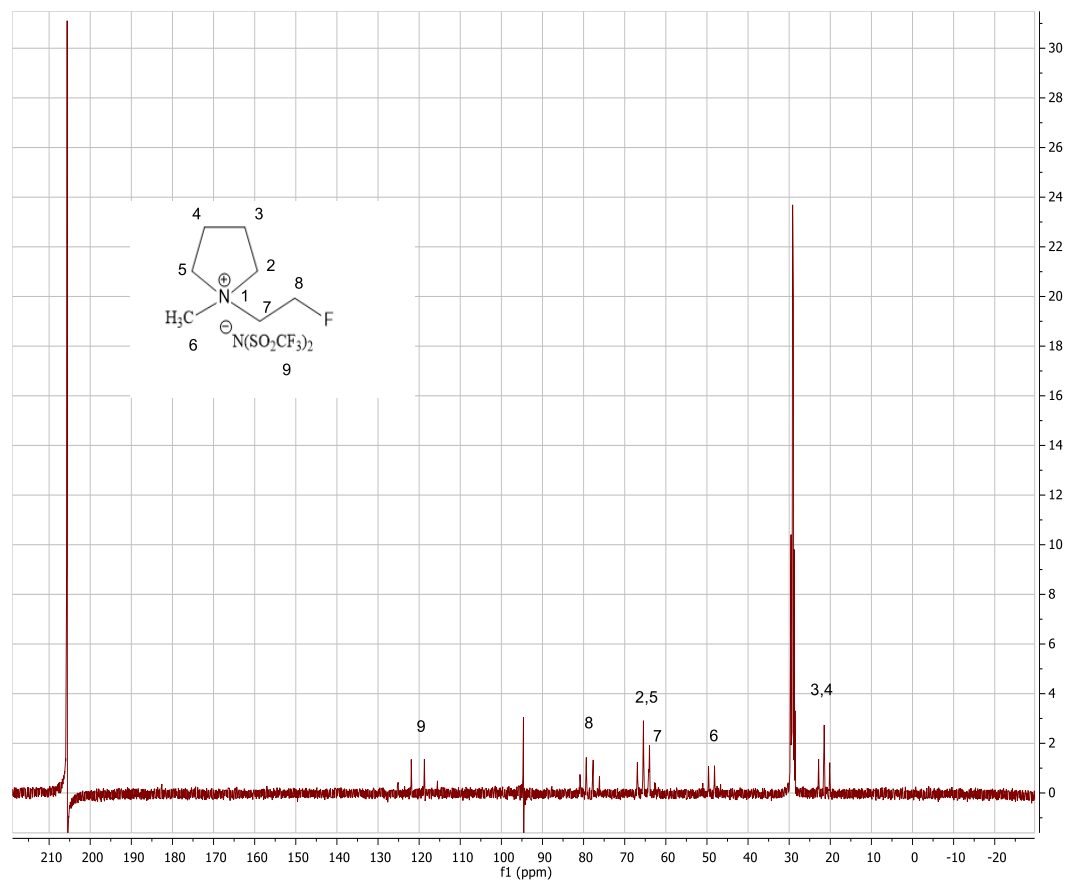


Figure A.18.  $^{13}\text{C}$  NMR ( $^1\text{H}$  coupled) (100 MHz, acetone- $d_6$ ) spectrum of 2-(fluoroethyl)-1-methylpyrrolidinium bis(trifluoromethanesulfonyl)imide <sup>45</sup>.

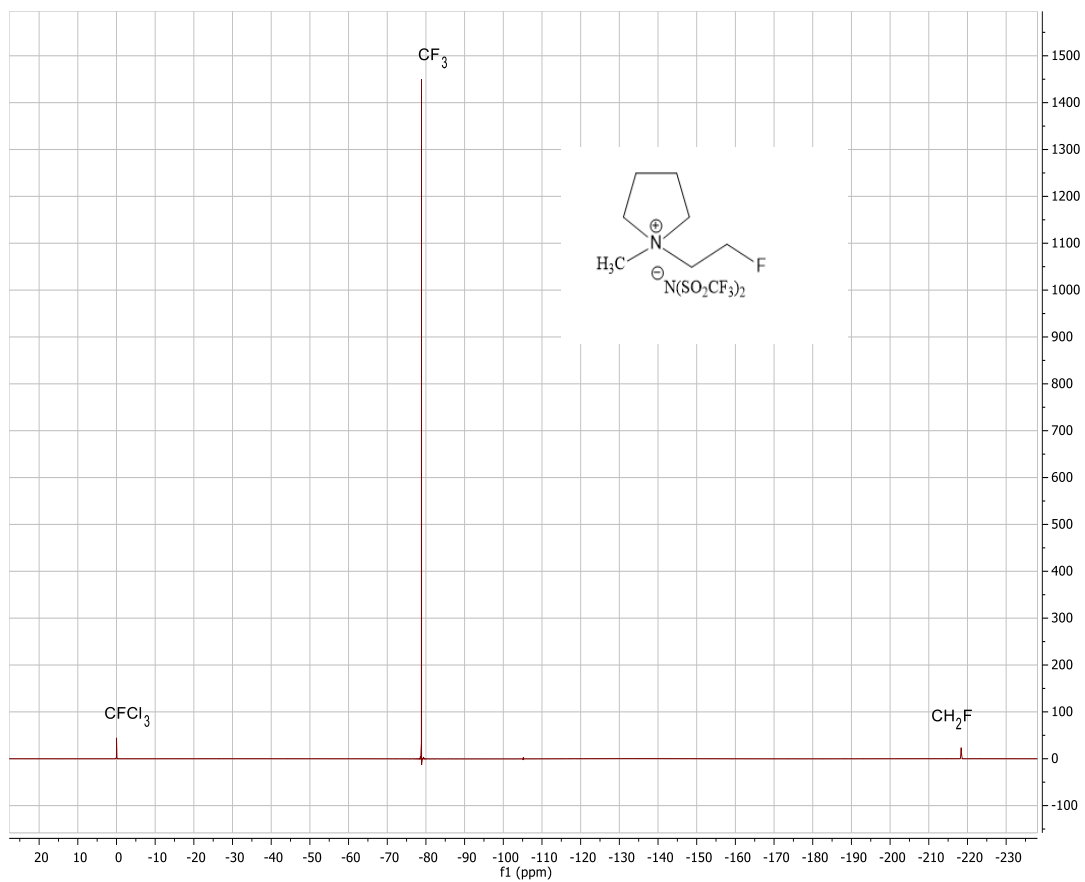


Figure A.19.  $^{19}\text{F}$  NMR (376 MHz, acetone- $d_6$ ) spectrum of 2-fluoroethyl-1-methylpyrrolidinium bis(trifluoromethanesulfonyl)imide <sup>45</sup>.

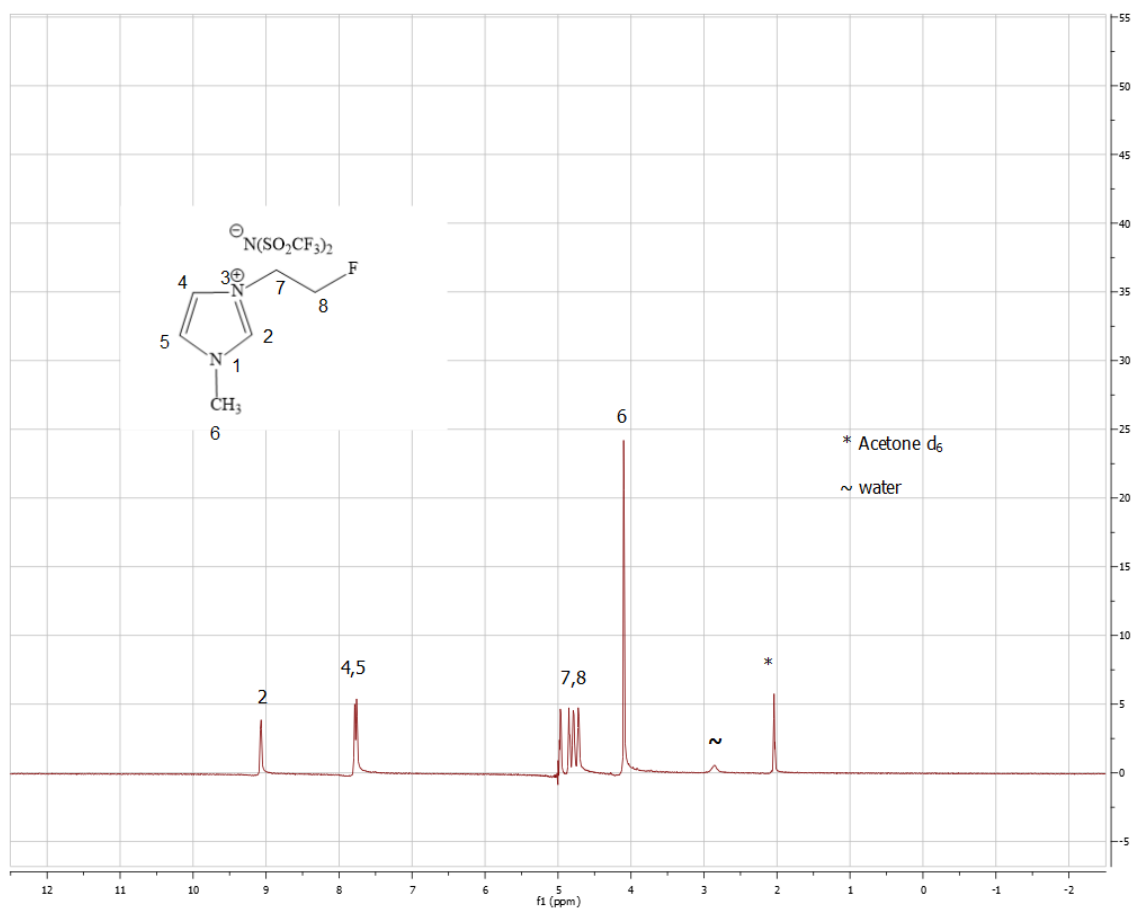


Figure A.20.  $^1\text{H}$  NMR (400 MHz, acetone- $d_6$ ) spectrum of 1-(2-fluoroethyl)-3-methylimidazolium bis(trifluoromethanesulfonyl)imide<sup>45</sup>.

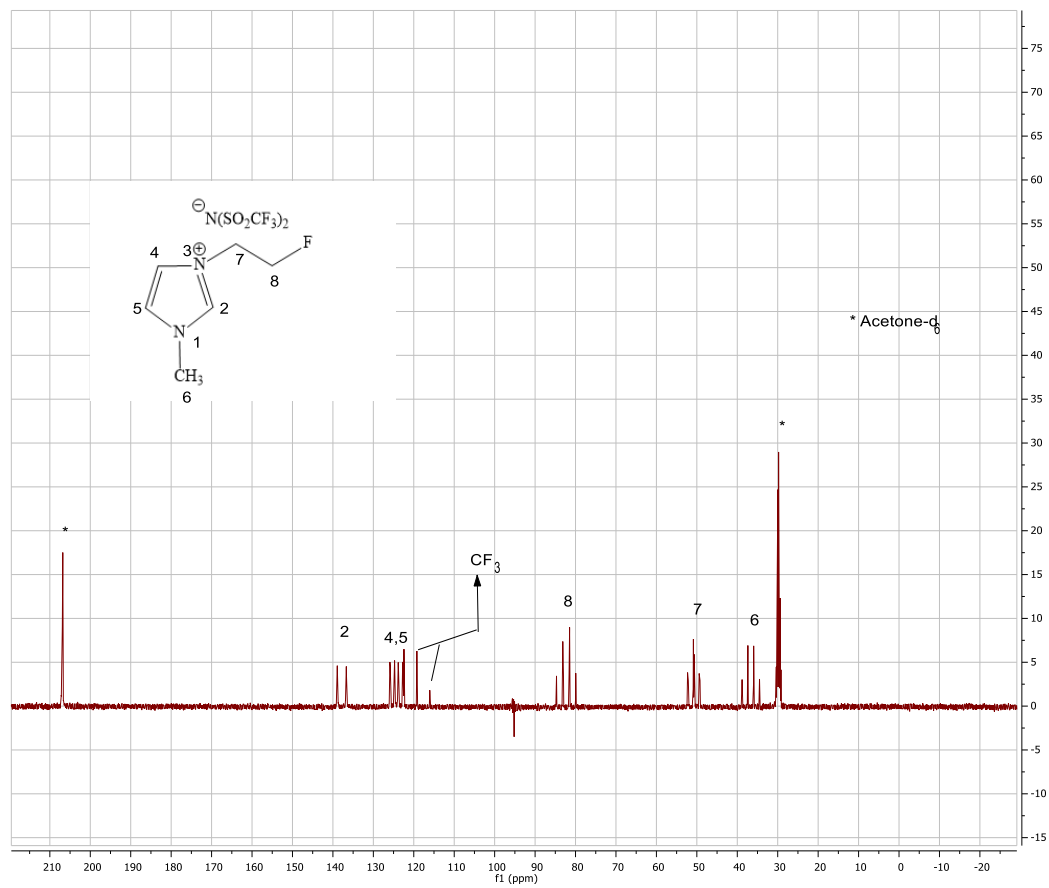


Figure A.21.  $^{13}\text{C}$  NMR ( $^1\text{H}$  coupled) (100 MHz, acetone- $d_6$ ) spectrum of 1-(2-fluoroethyl)-3-methylimidazolium bis(trifluoromethanesulfonyl)imide <sup>45</sup>.

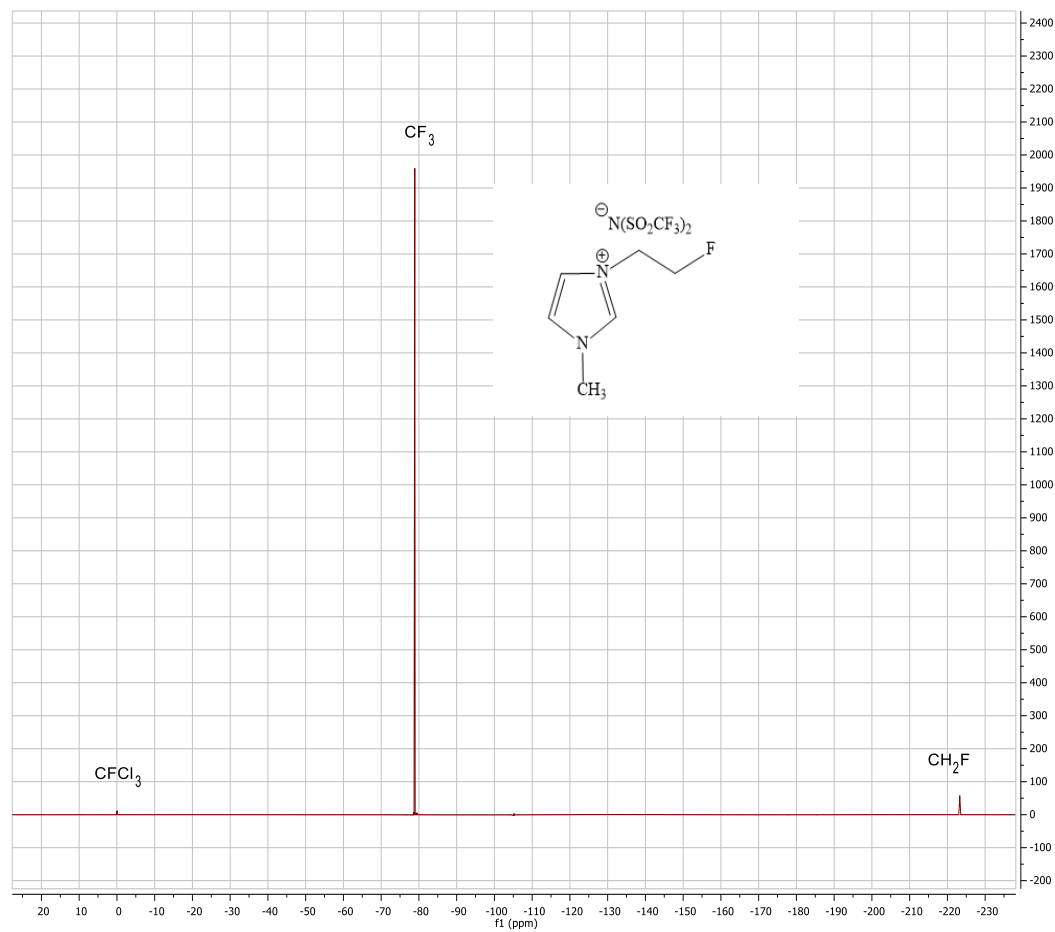


Figure A.22.  $^{19}\text{F}$  NMR (376 MHz, acetone- $d_6$ ) spectrum of 1-(2-fluoroethyl)-1-methylimidazolium bis(trifluoromethanesulfonyl)imide<sup>45</sup>.

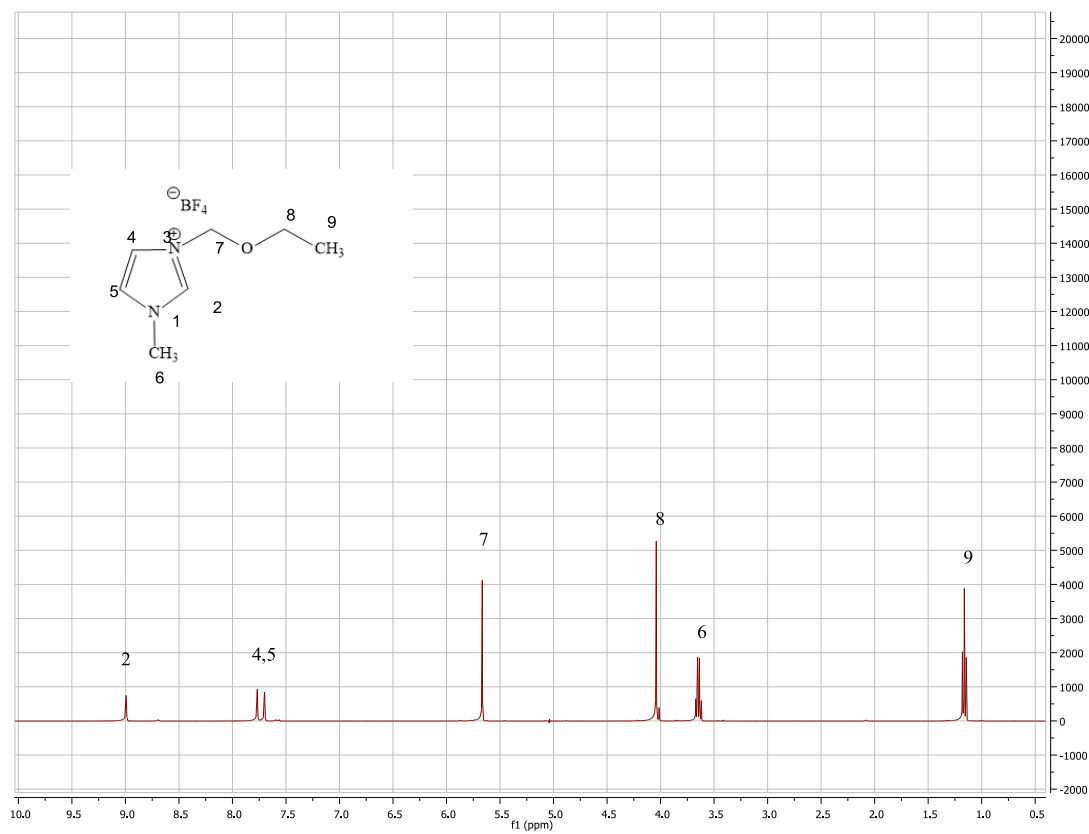


Figure. A.23.  $^1\text{H}$  NMR (400 MHz, acetone- $d_6$ ) Spectrum of 1-methyl-3-ethoxymethylimidazolium tetrafluoroborate <sup>45</sup>.

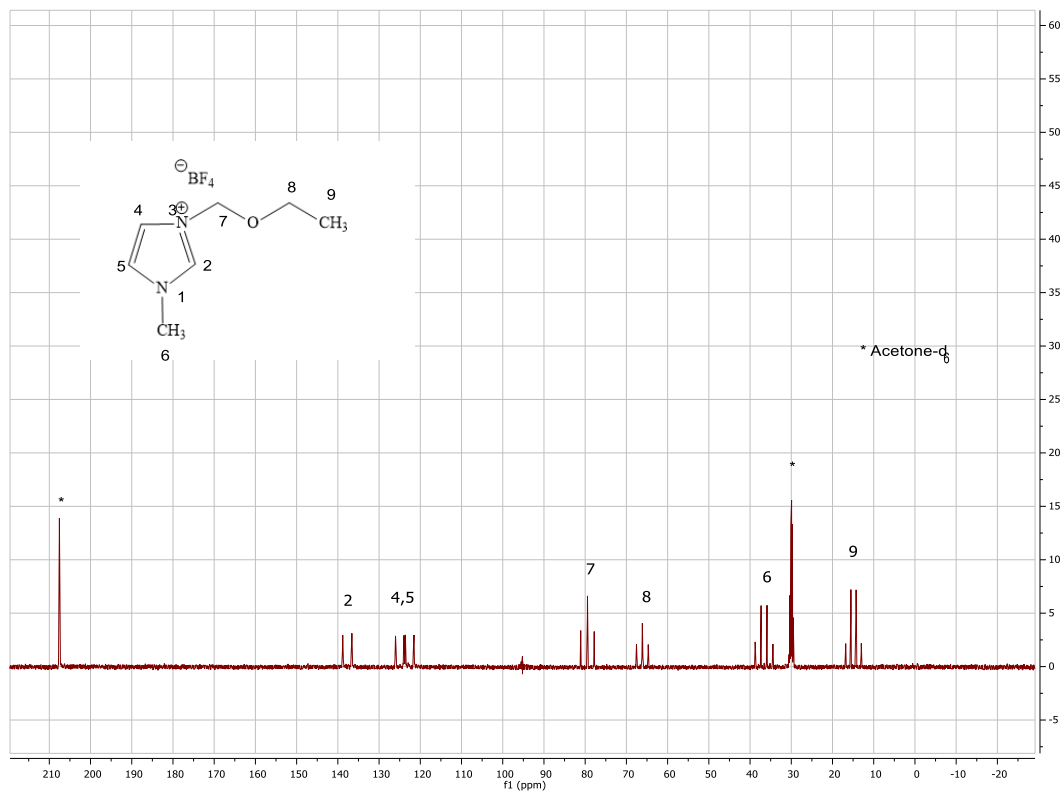


Figure A.24.  $^{13}\text{C}$  ( $^1\text{H}$  coupled) (100 MHz, acetone- $d_6$ ) spectra of 1-methyl-3-ethoxymethylimidazolium tetrafluoroborate <sup>45</sup>.



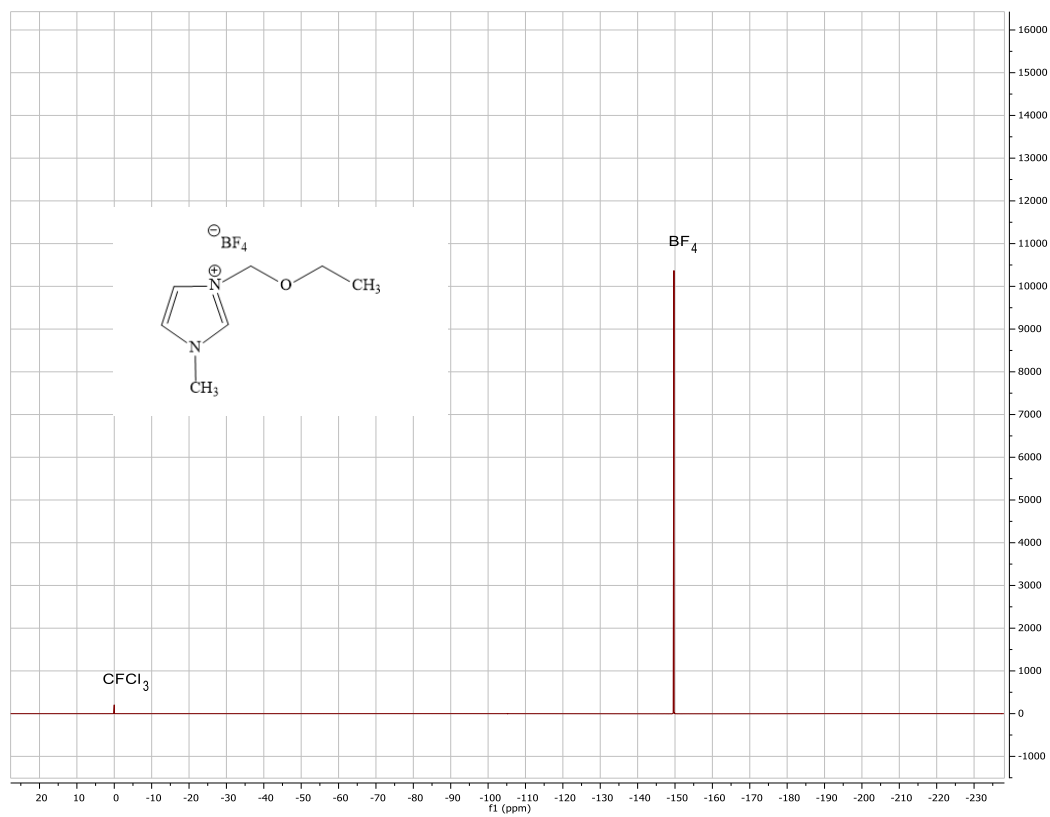


Figure.A.25.  $^{19}\text{F}$  NMR (376 MHz, acetone- $d_6$ ) spectra of 1-methyl-3-ethoxymethylimidazolium tetrafluoroborate <sup>45</sup>.

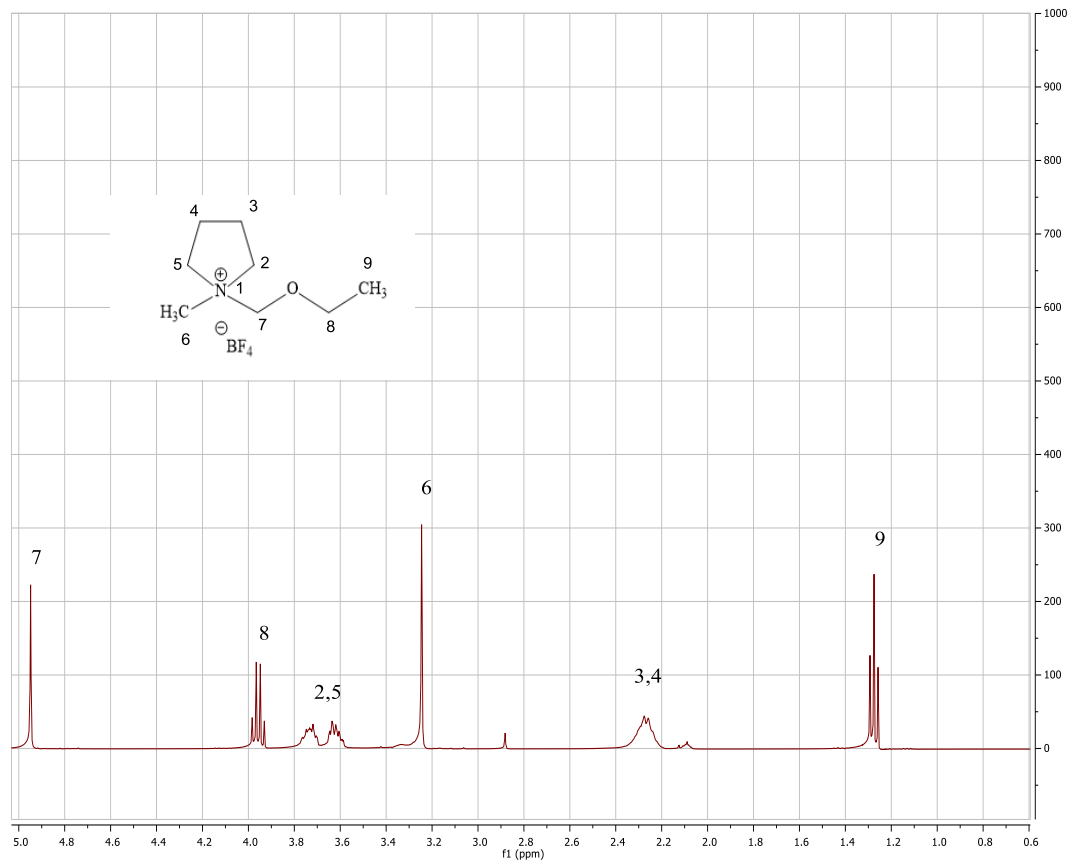


Figure A.26.  $^1\text{H}$  NMR (400 MHz, acetone- $d_6$ ) spectra of 1-ethoxymethyl-1-methylpyrrolidinium tetrafluoroborate <sup>45</sup>.

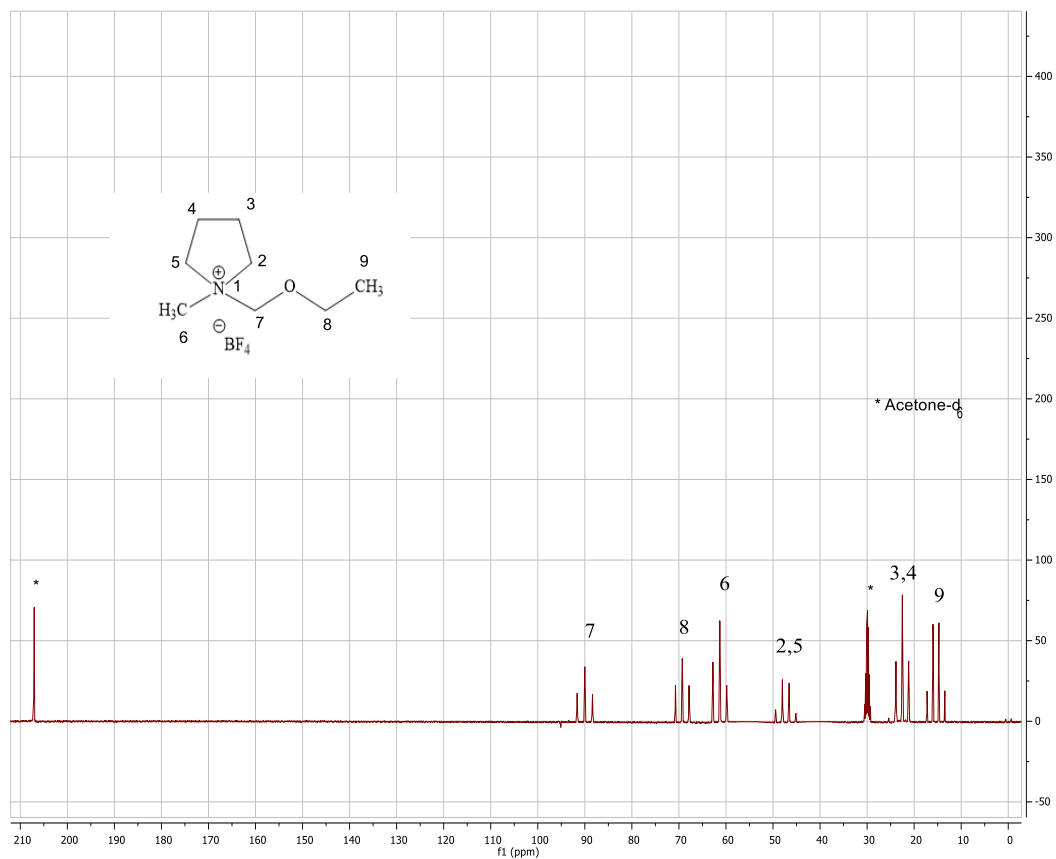


Figure A.27.  $^{13}\text{C}$  NMR ( $^1\text{H}$  coupled) (100 MHz, acetone- $d_6$ ) spectra of 1-ethoxymethyl-1-methyl-pyrrolidinium tetrafluoroborate <sup>45</sup>.

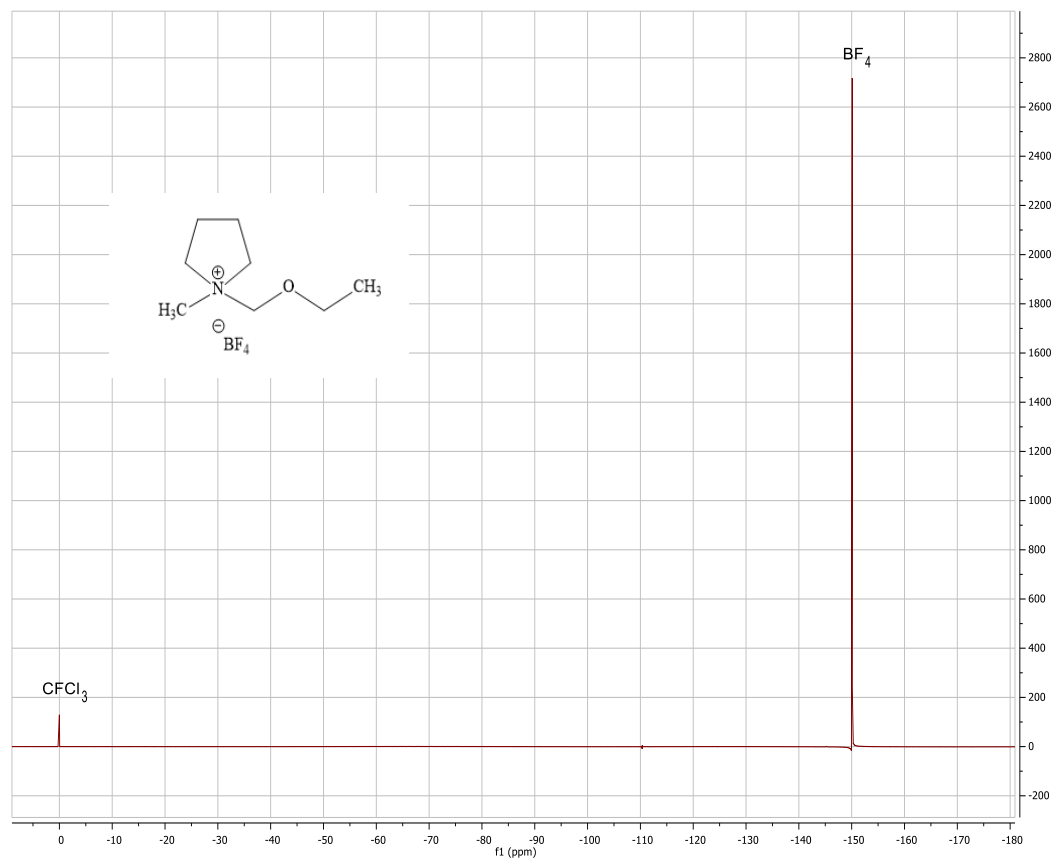


Figure A.28.  $^{19}\text{F}$  NMR (376 MHz, acetone- $d_6$ ) spectra of 1-ethoxymethyl-1-methylpyrrolidinium tetrafluoroborate <sup>45</sup>.

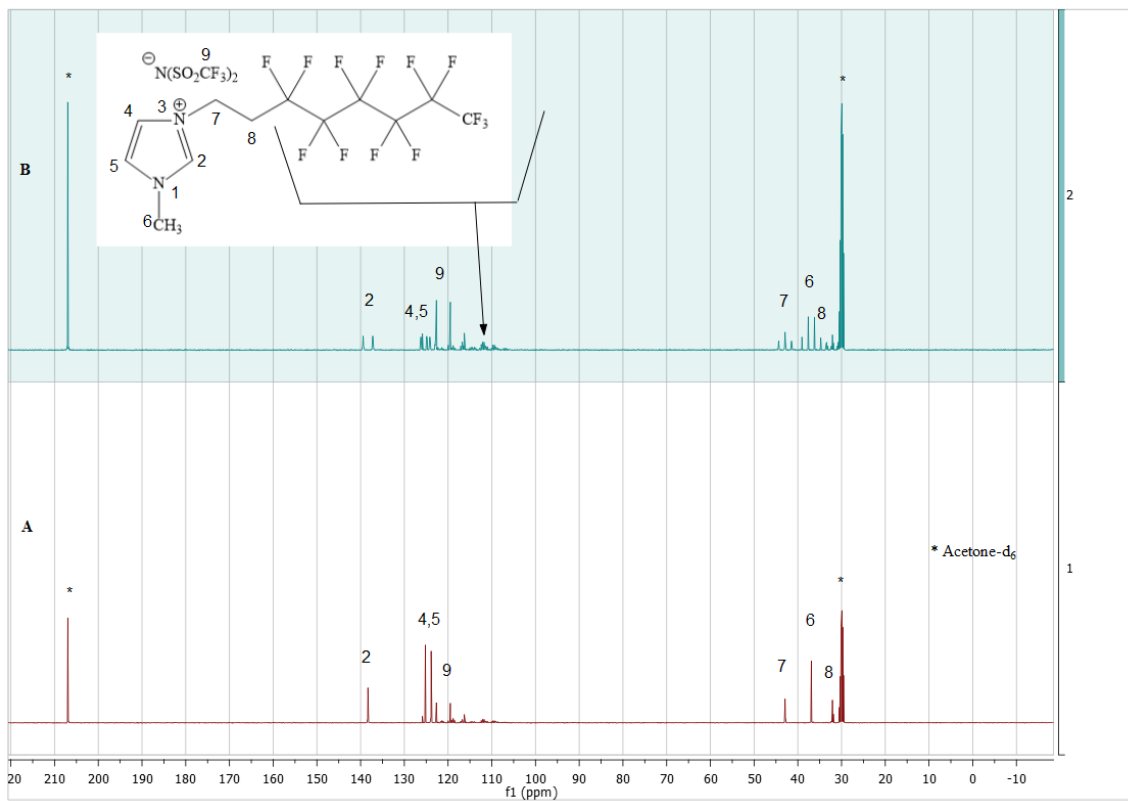


Figure.A.29.  $^{13}\text{C}$  NMR (100 MHz, **A**, proton decoupled, **B**, proton coupled) spectra of 1-Methyl-3-(3,3,4,4,5,5,6,6,7,7,8,8,8-tridecafluorooctyl)-imidazolium bis(trifluoromethanesulfonyl)imide.

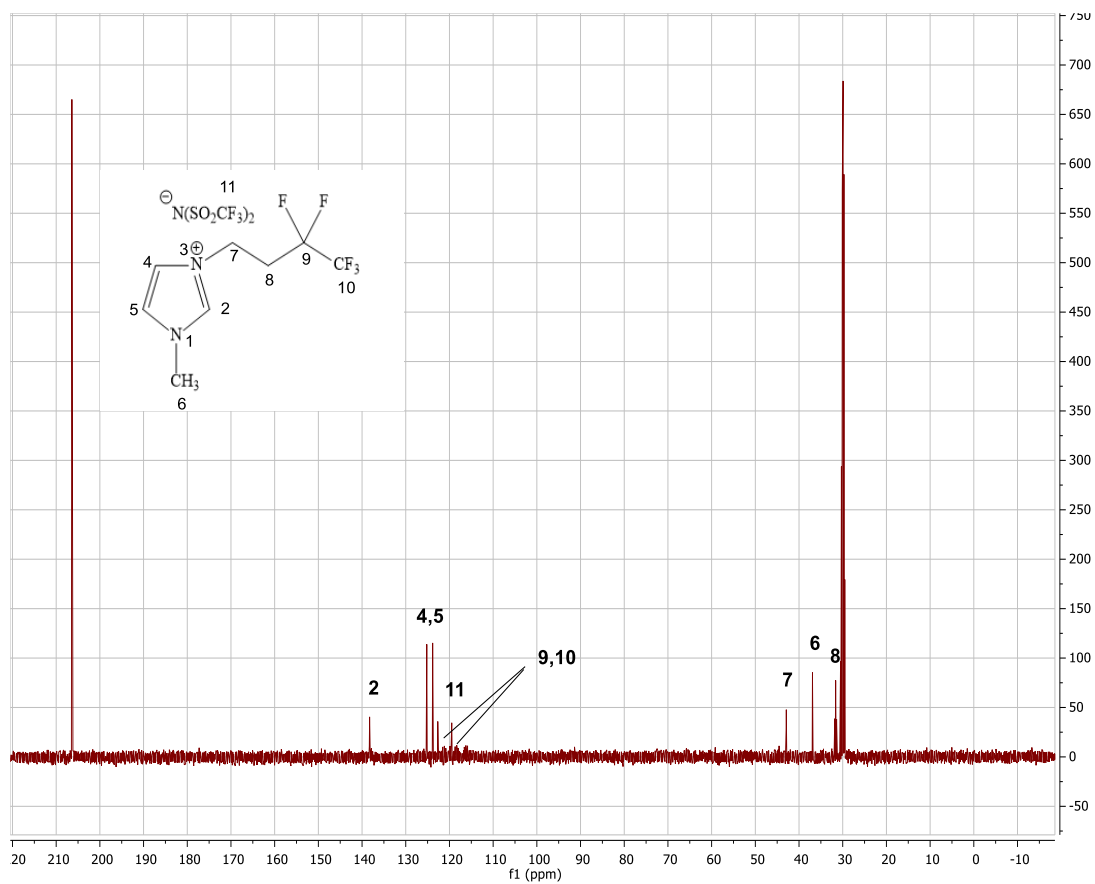


Figure.A.30.  $^{13}\text{C}$  NMR (100 MHz, proton decoupled) spectra of 1-methyl-3-(3,3,4,4,4-pentafluorobutyl)-imidazolium bis(trifluoromethanesulfonyl)imide.

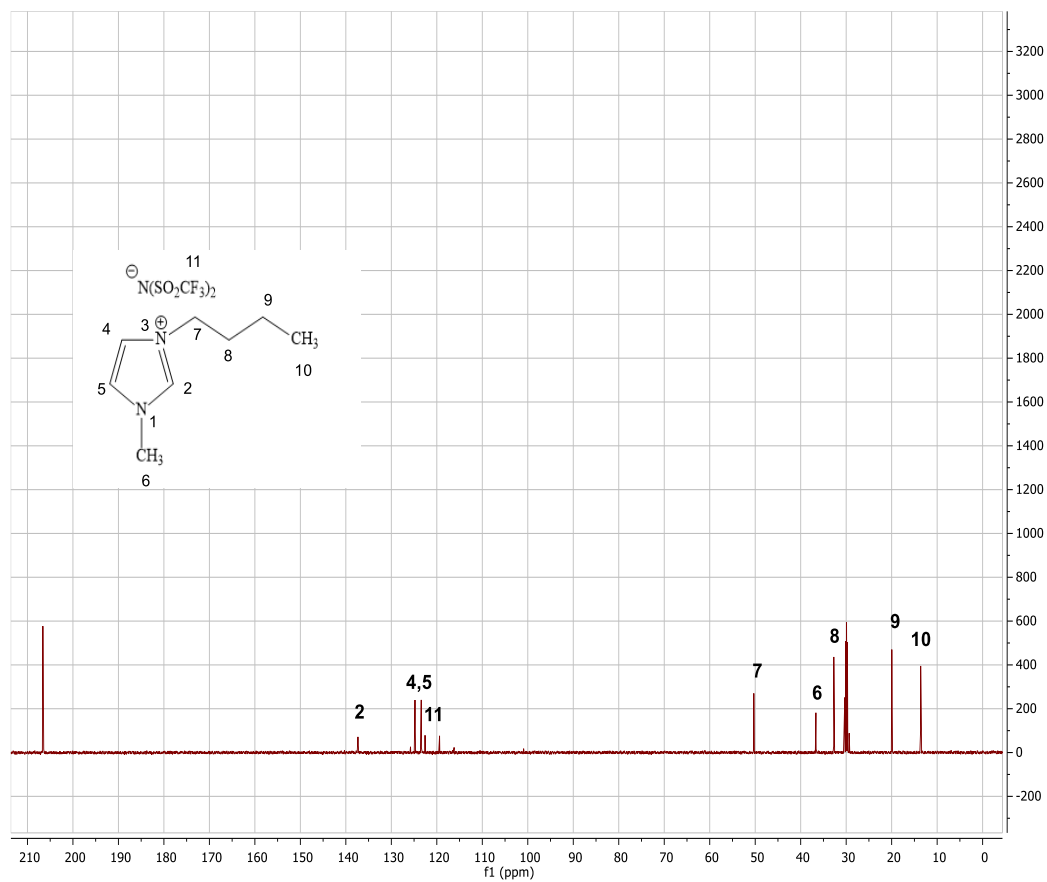


Figure.A.31.  $^{13}\text{C}$  NMR (100 MHz, proton decoupled) spectra of 1-methyl-3-butylimidazolium bis(trifluoromethanesulfonyl)imide.

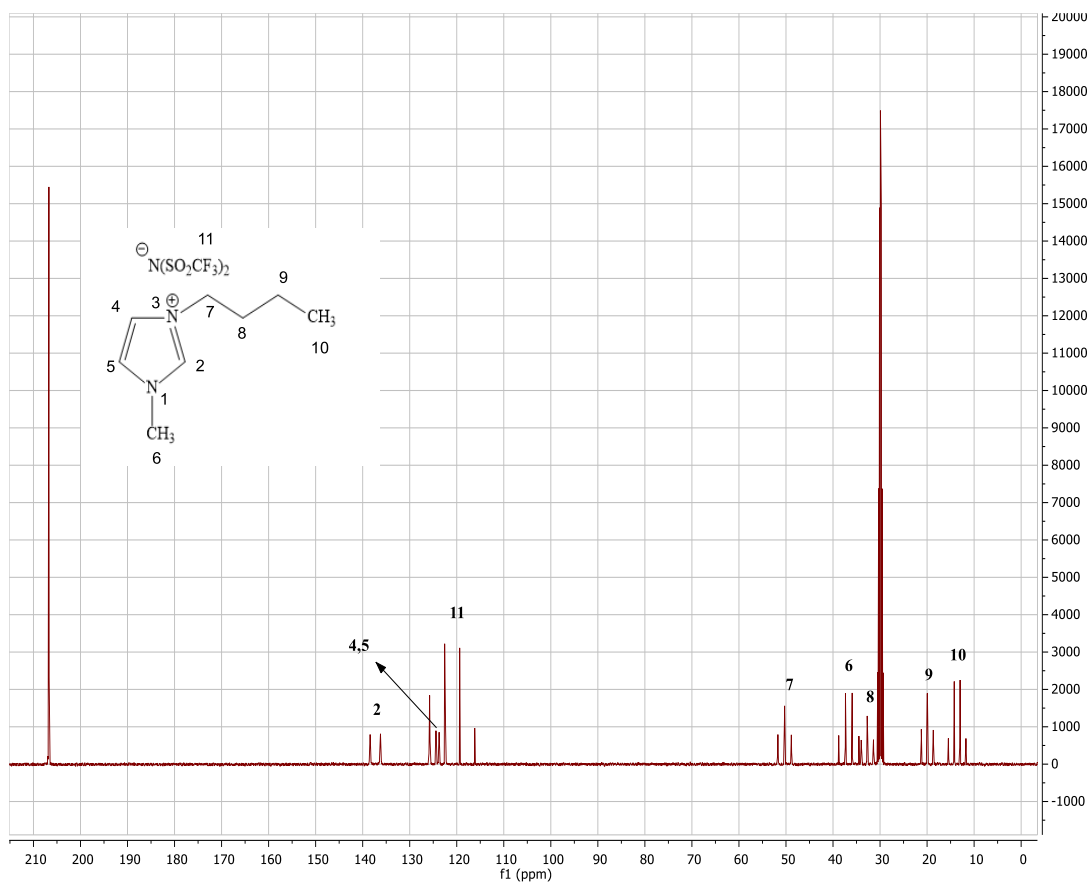


Figure.A.32.  $^{13}\text{C}$  NMR (100 MHz, proton coupled) spectra of 1-methyl-3-butylimidazolium bis(trifluoromethanesulfonyl)imide.



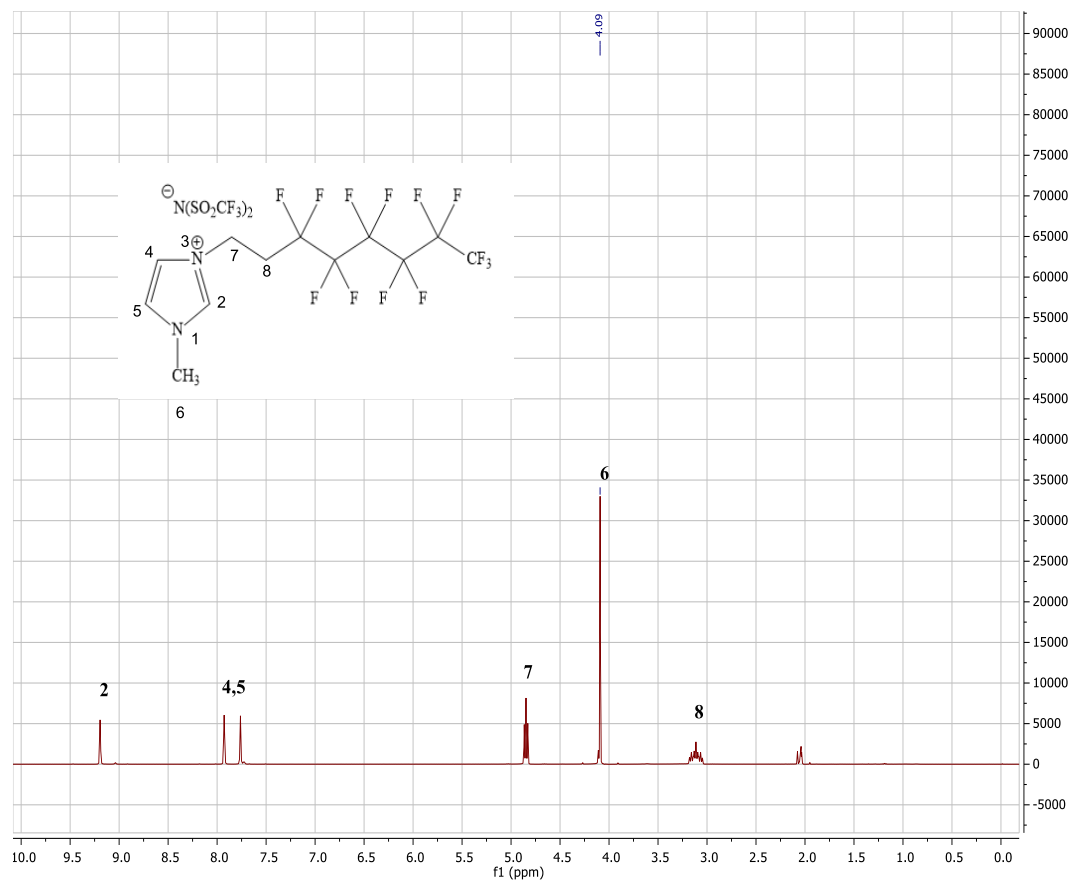


Figure A.33. <sup>1</sup>H NMR spectrum (400 MHz) of 1-Methyl-3-(3,3,4,4,5,5,7,7,8,8,8-tridecafluorohexyl)-imidazolium bis(trifluoromethanesulfonyl)imide.

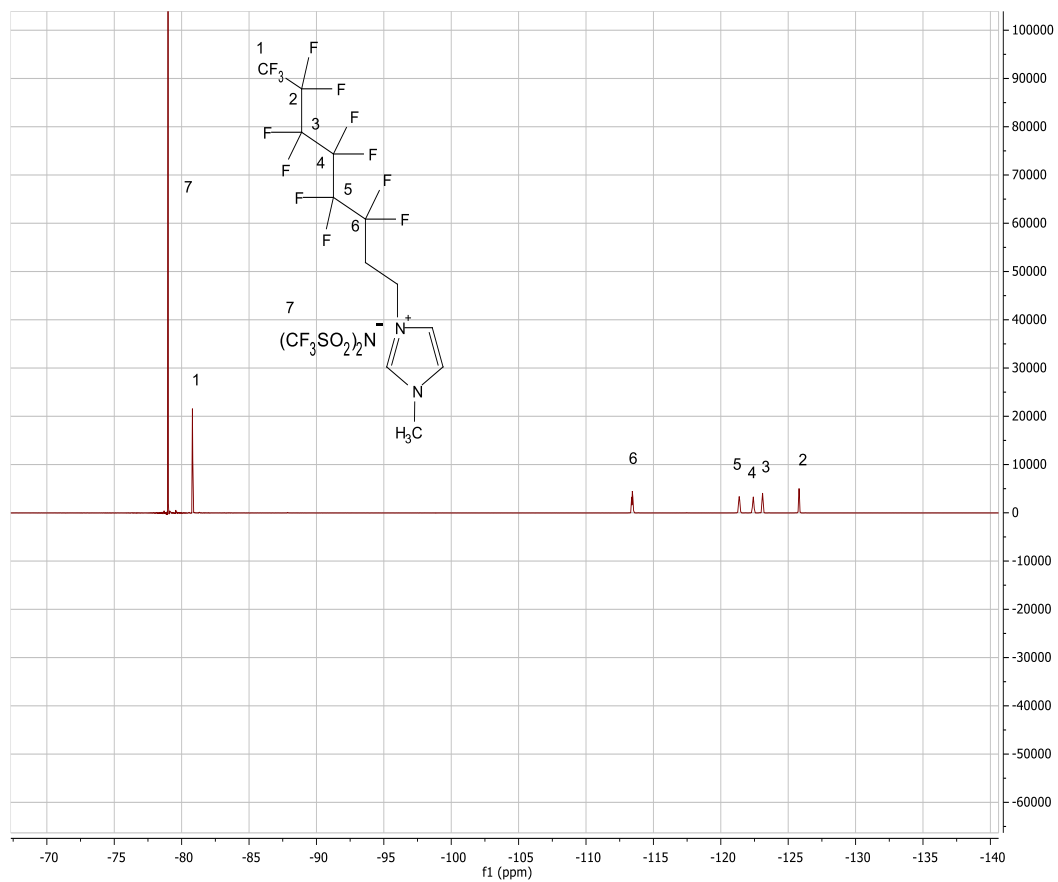


Figure A.34.  $^{19}\text{F}$  NMR (376 MHz) spectrum of 1-Methyl-3-(3,3,4,4,5,5,7,7,8,8,8-tridecafluorohexyl)-imidazolium bis(trifluoromethanesulfonyl)imide.

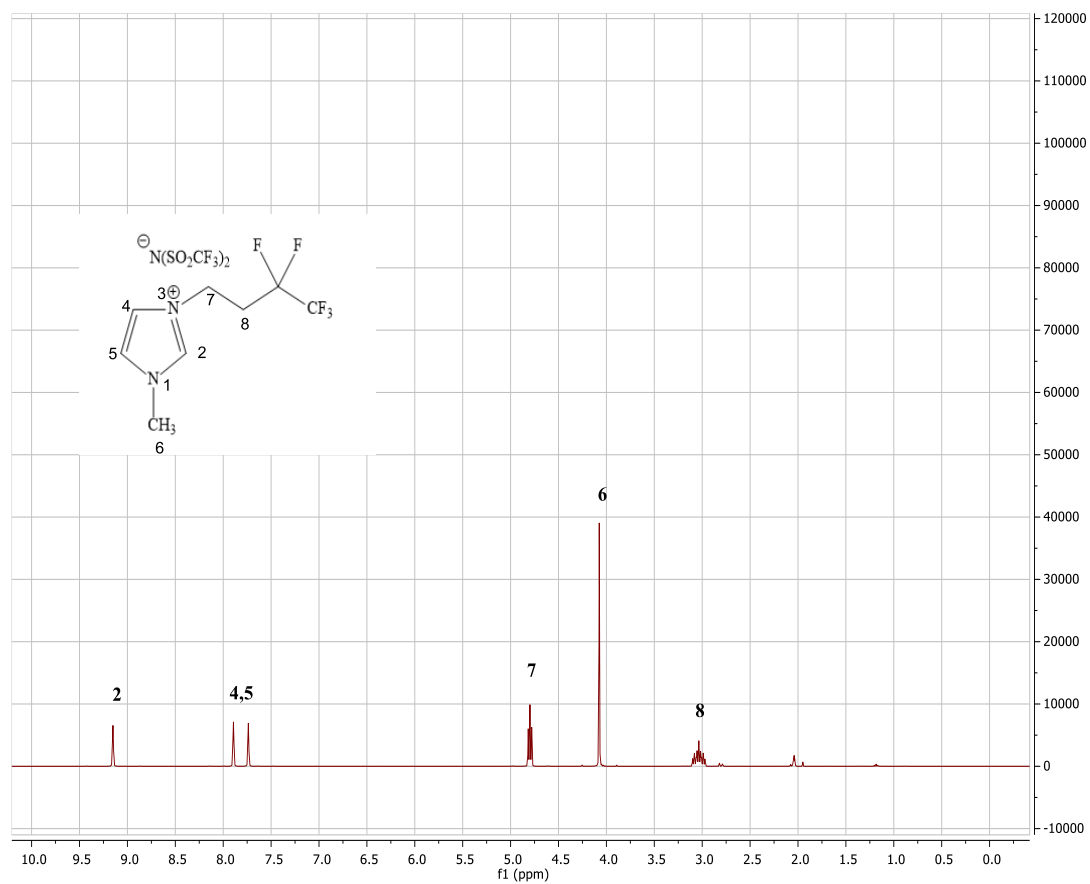


Figure A.35.  $^1\text{H}$  NMR spectrum (400 MHz) of 1-methyl-3-(3,3,4,4,4-pentafluorohexyl)imidazolium bis(trifluoromethanesulfonyl)imide.

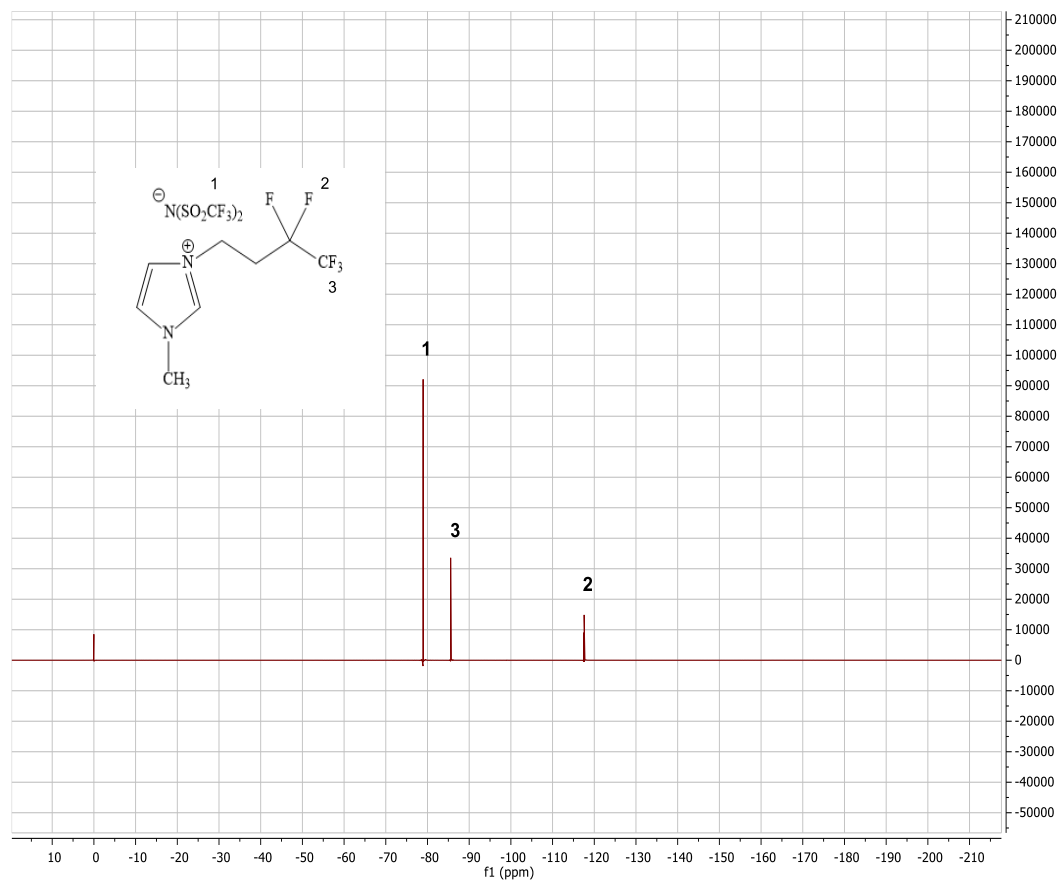


Figure A.36.  $^{19}\text{F}$  NMR (376 MHz) spectrum of 1-methyl-3-(3,3,4,4,4-pentafluorohexyl)imidazolium bis(trifluoromethanesulfonyl)imide.

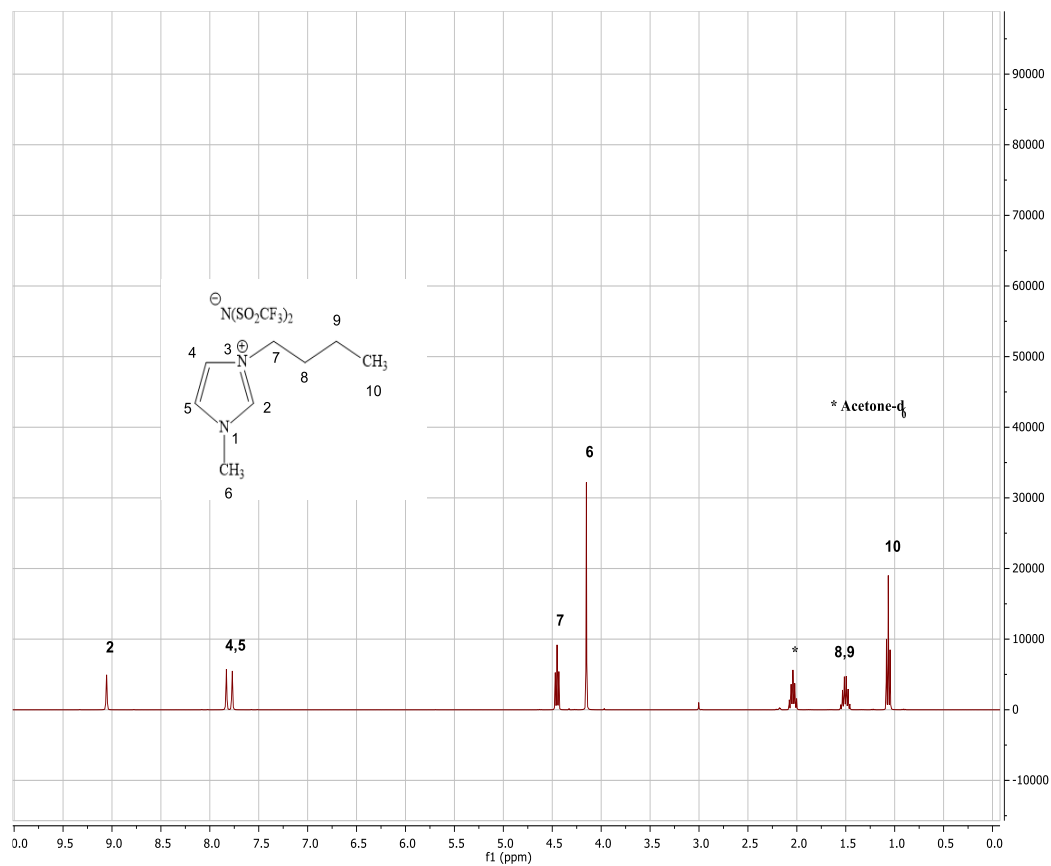


Figure A.37.  $^1\text{H}$  NMR spectrum (400 MHz) of 1-methyl-3-butylimidazolium bis(trifluoromethanesulfonyl)imide.

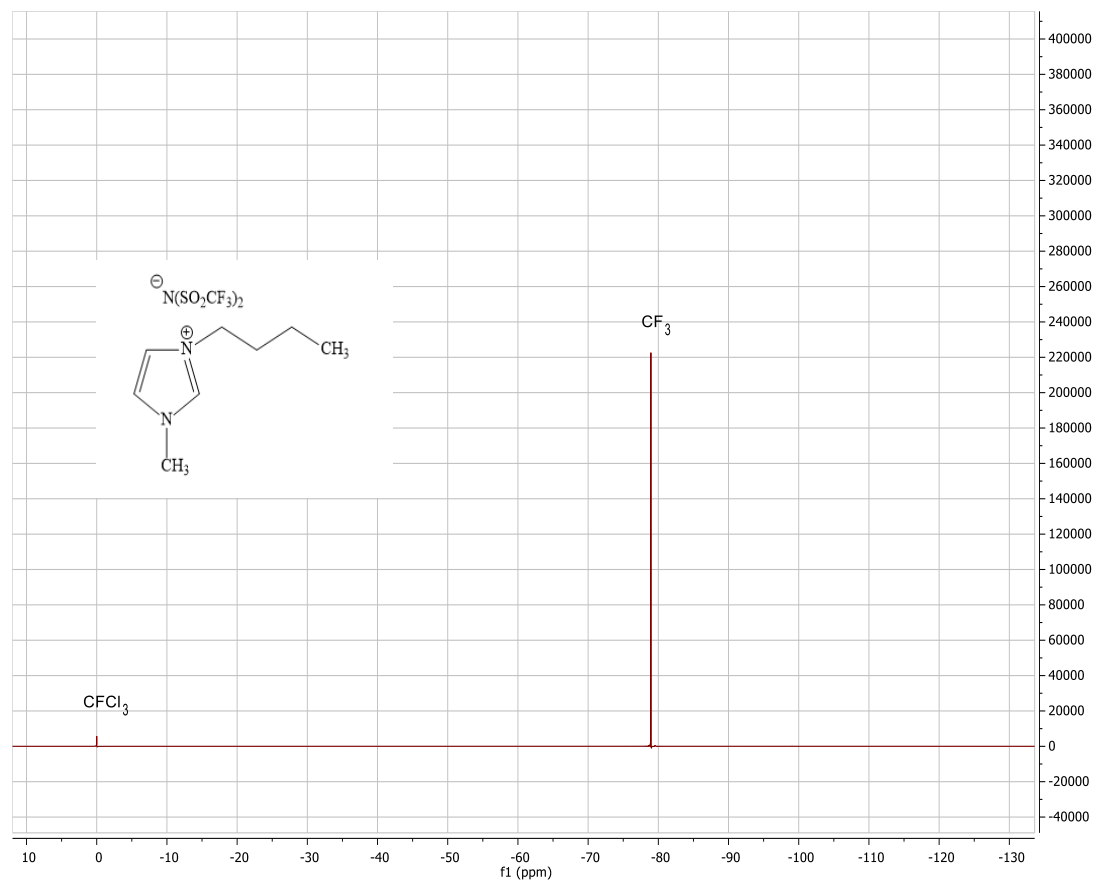


Figure A.38.  $^{19}\text{F}$  NMR (376 MHz) spectrum of 1-methyl-3-butylimidazolium bis(trifluoromethanesulfonyl)imide.

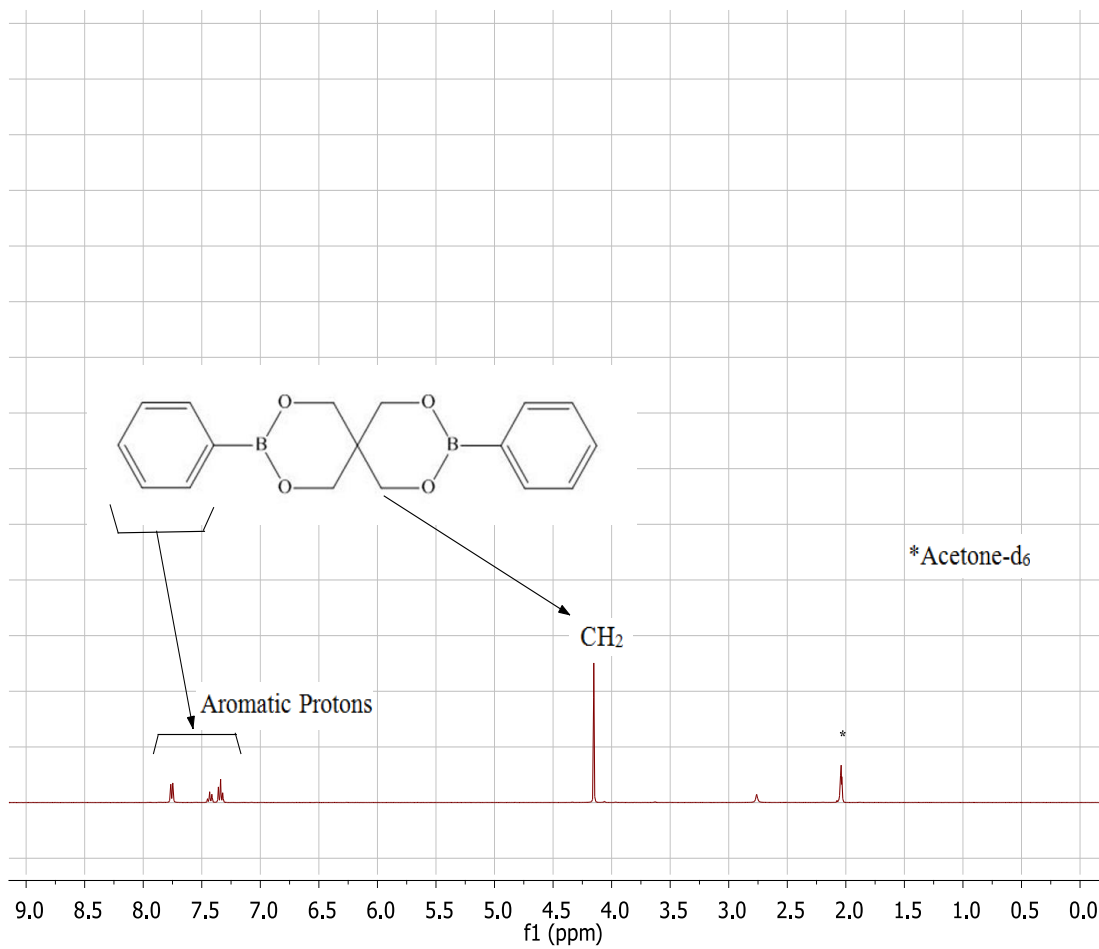


Figure A.39. <sup>1</sup>H NMR spectrum (400 MHz) of 3,9-diphenyl-2,4,8,10-tetraoxa-3,9-diborospiro[5.5]undecane.

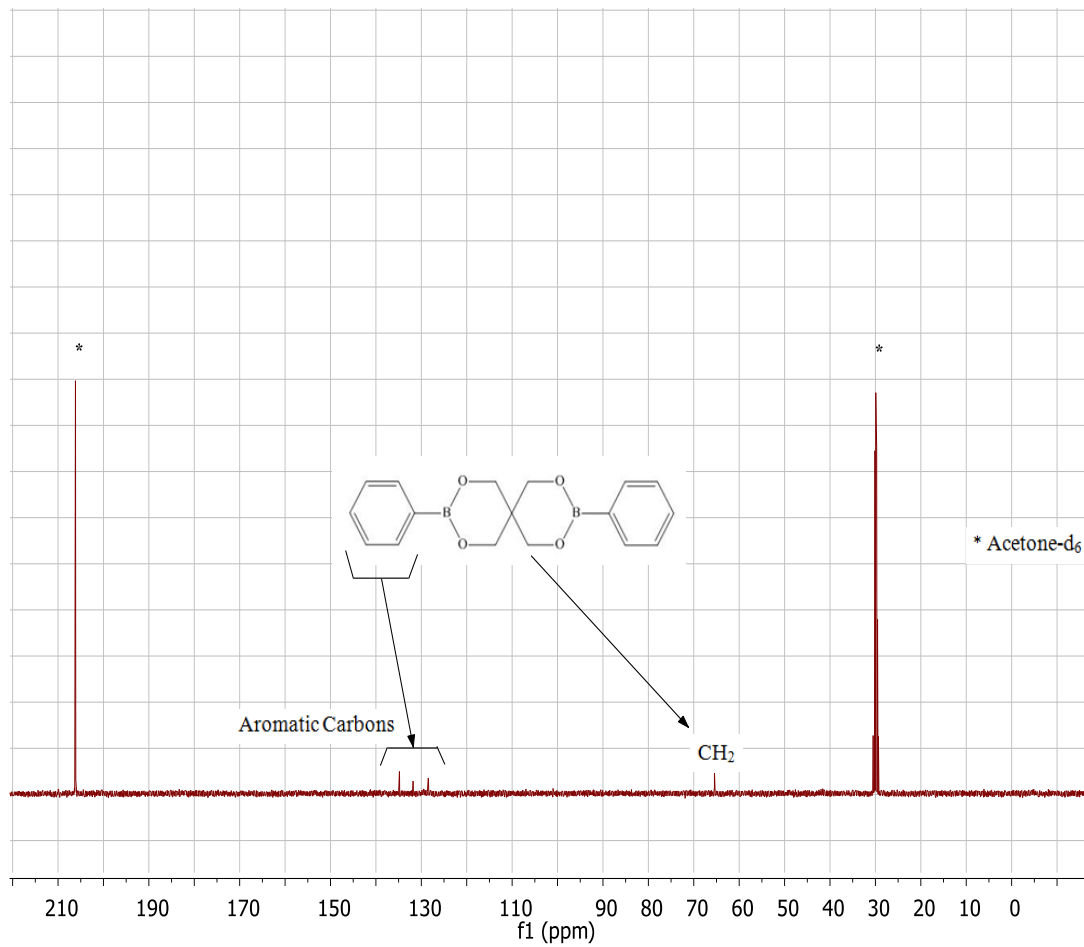


Figure A.40.  $^{13}\text{C}$  NMR spectrum (100 MHz) of 3,9-diphenyl-2,4,8,10-tetraoxa-3,9-diborospiro[5.5]undecane.



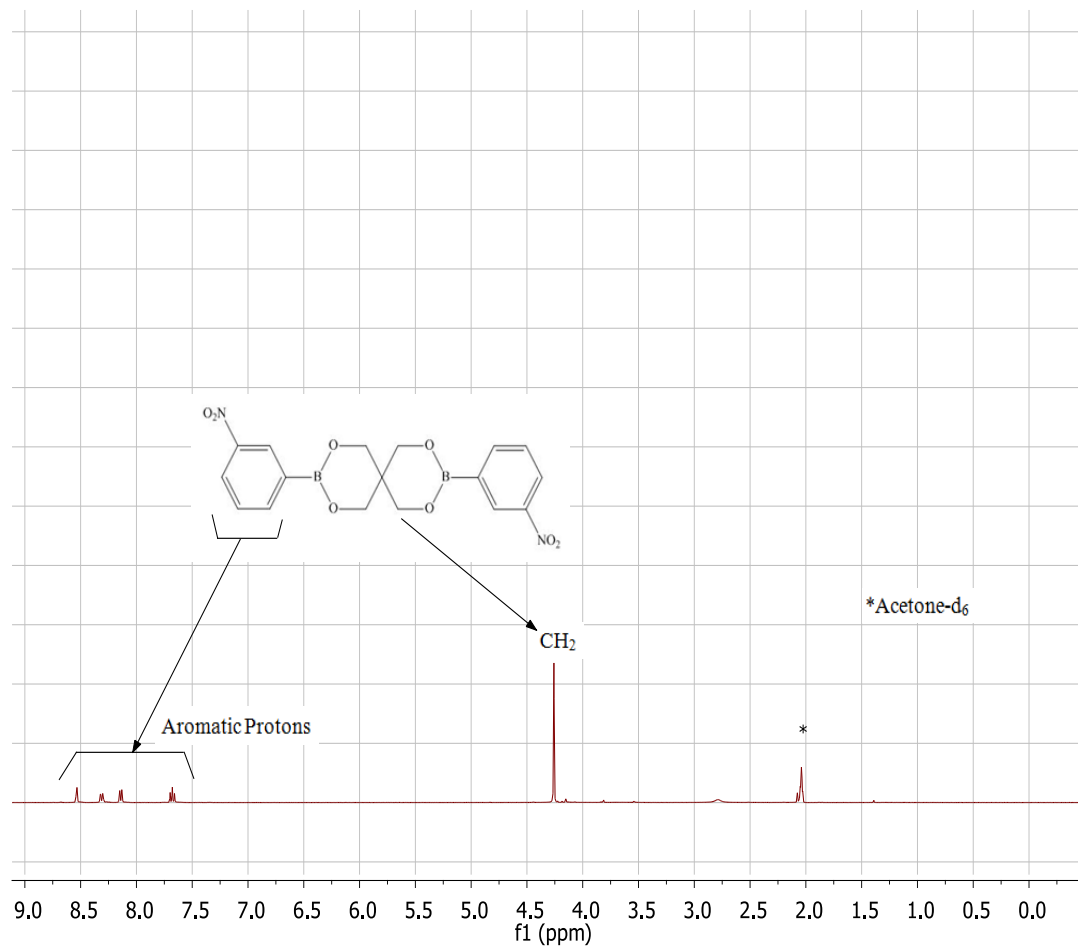


Figure A.41.  $^1\text{H}$  NMR spectrum (400 MHz) of 3,9-bis(3-nitrophenyl)-2,4,8,10-tetraoxa-3,9-diborasp[iro[5.5]undecane.

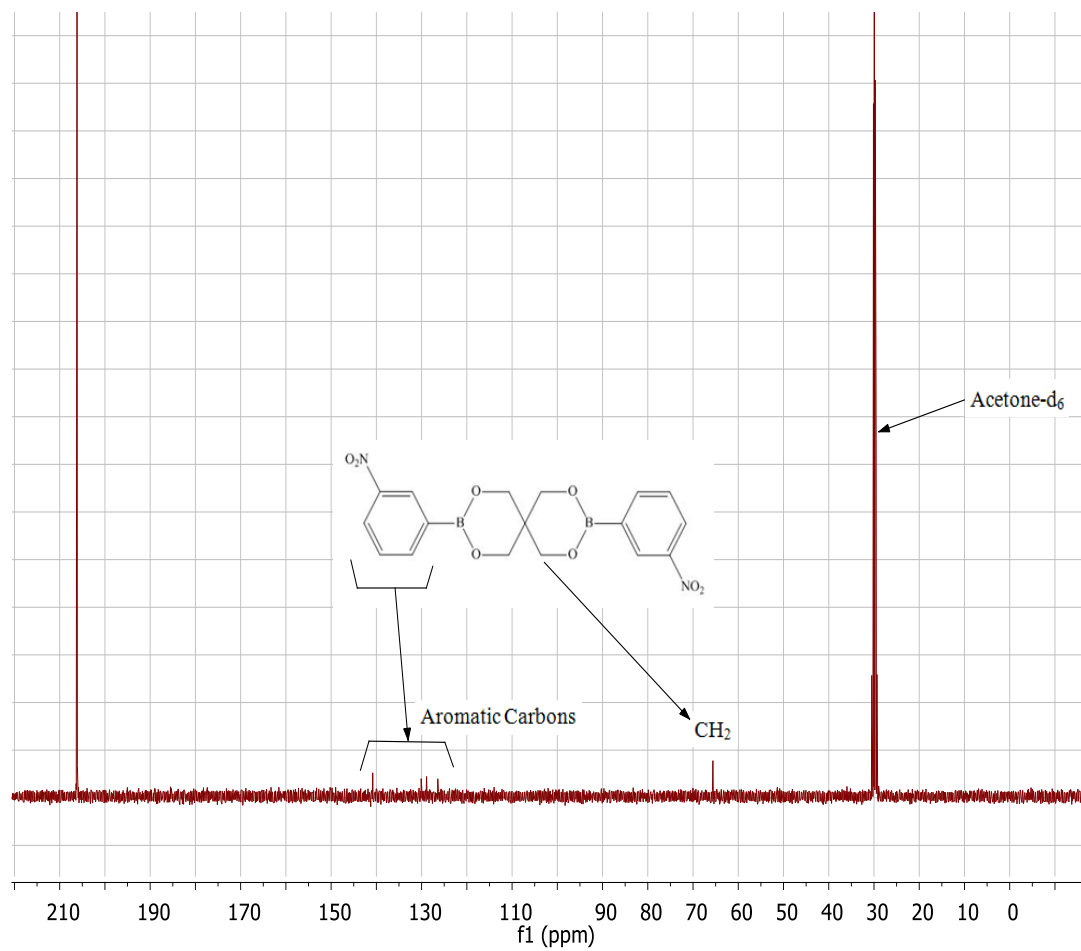


Figure A.42.  $^{13}\text{C}$  NMR spectrum (100 MHz) of 3,9-bis(3-nitrophenyl)-2,4,8,10-tetraoxa-3,9-diborasp[5.5]undecane.

## REFERENCES

- (1) Welton, T.: Room-Temperature Ionic Liquids. Solvents for Synthesis and Catalysis. *Chemical Reviews* **1999**, *99*, 2071-2084.
- (2) Walden, P.: Molecular weights and electrical conductivity of several fused salts. *Bull. Acad. Imper. Sci.* **1914**, 405-422.
- (3) Sugden, S.; Wilkins, H.: CLXVII.-The parachor and chemical constitution. Part XII. Fused metals and salts. *Journal of the Chemical Society (Resumed)* **1929**, 1291-1298.
- (4) Hurley, F. H.; Wier, T. P.: The Electrodeposition of Aluminum from Nonaqueous Solutions at Room Temperature. *Journal of the Electrochemical Society* **1951**, *98*, 207-212.
- (5) Chum, H. L.; Koch, V. R.; Miller, L. L.; Osteryoung, R. A.: An electrochemical scrutiny of organometallic iron complexes and hexamethylbenzene in a room temperature molten salt [32]. *Journal of the American Chemical Society* **1975**, *97*, 3264-3265.
- (6) Gale, R. J.; Gilbert, B.; Osteryoung, R. A.: Raman spectra of molten aluminum chloride: 1-butylpyridinium chloride systems at ambient temperatures. *Inorganic Chemistry* **1978**, *17*, 2728-2729.
- (7) Fry, S. E.; Pienta, N. J.: Effects of molten salts on reactions. Nucleophilic aromatic substitution by halide ions in molten dodecyltributylphosphonium salts. *Journal of the American Chemical Society* **1985**, *107*, 6399-6400.
- (8) Boon, J. A.; Levisky, J. A.; Pflug, J. L.; Wilkes, J. S.: Friedel-Crafts reactions in ambient-temperature molten salts. *Journal of Organic Chemistry* **1986**, *51*, 480-483.
- (9) Hussey, C. L.: Room-temperature molten salt systems. *Adv. molten Salt Chem.* **1983**, *5*, 185-230.

- (10) Wilkes, J. S.; Zaworotko, M. J.: Air and water stable 1-ethyl-3-methylimidazolium based ionic liquids. *Journal of the Chemical Society, Chemical Communications* **1992**, 965-967.
- (11) Davis Jr, J. H.; Forrester, K. J.; Merrigan, T.: Novel organic ionic liquids (OILs) incorporating cations derived from the antifungal drug miconazole. *Tetrahedron Letters* **1998**, *39*, 8955-8958.
- (12) del Valle, J. C.; García Blanco, F.; Catalán, J.: Empirical Parameters for Solvent Acidity, Basicity, Dipolarity, and Polarizability of the Ionic Liquids [BMIM][BF<sub>4</sub>] and [BMIM][PF<sub>6</sub>]. *The Journal of Physical Chemistry B* **2015**, *119*, 4683-4692.
- (13) Huddleston, J. G.; Visser, A. E.; Reichert, W. M.; Willauer, H. D.; Broker, G. A.; Rogers, R. D.: Characterization and comparison of hydrophilic and hydrophobic room temperature ionic liquids incorporating the imidazolium cation. *Green Chemistry* **2001**, *3*, 156-164.
- (14) Seddon, K. R.; Stark, A.; Torres, M. J.: Influence of chloride, water, and organic solvents on the physical properties of ionic liquids. *Pure and Applied Chemistry* **2000**, *72*, 2275-2287.
- (15) Fang, S.; Yang, L.; Wei, C.; Peng, C.; Tachibana, K.; Kamijima, K.: Low-viscosity and low-melting point asymmetric trialkylsulfonium based ionic liquids as potential electrolytes. *Electrochemistry Communications* **2007**, *9*, 2696-2702.
- (16) Fayer, M. D.: Dynamics and structure of room temperature ionic liquids. *Chem. Phys. Lett.* **2014**, *616-617*, 259-274.
- (17) Nishikawa, K.: The phase behaviour of 1-alkyl-3-methylimidazolium ionic liquids. John Wiley & Sons, Inc., 2014; pp 59-85.
- (18) Zhang, Y.; Maginn, E. J.: Molecular dynamics study of the effect of alkyl chain length on melting points of [C<sub>n</sub>MIM][PF<sub>6</sub>] ionic liquids. *Physical Chemistry Chemical Physics* **2014**, *16*, 13489-13499.

- (19) Leys, J.; Tripathi, C. S. P.; Glorieux, C.; Zahn, S.; Kirchner, B.; Longuemart, S.; Lethesh, K. C.; Nockemann, P.; Dehaen, W.; Binnemans, K.: Electrical conductivity and glass formation in nitrile-functionalized pyrrolidinium bis(trifluoromethylsulfonyl)imide ionic liquids: chain length and odd-even effects of the alkyl spacer between the pyrrolidinium ring and the nitrile group. *Physical Chemistry Chemical Physics* **2014**, *16*, 10548-10557.
- (20) McFarlane, D. R.; Sun, J.; Golding, J.; Meakin, P.; Forsyth, M.: High conductivity molten salts based on the imide ion. *Electrochimica Acta* **2000**, *45*, 1271-1278.
- (21) M. Gordon, C.; D. Holbrey, J.; R. Kennedy, A.; R. Seddon, K.: Ionic liquid crystals: hexafluorophosphate salts. *Journal of Materials Chemistry* **1998**, *8*, 2627-2636.
- (22) D. Holbrey, J.; R. Seddon, K.: The phase behaviour of 1-alkyl-3-methylimidazolium tetrafluoroborates; ionic liquids and ionic liquid crystals. *Journal of the Chemical Society, Dalton Transactions* **1999**, 2133-2140.
- (23) Wilkes, J. S.: Properties of ionic liquid solvents for catalysis. *Journal of Molecular Catalysis A: Chemical* **2004**, *214*, 11-17.
- (24) Tokuda, H.; Hayamizu, K.; Ishii, K.; Susan, M. A. B. H.; Watanabe, M.: Physicochemical Properties and Structures of Room Temperature Ionic Liquids. 2. Variation of Alkyl Chain Length in Imidazolium Cation. *The Journal of Physical Chemistry B* **2005**, *109*, 6103-6110.
- (25) Tokuda, H.; Hayamizu, K.; Ishii, K.; Susan, M. A. B. H.; Watanabe, M.: Physicochemical Properties and Structures of Room Temperature Ionic Liquids. 1. Variation of Anionic Species. *The Journal of Physical Chemistry B* **2004**, *108*, 16593-16600.
- (26) Dzyuba, S. V.; Bartsch, R. A.: Influence of Structural Variations in 1-Alkyl(aralkyl)-3-Methylimidazolium Hexafluorophosphates and Bis(trifluoromethylsulfonyl)imides on Physical Properties of the Ionic Liquids. *ChemPhysChem* **2002**, *3*, 161-166.
- (27) Seddon, K. R.; Stark, A.; Torres, M.-J.: Viscosity and density of 1-alkyl-3-methylimidazolium ionic liquids. *ACS Symp. Ser.* **2002**, *819*, 34-49.

- (28) Marsh, K. N.; Boxall, J. A.; Lichtenthaler, R.: Room temperature ionic liquids and their mixtures—a review. *Fluid Phase Equilibria* **2004**, *219*, 93-98.
- (29) Seddon, K. R.; Stark, A.; Torres, M.-J.: Influence of chloride, water, and organic solvents on the physical properties of ionic liquids. *Pure Appl. Chem.* **2000**, *72*, 2275-2287.
- (30) Bozym, D. J.; Uralcan, B.; Limmer, D. T.; Pope, M. A.; Szamreta, N. J.; Debenedetti, P. G.; Aksay, I. A.: Anomalous Capacitance Maximum of the Glassy Carbon–Ionic Liquid Interface through Dilution with Organic Solvents. *The Journal of Physical Chemistry Letters* **2015**, *6*, 2644-2648.
- (31) Pringle, J. M.; Golding, J.; Baranyai, K.; Forsyth, C. M.; Deacon, G. B.; Scott, J. L.; MacFarlane, D. R.: The effect of anion fluorination in ionic liquids-physical properties of a range of bis(methanesulfonyl)amide salts. *New Journal of Chemistry* **2003**, *27*, 1504-1510.
- (32) Del Sesto, R. E.; Corley, C.; Robertson, A.; Wilkes, J. S.: Tetraalkylphosphonium-based ionic liquids. *Journal of Organometallic Chemistry* **2005**, *690*, 2536-2542.
- (33) Maton, C.; De Vos, N.; Stevens, C. V.: Ionic liquid thermal stabilities: decomposition mechanisms and analysis tools. *Chemical Society Reviews* **2013**, *42*, 5963-5977.
- (34) Ngo, H. L.; LeCompte, K.; Hargens, L.; McEwen, A. B.: Thermal properties of imidazolium ionic liquids. *Thermochimica Acta* **2000**, *357–358*, 97-102.
- (35) Crosthwaite, J. M.; Muldoon, M. J.; Dixon, J. K.; Anderson, J. L.; Brennecke, J. F.: Phase transition and decomposition temperatures, heat capacities and viscosities of pyridinium ionic liquids. *The Journal of Chemical Thermodynamics* **2005**, *37*, 559-568.
- (36) Ngo, H. L.; LeCompte, K.; Hargens, L.; McEwen, A. B.: Thermal properties of imidazolium ionic liquids. *Thermochimica Acta* **2000**, *357-358*, 97-102.
- (37) MacFarlane, D. R.; Forsyth, S. A.; Golding, J.; Deacon, G. B.: Ionic liquids based on imidazolium, ammonium and pyrrolidinium salts of the dicyanamide anion. *Green Chemistry* **2002**, *4*, 444-448.

- (38) Awad, W. H.; Gilman, J. W.; Nyden, M.; Harris Jr, R. H.; Sutto, T. E.; Callahan, J.; Trulove, P. C.; DeLong, H. C.; Fox, D. M.: Thermal degradation studies of alkyl-imidazolium salts and their application in nanocomposites. *Thermochimica Acta* **2004**, *409*, 3-11.
- (39) Tokuda, H.; Ishii, K.; Susan, M. A. B. H.; Tsuzuki, S.; Hayamizu, K.; Watanabe, M.: Physicochemical Properties and Structures of Room-Temperature Ionic Liquids. 3. Variation of Cationic Structures. *The Journal of Physical Chemistry B* **2006**, *110*, 2833-2839.
- (40) Fredlake, C. P.; Crosthwaite, J. M.; Hert, D. G.; Aki, S. N. V. K.; Brennecke, J. F.: Thermophysical Properties of Imidazolium-Based Ionic Liquids. *Journal of Chemical & Engineering Data* **2004**, *49*, 954-964.
- (41) Fox, D. M.; Awad, W. H.; Gilman, J. W.; Maupin, P. H.; De Long, H. C.; Trulove, P. C.: Flammability, thermal stability, and phase change characteristics of several trialkylimidazolium salts. *Green Chemistry* **2003**, *5*, 724-727.
- (42) Kroon, M. C.; Buijs, W.; Peters, C. J.; Witkamp, G.-J.: Quantum chemical aided prediction of the thermal decomposition mechanisms and temperatures of ionic liquids. *Thermochimica Acta* **2007**, *465*, 40-47.
- (43) Chowdhury, A.; Thynell, S. T.: Confined rapid thermolysis/FTIR/ToF studies of imidazolium-based ionic liquids. *Thermochimica Acta* **2006**, *443*, 159-172.
- (44) Suarez, P. A. Z.; Einloft, S.; Dullius, J. E. L.; de Souza, R. F.; Dupont, J.: Synthesis and physical-chemical properties of ionic liquids based on 1-butyl-3-methylimidazolium cation. *J. Chim. Phys.* **1998**, *95*, 1626-1639.
- (45) Madria, N.; Arunkumar, T. A.; Nair, N. G.; Vadapalli, A.; Huang, Y.-W.; Jones, S. C.; Reddy, V. P.: Ionic liquid electrolytes for lithium batteries: Synthesis, electrochemical, and cytotoxicity studies. *Journal of Power Sources* **2013**, *234*, 277-284.
- (46) Freire, M. G.; Carvalho, P. J.; Fernandes, A. M.; Marrucho, I. M.; Queimada, A. J.; Coutinho, J. A. P.: Surface tensions of imidazolium based ionic liquids: Anion, cation, temperature and water effect. *Journal of Colloid and Interface Science* **2007**, *314*, 621-630.

- (47) Rolo, L. I.; Caço, A. I.; Queimada, A. J.; Marrucho, I. M.; Coutinho, J. A. P.: Surface Tension of Heptane, Decane, Hexadecane, Eicosane, and Some of Their Binary Mixtures. *Journal of Chemical & Engineering Data* **2002**, *47*, 1442-1445.
- (48) Queimada, A. J.; Caço, A. I.; Marrucho, I. M.; Coutinho, J. A. P.: Surface Tension of Decane Binary and Ternary Mixtures with Eicosane, Docosane, and Tetracosane. *Journal of Chemical & Engineering Data* **2005**, *50*, 1043-1046.
- (49) Queimada, A. J.; Silva, F. A. E.; Caço, A. I.; Marrucho, I. M.; Coutinho, J. A. P.: Measurement and modeling of surface tensions of asymmetric systems: heptane, eicosane, docosane, tetracosane and their mixtures. *Fluid Phase Equilibria* **2003**, *214*, 211-221.
- (50) Deetlefs, M.; Hardacre, C.; Nieuwenhuyzen, M.; Padua, A. A. H.; Sheppard, O.; Soper, A. K.: Liquid Structure of the Ionic Liquid 1,3-Dimethylimidazolium Bis{(trifluoromethyl)sulfonyl}amide. *The Journal of Physical Chemistry B* **2006**, *110*, 12055-12061.
- (51) Law, G.; Watson, P. R.: Surface Tension Measurements of N-Alkylimidazolium Ionic Liquids. *Langmuir* **2001**, *17*, 6138-6141.
- (52) Ignat'ev, N. V.; Welz-Biermann, U.; Kucheryna, A.; Bissky, G.; Willner, H.: New ionic liquids with tris(perfluoroalkyl)trifluorophosphate (FAP) anions. *Journal of Fluorine Chemistry* **2005**, *126*, 1150-1159.
- (53) Buzzeo, M. C.; Evans, R. G.; Compton, R. G.: Non-Haloaluminate Room-Temperature Ionic Liquids in Electrochemistry—A Review. *ChemPhysChem* **2004**, *5*, 1106-1120.
- (54) MacFarlane, D. R.; Meakin, P.; Sun, J.; Amini, N.; Forsyth, M.: Pyrrolidinium Imides: A New Family of Molten Salts and Conductive Plastic Crystal Phases. *The Journal of Physical Chemistry B* **1999**, *103*, 4164-4170.
- (55) Ong, S. P.; Andreussi, O.; Wu, Y.; Marzari, N.; Ceder, G.: Electrochemical windows of room-temperature ionic liquids from molecular dynamics and density functional theory calculations. *Chemistry of Materials* **2011**, *23*, 2979-2986.
- (56) McEwen, A. B.; Ngo, H. L.; LeCompte, K.; Goldman, J. L.: Electrochemical Properties of Imidazolium Salt Electrolytes for Electrochemical Capacitor Applications. *Journal of the Electrochemical Society* **1999**, *146*, 1687-1695.



- (57) Hapiot, P.; Lagrost, C.: Electrochemical Reactivity in Room-Temperature Ionic Liquids. *Chemical Reviews* **2008**, *108*, 2238-2264.
- (58) Galiński, M.; Lewandowski, A.; Stępnia, I.: Ionic liquids as electrolytes. *Electrochimica Acta* **2006**, *51*, 5567-5580.
- (59) Rogers, E. I.; Šljukić, B.; Hardacre, C.; Compton, R. G.: Electrochemistry in Room-Temperature Ionic Liquids: Potential Windows at Mercury Electrodes. *Journal of Chemical & Engineering Data* **2009**, *54*, 2049-2053.
- (60) Villagrán, C.; Aldous, L.; Lagunas, M. C.; Compton, R. G.; Hardacre, C.: Electrochemistry of phenol in bis{(trifluoromethyl)sulfonyl}amide ([NTf<sub>2</sub>]<sup>-</sup>) based ionic liquids. *Journal of Electroanalytical Chemistry* **2006**, *588*, 27-31.
- (61) Schroder, U.; Wadhawan, J. D.; Compton, R. G.; Marken, F.; Suarez, P. A. Z.; Consorti, C. S.; de Souza, R. F.; Dupont, J.: Water-induced accelerated ion diffusion: voltammetric studies in 1-methyl-3-[2,6-(S)-dimethylocten-2-yl]imidazolium tetrafluoroborate, 1-butyl-3-methylimidazolium tetrafluoroborate and hexafluorophosphate ionic liquids. *New Journal of Chemistry* **2000**, *24*, 1009-1015.
- (62) Visser, A. E.; Swatloski, R. P.; Reichert, W. M.; Griffin, S. T.; Rogers, R. D.: Traditional Extractants in Nontraditional Solvents: Groups 1 and 2 Extraction by Crown Ethers in Room-Temperature Ionic Liquids†. *Industrial & Engineering Chemistry Research* **2000**, *39*, 3596-3604.
- (63) Smiglak, M.; Reichert, W. M.; Holbrey, J. D.; Wilkes, J. S.; Sun, L.; Thrasher, J. S.; Kirichenko, K.; Singh, S.; Katritzky, A. R.; Rogers, R. D.: Combustible ionic liquids by design: is laboratory safety another ionic liquid myth? *Chemical Communications* **2006**, 2554-2556.
- (64) Zhang, Y.; Gao, H.; Joo, Y.-H.; Shreeve, J. n. M.: Ionic Liquids as Hypergolic Fuels. *Angewandte Chemie International Edition* **2011**, *50*, 9554-9562.
- (65) Xue, H.; Shreeve, J. M.: Energetic Ionic Liquids from Azido Derivatives of 1,2,4-Triazole. *Advanced Materials* **2005**, *17*, 2142-2146.

- (66) Fox, D. M.; Gilman, J. W.; Morgan, A. B.; Shields, J. R.; Maupin, P. H.; Lyon, R. E.; De Long, H. C.; Trulove, P. C.: Flammability and Thermal Analysis Characterization of Imidazolium-Based Ionic Liquids. *Industrial & Engineering Chemistry Research* **2008**, *47*, 6327-6332.
- (67) Paulechka, Y. U.; Kabo, G. J.; Blokhin, A. V.; Vydrov, O. A.; Magee, J. W.; Frenkel, M.: Thermodynamic Properties of 1-Butyl-3-methylimidazolium Hexafluorophosphate in the Ideal Gas State†. *Journal of Chemical & Engineering Data* **2003**, *48*, 457-462.
- (68) Earle, M. J.; Esperanca, J. M. S. S.; Gilea, M. A.; Canongia Lopes, J. N.; Rebelo, L. P. N.; Magee, J. W.; Seddon, K. R.; Widegren, J. A.: The distillation and volatility of ionic liquids. *Nature* **2006**, *439*, 831-834.
- (69) D. Sun, T. R., M. Destephen, R. Higgins,: Proceedings of the Power Sources Conference 44th. 2010; pp 116-118.
- (70) D. Zhang, E. N., M. Yang,: Proceedings of the Power Sources Conference 44th. 2010; pp 113-115.
- (71) Yazami, R.; Hamwi, A.; Guérin, K.; Ozawa, Y.; Dubois, M.; Giraudet, J.; Masin, F.: Fluorinated carbon nanofibres for high energy and high power densities primary lithium batteries. *Electrochemistry Communications* **2007**, *9*, 1850-1855.
- (72) Yim, T.; Kwon, M. S.; Mun, J.; Lee, K. T.: Room temperature ionic liquid-based electrolytes as an alternative to carbonate-based electrolytes. *Israel Journal of Chemistry* **2015**, *55*, 586-598.
- (73) Kim, G. T.; Jeong, S. S.; Xue, M. Z.; Balducci, A.; Winter, M.; Passerini, S.; Alessandrini, F.; Appetecchi, G. B.: Development of ionic liquid-based lithium battery prototypes. *Journal of Power Sources* **2012**, *199*, 239-246.
- (74) Pandian, S.; Raju, S. G.; Hariharan, K. S.; Kolake, S. M.; Park, D. H.; Lee, M. J.: Functionalized ionic liquids as electrolytes for lithium-ion batteries. *Journal of Power Sources* **2015**, *286*, 204-209.
- (75) Macfarlane, D. R.; Tachikawa, N.; Forsyth, M.; Pringle, J. M.; Howlett, P. C.; Elliott, G. D.; Davis, J. H.; Watanabe, M.; Simon, P.; Angell, C. A.: Energy applications of ionic liquids. *Energy and Environmental Science* **2014**, *7*, 232-250.

- (76) Cui, Y.; Xu, M.; Yao, W.; Mao, J.: Room-temperature ionic liquids enhanced green synthesis of  $\beta$ -glycosyl 1-ester. *Carbohydrate Research* **2015**, *407*, 51-54.
- (77) Li, L.-L.; Zhang, W.-M.; Yuan, Q.; Li, Z.-X.; Fang, C.-J.; Sun, L.-D.; Wan, L.-J.; Yan, C.-H.: Room Temperature Ionic Liquids Assisted Green Synthesis of Nanocrystalline Porous SnO<sub>2</sub> and Their Gas Sensor Behaviors. *Crystal Growth & Design* **2008**, *8*, 4165-4172.
- (78) Kunze, M.; Jeong, S.; Appetecchi, G. B.; Schönhoff, M.; Winter, M.; Passerini, S.: Mixtures of ionic liquids for low temperature electrolytes. *Electrochimica Acta* **2012**, *82*, 69-74.
- (79) Lei, Z.; Liu, Z.; Wang, H.; Sun, X.; Lu, L.; Zhao, X. S.: A high-energy-density supercapacitor with graphene-CMK-5 as the electrode and ionic liquid as the electrolyte. *Journal of Materials Chemistry A* **2013**, *1*, 2313-2321.
- (80) Maiti, S.; Pramanik, A.; Mahanty, S.: Influence of imidazolium-based ionic liquid electrolytes on the performance of nano-structured MnO<sub>2</sub> hollow spheres as electrochemical supercapacitor. *RSC Advances* **2015**, *5*, 41617-41626.
- (81) Wang, J.; He, X.; Zhu, H.; Chen, D.: Preparation of a ROMP-type imidazolium-functionalized norbornene ionic liquid block copolymer and the electrochemical property for lithium-ion batteries polyelectrolyte membranes. *RSC Advances* **2015**, *5*, 43581-43588.
- (82) Srour, H.; Traïkia, M.; Fenet, B.; Rouault, H.; Costa Gomes, M. F.; Santini, C. C.; Husson, P.: Effect of Nitrile-Functionalization of Imidazolium-Based Ionic Liquids on Their Transport Properties, Both Pure and Mixed with Lithium Salts. *Journal of Solution Chemistry* **2014**.
- (83) Yin, K.; Zhang, Z.; Yang, L.; Hirano, S. I.: An imidazolium-based polymerized ionic liquid via novel synthetic strategy as polymer electrolytes for lithium ion batteries. *Journal of Power Sources* **2014**, *258*, 150-154.
- (84) Xue, H.; Shreeve, J. M.: Ionic liquids with fluorine-containing cations. *European Journal of Inorganic Chemistry* **2005**, 2573-2580.
- (85) Lee, H.; Cho, M. H.; Lee, B. S.; Palgunadi, J.; Kim, H.; Kim, H. S.: Alkyl-fluoroalkylimidazolium-based ionic liquids as efficient CO<sub>2</sub> absorbents. *Energy and Fuels* **2010**, *24*, 6689-6692.

- (86) Jin, Y.; Fang, S.; Chai, M.; Yang, L.; Hirano, S. I.: Ether-functionalized trialkylimidazolium ionic liquids: Synthesis, characterization, and properties. *Industrial and Engineering Chemistry Research* **2012**, *51*, 11011-11020.
- (87) Yoshida, K.; Nakamura, M.; Kazue, Y.; Tachikawa, N.; Tsuzuki, S.; Seki, S.; Dokko, K.; Watanabe, M.: Oxidative-stability enhancement and charge transport mechanism in glyme-lithium salt equimolar complexes. *Journal of the American Chemical Society* **2011**, *133*, 13121-13129.
- (88) Beyaz, A.; Oh, W. S.; Reddy, V. P.: Synthesis and CMC studies of 1-methyl-3-(pentafluorophenyl)imidazolium quaternary salts. *Colloids and Surfaces B: Biointerfaces* **2004**, *36*, 71-74.
- (89) Beyaz, A.; Oh, W. S.; Reddy, V. P.: Ionic liquids as modulators of the critical micelle concentration of sodium dodecyl sulfate. *Colloids and Surfaces B: Biointerfaces* **2004**, *35*, 119-124.
- (90) Abraham, K. M.; Jiang, Z.: A Polymer Electrolyte-Based Rechargeable Lithium/Oxygen Battery. *Journal of the Electrochemical Society* **1996**, *143*, 1-5.
- (91) Girishkumar, G.; McCloskey, B.; Luntz, A. C.; Swanson, S.; Wilcke, W.: Lithium–Air Battery: Promise and Challenges. *The Journal of Physical Chemistry Letters* **2010**, *1*, 2193-2203.
- (92) Zheng, J. P.; Liang, R. Y.; Hendrickson, M.; Plichta, E. J.: Theoretical Energy Density of Li–Air Batteries. *Journal of the Electrochemical Society* **2008**, *155*, A432-A437.
- (93) Read, J.; Mutolo, K.; Ervin, M.; Behl, W.; Wolfenstine, J.; Driedger, A.; Foster, D.: Oxygen Transport Properties of Organic Electrolytes and Performance of Lithium/Oxygen Battery. *Journal of the Electrochemical Society* **2003**, *150*, A1351-A1356.
- (94) Pilarek, M.; Glazyrina, J.; Neubauer, P.: Enhanced growth and recombinant protein production of *Escherichia coli* by a perfluorinated oxygen carrier in miniaturized fed-batch cultures. *Microbial Cell Factories* **2011**, *10*, 50-50.
- (95) Hirai, M.; Gabbai, F. P.: Lewis acidic stiborafluorenes for the fluorescence turn-on sensing of fluoride in drinking water at ppm concentrations. *Chemical Science* **2014**, *5*, 1886-1893.

- (96) Madhu, S.; Ravikanth, M.: Boron-dipyrromethene based reversible and reusable selective chemosensor for fluoride detection. *Inorganic Chemistry* **2014**, *53*, 1646-1653.
- (97) Ashokkumar, P.; Weißhoff, H.; Kraus, W.; Rurack, K.: Test-Strip-Based Fluorometric Detection of Fluoride in Aqueous Media with a BODIPY-Linked Hydrogen-Bonding Receptor. *Angewandte Chemie International Edition* **2014**, *53*, 2225-2229.
- (98) Bull, S. D.; Davidson, M. G.; van den Elsen, J. M. H.; Fossey, J. S.; Jenkins, A. T. A.; Jiang, Y.-B.; Kubo, Y.; Marken, F.; Sakurai, K.; Zhao, J.; James, T. D.: Exploiting the Reversible Covalent Bonding of Boronic Acids: Recognition, Sensing, and Assembly. *Accounts of Chemical Research* **2013**, *46*, 312-326.
- (99) Thakur, A.; Mandal, D.; Sao, S.; Ghosh, S.: Catecholboryl-functionalized ferrocene based Lewis acid system: A selective probe for fluoride ion through multiple channels. *Journal of Organometallic Chemistry* **2012**, *715*, 129-135.
- (100) Huynh, T.-P.; Sharma, P. S.; Sosnowska, M.; D'Souza, F.; Kutner, W.: Functionalized polythiophenes: Recognition materials for chemosensors and biosensors of superior sensitivity, selectivity, and detectability. *Progress in Polymer Science* **2015**, *47*, 1-25.
- (101) Prakash Reddy, V.; Blanco, M.; Bugga, R.: Boron-based anion receptors in lithium-ion and metal-air batteries. *Journal of Power Sources* **2014**, *247*, 813-820.
- (102) Choi, N.-S.; Jeong, G.; Koo, B.; Lee, Y.-W.; Lee, K. T.: Tris(pentafluorophenyl) borane-containing electrolytes for electrochemical reversibility of lithium peroxide-based electrodes in lithium–oxygen batteries. *Journal of Power Sources* **2013**, *225*, 95-100.
- (103) Shanmukaraj, D.; Grugeon, S.; Gachot, G.; Laruelle, S.; Mathiron, D.; Tarascon, J.-M.; Armand, M.: Boron Esters as Tunable Anion Carriers for Non-Aqueous Batteries Electrochemistry. *Journal of the American Chemical Society* **2010**, *132*, 3055-3062.
- (104) Goodenough, J. B.; Park, K.-S.: The Li-Ion Rechargeable Battery: A Perspective. *Journal of the American Chemical Society* **2013**, *135*, 1167-1176.

- (105) Kalhoff, J.; Eshetu, G. G.; Bresser, D.; Passerini, S.: Safer Electrolytes for Lithium-Ion Batteries: State of the Art and Perspectives. *ChemSusChem* **2015**, *8*, 2154-2175.
- (106) Liu, X.; Xu, Q.; Yuan, X.; Jin, X.; Zhou, L.: Progress of research on Li-rich cathode materials  $x\text{Li}_2\text{MnO}_3 \cdot (1-x)\text{LiMO}_2$  (M=Ni, Co, Mn...) for Li-ion battery. *Adv. Mater. Res. (Durten-Zurich, Switz.)* **2015**, *1070-1072*, 543-548.
- (107) Zhang, Y.; Wu, X.; Feng, H.; Wang, L.; Zhang, A.; Xia, T.; Dong, H.: Effect of nanosized  $\text{Mg}_{0.8}\text{Cu}_{0.2}\text{O}$  on electrochemical properties of Li/S rechargeable batteries. *International Journal of Hydrogen Energy* **2009**, *34*, 1556-1559.
- (108) Han, C. H.; Kim, J. H.; Paeng, S. H.; Kwak, D. J.; Sung, Y. M.: Electrochemical characteristics of  $\text{LiNiO}_2$  films prepared for charge storable electrode application. *Thin Solid Films* **2009**, *517*, 4215-4217.
- (109) Nam, K. W.; Kim, J. S.; Lee, H. B.: Room temperature strength and crack healing morphology of Si  $3\text{N}_4$  composite ceramics with  $\text{SiO}_2$  colloidal. *Transactions of the Korean Society of Mechanical Engineers, A* **2009**, *33*, 652-657.
- (110) Xiong, L.; Xu, Y.; Tao, T.; Goodenough, J. B.: Synthesis and electrochemical characterization of multi-cations doped spinel  $\text{LiMn}_2\text{O}_4$  used for lithium ion batteries. *Journal of Power Sources* **2012**, *199*, 214-219.
- (111) Fergus, J. W.: Recent developments in cathode materials for lithium ion batteries. *Journal of Power Sources* **2010**, *195*, 939-954.
- (112) Hwang, S. S.; Cho, C. G.; Park, K.-S.: Stabilizing  $\text{LiCoO}_2$  electrode with an overlayer of  $\text{LiNi}_{0.5}\text{Mn}_{1.5}\text{O}_4$  by using a Gravure printing method. *Electrochemistry Communications* **2011**, *13*, 279-283.
- (113) Arumugam, D.; Kalaignan, G. P.: Electrochemical characterizations of surface modified  $\text{LiMn}_2\text{O}_4$  cathode materials for high temperature lithium battery applications. *Thin Solid Films* **2011**, *520*, 338-343.
- (114) Thirunakaran, R.; Kalaiselvi, N.; Periasamy, P.; Renganathan, N. G.: Mg substituted  $\text{LiCoO}_2$  for reversible lithium intercalation. *Ionics* **2003**, *9*, 388-394.

- (115) Rougier, A.; Gravereau, P.; Delmas, C.: Optimization of the Composition of the  $\text{Li}_{1-z}\text{Ni}_z\text{O}_2$  Electrode Materials: Structural, Magnetic, and Electrochemical Studies. *Journal of the Electrochemical Society* **1996**, *143*, 1168-1175.
- (116) Arai, H.; Okada, S.; Sakurai, Y.; Yamaki, J. I.: Thermal behavior of  $\text{Li}_{1-y}\text{NiO}_2$  and the decomposition mechanism. *Solid State Ionics* **1998**, *109*, 295-302.
- (117) Zhang, W.-J.: Structure and performance of  $\text{LiFePO}_4$  cathode materials: A review. *Journal of Power Sources* **2011**, *196*, 2962-2970.
- (118) Zhao, Z.-w.; Si, X.-f.; Liang, X.-x.; Liu, X.-h.; He, L.-h.: Electrochemical behavior of  $\text{Li}^+$ ,  $\text{Mg}^{2+}$ ,  $\text{Na}^+$  and  $\text{K}^+$  in  $\text{LiFePO}_4/\text{FePO}_4$  structures. *Transactions of Nonferrous Metals Society of China* **2013**, *23*, 1157-1164.
- (119) Zhang, Y.; Huo, Q.-y.; Du, P.-p.; Wang, L.-z.; Zhang, A.-q.; Song, Y.-h.; Lv, Y.; Li, G.-y.: Advances in new cathode material  $\text{LiFePO}_4$  for lithium-ion batteries. *Synthetic Metals* **2012**, *162*, 1315-1326.
- (120) Jung, J.; Cho, M.; Zhou, M.: Ab initio study of the fracture energy of  $\text{LiFePO}_4/\text{FePO}_4$  interfaces. *Journal of Power Sources* **2013**, *243*, 706-714.
- (121) Yoon, M.-S.; Islam, M.; Ur, S.-C.: The role of impurities on electrochemical properties of  $\text{LiFePO}_4$  cathode material. *Ceramics International* **2013**, *39*, Supplement 1, S647-S651.
- (122) Vediappan, K.; Guerfi, A.; Gariépy, V.; Demopoulos, G. P.; Hovington, P.; Trottier, J.; Mauger, A.; Julien, C. M.; Zaghbi, K.: Stirring effect in hydrothermal synthesis of nano C- $\text{LiFePO}_4$ . *Journal of Power Sources* **2014**, *266*, 99-106.
- (123) Purwadi, A.; Dozeno, J.; Heryana, N.: Testing Performance of 10 kW BLDC Motor and  $\text{LiFePO}_4$  Battery on ITB-1 Electric Car Prototype. *Procedia Technology* **2013**, *11*, 1074-1082.
- (124) Ren, Y.; Bruce, P. G.: Mesoporous  $\text{LiFePO}_4$  as a cathode material for rechargeable lithium ion batteries. *Electrochemistry Communications* **2012**, *17*, 60-62.

- (125) Doughty, D.; Roth, E. P.: A general discussion of Li Ion battery safety. *Electrochemical Society Interface* **2012**, *21*, 37-44.
- (126) Jiang, J.; Eberman, K. W.; Krause, L. J.; Dahn, J. R.: Structure, electrochemical properties, and thermal stability studies of cathode materials in the  $x\text{Li}[\text{Mn}_{1/2}\text{Ni}_{1/2}]\text{O}_2 \cdot y\text{LiCoO}_2 \cdot z\text{Li}[\text{Li}_{1/3}\text{Mn}_{2/3}]\text{O}_2$  pseudoternary system ( $x + y + z = 1$ ). *Journal of the Electrochemical Society* **2005**, *152*, A1879-A1889.
- (127) Zhang, L.; Takada, K.; Ohta, N.; Fukuda, K.; Osada, M.; Wang, L.; Sasaki, T.; Watanabe, M.: Layered  $(1 - x - y)\text{LiNi}_{1/2}\text{Mn}_{1/2}\text{O}_2 \cdot x\text{Li}[\text{Li}_{1/3}\text{Mn}_{2/3}]\text{O}_2 \cdot y\text{LiCoO}_2$  ( $0 \leq x = y \leq 0.3$  and  $x + y = 0.5$ ) Cathode Materials. *Journal of the Electrochemical Society* **2005**, *152*, A171-A178.
- (128) Kang, S. H.; Amine, K.: Layered  $\text{Li}(\text{Li}_{0.2}\text{Ni}_{0.15} + 0.5z\text{Co}_{0.10}\text{Mn}_{0.55 - 0.5z})\text{O}_2 - z\text{Fz}$  cathode materials for Li-ion secondary batteries. *Journal of Power Sources* **2005**, *146*, 654-657.
- (129) Oljaca, M.; Blizanac, B.; Du Pasquier, A.; Sun, Y.; Bontchev, R.; Suszko, A.; Wall, R.; Koehlert, K.: Novel  $\text{Li}(\text{Ni}_{1/3}\text{Co}_{1/3}\text{Mn}_{1/3})\text{O}_2$  cathode morphologies for high power Li-ion batteries. *Journal of Power Sources* **2014**, *248*, 729-738.
- (130) Xia, J.; Madec, L.; Ma, L.; Ellis, L. D.; Qiu, W.; Nelson, K. J.; Lu, Z.; Dahn, J. R.: Study of triallyl phosphate as an electrolyte additive for high voltage lithium-ion cells. *Journal of Power Sources* **2015**, *295*, 203-211.
- (131) Lee, H.; Choi, S.; Kim, H. J.; Choi, Y.; Yoon, S.; Cho, J. J.: SEI layer-forming additives for  $\text{LiNi}_{0.5}\text{Mn}_{1.5}\text{O}_4/\text{graphite}$  5 V Li-ion batteries. *Electrochemistry Communications* **2007**, *9*, 801-806.
- (132) Zuo, X.; Fan, C.; Xiao, X.; Liu, J.; Nan, J.: Methylene Methanedisulfonate as an Electrolyte Additive for Improving the Cycling Performance of  $\text{LiNi}_{0.5}\text{Co}_{0.2}\text{Mn}_{0.3}\text{O}_2/\text{Graphite}$  Batteries at 4.4 V Charge Cutoff Voltage. *ECS Electrochemistry Letters* **2012**, *1*, A50-A53.
- (133) Ryou, M.-H.; Lee, Y. M.; Lee, Y.; Winter, M.; Bieker, P.: Mechanical Surface Modification of Lithium Metal: Towards Improved Li Metal Anode Performance by Directed Li Plating. *Advanced Functional Materials* **2015**, *25*, 834-841.
- (134) Xu, K.: Nonaqueous liquid electrolytes for lithium-based rechargeable batteries. *Chemical Reviews* **2004**, *104*, 4303-4417.



- (135) Gireaud, L.; Grugeon, S.; Laruelle, S.; Yrieix, B.; Tarascon, J. M.: Lithium metal stripping/plating mechanisms studies: A metallurgical approach. *Electrochemistry Communications* **2006**, 8, 1639-1649.
- (136) Park, M. S.; Yoon, W. Y.: Characteristics of a Li/MnO<sub>2</sub> battery using a lithium powder anode at high-rate discharge. *Journal of Power Sources* **2003**, 114, 237-243.
- (137) Arie, A. A. a. L., Joong Kee: Nano-Carbon Coating Layer Prepared by the Thermal Evaporation of Fullerene C<sub>60</sub> for Lithium Metal Anodes in Rechargeable Lithium Batteries. *Journal of Nanoscience and Nanotechnology* **2011**, 11, 6569-6574.
- (138) Ryou, M. H.; Lee, D. J.; Lee, J. N.; Lee, Y. M.; Park, J. K.; Choi, J. W.: Excellent cycle life of lithium-metal anodes in lithium-ion batteries with mussel-inspired polydopamine-coated separators. *Advanced Energy Materials* **2012**, 2, 645-650.
- (139) Lee, Y.-S.; Lee, J. H.; Choi, J.-A.; Yoon, W. Y.; Kim, D.-W.: Cycling Characteristics of Lithium Powder Polymer Batteries Assembled with Composite Gel Polymer Electrolytes and Lithium Powder Anode. *Advanced Functional Materials* **2013**, 23, 1019-1027.
- (140) Kim, J. S.; Yoon, W. Y.; Kim, B. K.: Morphological differences between lithium powder and lithium foil electrode during discharge/charge. *Journal of Power Sources* **2006**, 163, 258-263.
- (141) Lee, Y. M.; Seo, J. E.; Lee, Y.-G.; Lee, S. H.; Cho, K. Y.; Park, J.-K.: Effects of Triacetoxymethylsilane as SEI Layer Additive on Electrochemical Performance of Lithium Metal Secondary Battery. *Electrochemical and Solid-State Letters* **2007**, 10, A216-A219.
- (142) Ota, H.; Shima, K.; Ue, M.; Yamaki, J. I.: Effect of vinylene carbonate as additive to electrolyte for lithium metal anode. *Electrochimica Acta* **2004**, 49, 565-572.
- (143) Mogi, R.; Inaba, M.; Jeong, S. K.; Iriyama, Y.; Abe, T.; Ogumi, Z.: Effects of some organic additives on lithium deposition in propylene carbonate. *Journal of the Electrochemical Society* **2002**, 149, A1578-A1583.

## VITA

Avinash Raju Vadapalli was born in 1984 in Andhra Pradesh, India. He received his primary, middle and high school education, in Jadugoda, India. He received his Bachelor Degree in Biotechnology from Bangalore University in May 2005 and a Master's Degree in Organic Chemistry, with first class distinction, in May 2009 from Osmania University. In January 2010, Avinash joined the Missouri University of Science and Technology to pursue his Ph.D. He worked as a Teaching Assistant for the Department of Chemistry and as a Research Assistant for Dr. V. Prakash Reddy. In December 2015, Avinash received his Ph.D. in Chemistry from Missouri University of Science and Technology.